Molecular Mechanisms of Circadian Photoreception in *Neurospora crassa*

Dissertation
der Fakultät für Biologie
der Ludwig-Maximilians-Universität München

von
Zdravko Dragovic
aus
Batajnica in Serbien

Inaugural dissertation
zur Erlangung des Doktorgrades
der Fakultät für Biologie
der Ludwig-Maximilians-Universität München

vorgelegt von
Diplom Biologer Zdravko Dragovic
aus Batajnica in Serbien

Erstgutachter: Herr Prof. Reinhold Herrmann

Zweitgutachter: Herr Prof. Eberhard Gwinner

Sondergutachter: Herr Prof. Till Roenneberg

Mündliche Prüfüng am 16. Februar 2004

1 Introduction 7
1.1 Circadian rhythms 7
1.2 Properties of circadian systems 8
1.2.1 Free-running and self-sustainment 8
1.2.2 Period length 9
1.2.3 Circadian rhythms are entrainable 9
1.2.4 Circadian rhythms are compensated 9
1.2.5 Modules of circadian clock 9
1.3 Entrainment of circadian rhythms by light 10
1.3.1 Phase response curves (PRCs) 10
1.3.2 Circadian photosensory system 11
1.3.3 The *Gonyaulax* story 12
1.3.4 Circadian photoreception in *Arabidopsis* 12
1.3.4.1 Cryptochromes 12
1.3.4.2 Phytochromes 13
1.3.4.3 Resetting of the *Arabidopsis* clock with light 14
1.3.5 Circadian Photoreception in mice 15
1.3.5.1 Specialized circadian photoreceptor cells in eye 15
1.3.5.2 Resetting of the clock within an SCN cell 16
1.4 Neurospora crassa: A simple model system for clock and photobiology studies 17
1.4.1 The biology of *Neurospora crassa* 17
1.4.2 Asexual propagation 17
1.4.3 Sexual cycle 18
1.5 Circadian Rhythms in *Neurospora crassa* 19
1.5.1 Conidiation is major output of circadian rhythm 19
1.5.2 Genetic analysis of the clock 20
1.5.3 Genetic analysis of the light input pathway 21
1.5.4 The *Neurospora* genome suggests additional photoreceptors 21
1.6 Action spectra analysis 22
1.7 Molecular studies of the photoreception in *Neurospora* 23
1.7.1 White Collars 23
1.7.2 FRQ protein 24
1.7.3 Resetting of the *Neurospora* clock by light 25
1.7.4 Photoadaptation and circadian photoreception 26
1.8 Open questions 27
2 Results 28
2.1 Molecular and genetic regulation of the light input pathway in *Neurospora crassa* 28
2.1.1 Rhythmicity in DD: FRQ and WC-1 29
2.1.2 Regulation of *frq* and *wc-1* is interdependent: WC-1 regulates *frq* and FRQ regulates *wc-1* 32
2.1.3 frq and the light signaling pathway 35
2.1.4 Circadian regulation of light signaling 37
2.2 Posttranscriptional control of *wc-1* expression 38
2.2.1 Identification of putative protein binding sites in *wc-1* UTRs 38

2.2.2 Proteins bind to 5' and 3' UTRs of *wc-1* mRNA 40
2.2.3 Examining specificity of protein-UTR complexes 41
2.2.4 Circadian regulation of complex formation is not observable 42
2.2.5 Light regulates UTR complex formation 45
2.3 Light-regulated behavior in *white collar* mutants 46
2.3.1 *white collar* mutants synchronize conidiation in response to light..... 47
2.3.2 Fluence titration of light induced conidiation in *wc* mutant strains..... 53
2.3.3 A self–sustained circadian rhythm in the wc mutants..... 54
2.4 Molecular characterization of a series of white collar alleles 55
2.4.1 Light induction of FRQ protein in different *wc* background..... 55
2.4.2 Verification of the *wc* strains..... 56
2.4.3 Molecular dissection of light input mechanisms 59
2.4.4 Presence of FRQ but not quantitative or qualitative changes are required for the regulation of conidiation by light..... 63
2.4.5 Fluence titration of light induction of FRQ protein 64
2.5 Identification of light induced genes in *wc-2* mutant..... 65
2.6 Action spectrum for FRQ protein induction 68
2.6.1 Equal Intensity action spectrum..... 69
2.6.2 Range of reciprocity for FRQ protein light induction..... 71
2.6.3 Dose response curves 73
2.6.4 Action spectrum for FRQ protein induction..... 75
2.7 Novel photoreceptor candidates 77
3 DISCUSSION 85
3.1 Regulation of the light input pathway in *N. crassa* 85
3.1.1 Levels of WC-1 protein are circadianly regulated..... 85
3.1.2 Interdependent regulation of FRQ and WC-1 86
3.1.3 Circadian regulation of light responses..... 86
3.2 Novel photoreceptors in *Neurospora*..... 87
3.2.1 *wc* mutants respond to light..... 87
3.2.2 What are the photoreceptors in *Neurospora*?..... 89
3.2.3 Dual light input pathway in *N. crassa*..... 91
3.2.4 FRQ role in regulation of conidiation and carotenogenesis 92
3.2.5 A self-sustained circadian rhythm in the *wc* mutants 93
3.2.6 Action spectrum of FRQ protein induction..... 93
3.3 Posttranscriptional regulation of *wc-1* expression..... 94
3.3.1 Regulation of translation efficiency by binding to the 5' UTR..... 95
3.3.2 Adaptation in constant light and regulation of mRNA stability by binding to the 3' UTR 96
4 Materials and Methods 98
4.1 Physiological Methods..... 98
4.1.1 Strain maintenance..... 98
4.1.2 Media supplements 98
4.1.3 Stock management 98
4.1.4 Lab practice 99
4.1.5 Conidial suspensions -inoculum 99
4.1.6 Liquid cultures 99

4.1.7 Sexual crossing 100
4.1.8 Carotenoid assay 100
4.1.9 Race-tube assay 101
4.1.10 Light induction and light dark experiments with liquid cultures 102
4.2 Strains 102
4.3 DNA methods 104
4.3.1 DNA purification 104
4.3.1.1 Plasmid isolation from E. coli 104
4.3.1.1.1 Phenol extraction –"Mini-preps" 104
4.3.1.1.2 Silica columns – "Midi & Maxi-preps" 104
4.3.1.2 DNA extraction from conidia 104
4.3.1.3 DNA extraction from mycelia 105
4.3.1.3.1 DNA extraction with phenol 105
4.3.1.3.2 DNA extraction with CTAB 105
4.3.2 Separation and purification of DNA on agarose gels 106
4.3.3 DNA quantification 106
4.3.4 Sheering of DNA 106
4.3.5 Digestion, ligation and transformation of DNA molecules 107
4.3.6 Production of electrocompetent E. coli cells 107
4.3.7 Transformation of E. coli cells by electroporation 108
4.3.8 PCR 108
4.3.9 Real Time PCR analysis 109
4.3.9.1 DNase digestion and reverse transcription 110
4.3.9.2 Primer design 110
4.3.9.3 Real Time PCR analysis 111
4.4 RNA methods 114
4.4.1 RNA extraction 114
4.4.2 RNA quantification 114
4.4.3 Northern blot analysis 114
4.4.4 Synthesis of radioactive RNA probes 115
4.4.4.1 in vitro transcription 116
4.4.4.2 Polyacrylamide gel purification of labeled RNA 116
4.4.5 Radioactive labeling of Northerns 118
4.4.6 Gel mobility shift assay 118
4.4.6.1 Preparation of RNA and protein 118
4.4.6.2 RNA-protein binding reaction 119
4.4.6.3 Preparation, loading and running of native polyacrilamide gels 119
4.4.6.4 Drying and autoradiography of gels 119
4.4.7 Microarray experiments 120
4.5 Protein methods 120
4.5.1 Protein extraction 120
4.5.2 Protein quantitation- Bradford Assay 120
4.5.3 TCA precipitation 121
4.5.4 Protein electrophoresis SDS-PAGE 121
4.5.5 Western blotting 122
4.5.5.1 Wet blotting 122

4.5.5.2 Semi-dry blotting 123
4.5.6 Staining of SDS-polyacrilamide gels with coomasssie blue (CB) 123
4.5.7 Staining of nitrocellulose membranes with ponceau-S 123
4.5.8 Immunodetection of proteins 124
4.6 Densitometric analysis of the western and northern blots 124
4.7 Mathematical fits 125
4.8 Time measurement in chronobiology 126
5 SUMMARRY 127
6 Appendix 129
6.1 List of Instruments 129
6.2 List of chemicals 131
6.3 List of Biochemicals 134
6.4 Abbreviations 135
6.5 Recipes 137
6.6 List of software 149
7 REFERENCES 150
8 ERKLÄRUNG 161
9 Danksagung /Acknowledgements / Zahvalnica 162

1 INTRODUCTION

1.1 Circadian rhythms

Almost all organisms on Earth recruit their energy from sunlight stored in chemical bonds. This energy is not continually available, but is delivered in cycles created by the rotation of the Earth (Fig. 1). These day and night cycles also drive changes of other important environmental factors such as temperature and humidity.

Figure 1. Series of photographs taken throughout a mid-summer day, north of the artic circle. Light intensity and spectral composition change over the course of the day.

Many species have developed strategies to cope with these highly systematic environmental changes. They posses an endogenous clock that regulates daily rhythms of physiology and behavior. The clock that controls daily rhythms of an organism is called the circadian (circa dies, about a day) clock. Oscillations in physiological and behavioral functions with circa 24 h period are called circadian rhythms.

Circadian rhythms have been described in all phyla and they regulate important molecular, physiological and social aspects of biology. The internal clock generates a temporal program optimizing the sequence of daily events and preparing the organism for coming events, e.g., fungi release their spores during a clock regulated window of time (Merrow and Dunlap, 1994; Roenneberg and Merrow, 2001b); plants circadianly regulate photosynthesis, stomatal opening, leaf movement and growth (McClung, 1992; Quail

2002). In almost all animals, ranging from flies to mammals, locomotor activity is circadianly regulated. Experimental evidence demonstrates a survival advantage conferred by circadian clocks (DeCoursey and Krulas, 1998; Yan et al., 1998), suggesting selective pressure as the main driving force for the evolution of circadian clocks.

Circadian rhythmicity has great impact on human biology and human society (Moore, 1997). Circadian variations in hormone levels, mental and physical performance, pharmacokinetics and aspects of disease reveal the significant influence of the circadian clock on human physiology and pathology (McFadden, 1988; Moore-Ede et al., 1982; Rocco et al., 1987). In developed countries about 20% of employees work on night shifts. During shift work, circadian systems often remain entrained to local time rather than adjusting to night shifts. Thus, shift workers are active and alert when their physiology and psychology are adjusted for sleep (Scott, 2000; Waterhouse et al., 1997). Understanding how light regulates clock genes and their protein products will provide us with valuable information on how to adjust functions of the human body to shift work.

1.2 Properties of circadian systems

Molecular clock components differ significantly among cyanobacteria, fungi, plants and animals. Importantly though several mechanistic features are common to all circadian systems:

1.2.1 Free-running and self-sustainment

Circadian rhythms persist even when environmental cues, such as light and temperature, are removed. This property of circadian rhythms is called **self-sustainment**. When the rhythms are observed under constant conditions they are called **free-running rhythms.** Examples of free-running circadian rhythms are activity in mammals in darkness, asexual spore formation in the filamentous fungus *Neurospora crassa* in darkness or bioluminescence of some photosynthetic algae in constant light. Rhythms can persist indefinitely, but sometimes the amplitude of the oscillations decreases until the rhythm is no longer observed, a condition called “damping”.

Circadian rhythms are often studied under free-running conditions. Physiological and molecular changes, which would occur in the morning under entrained conditions, occur in the "subjective morning" under free-running conditions. Analogously, free running rhythms are structured into the subjective night and subjective day.

1.2.2 Period length

The period of free-running circadian rhythms is called free-running period (FRP) and it is always close to 24 h. Biological rhythms can also be significantly shorter or longer than a day, called ultradian and infradian respectively. Among the infradian rhythms are the circalunar (circa-monthly) and circannual.

1.2.3 Circadian rhythms are entrainable

Entrainment is the synchronization of circadian rhythms by external cues. Natural light and temperature cycles entrain the circadian clock on a daily basis and keep physiological functions synchronized with environment.

1.2.4 Circadian rhythms are compensated

Circadian rhythms have a stable FRP in different nutritional conditions and over a broad range of temperatures (10°C or more), showing that endogenous timing is preserved despite large changes in metabolic rate. Compensated circadian clocks reliably regulate timing of important functions even under suboptimal conditions.

1.2.5 Modules of circadian clock

According to Eskin, (Fig. 2; Eskin, 1979) circadian clocks consist of three major functional components: **input pathway**, **rhythm generator** and **output pathway** (Fig. 2). **Zeitgeber** signals are, through the input pathway, transduced to the oscillator. The oscillator generates the self-sustained rhythmicity of the clock. Output pathway carries the signal to its functional role. Because of its simplicity Eskin's model generally describes circadian systems of all known model-organisms.

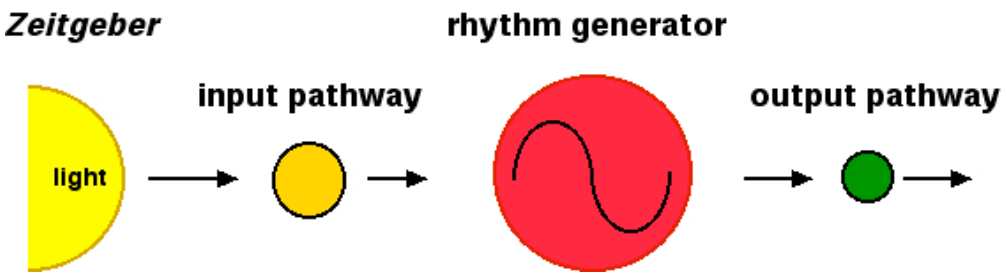

Figure 2. Basic model of a circadian system. The input pathway transduces zeitgeber signals, such as light, to the rhythm generator. The oscillator generates a self-sustained rhythmicity and regulates various output pathways (Eskin, 1979; Roenneberg and Merrow, 1998).

1.3 Entrainment of circadian rhythms by light

The period of the circadian rhythm in constant conditions deviates from 24 h. Thus, to be of use for an organism, circadian clock has to be set (or entrained) on daily base to match the 24 day. The most common external cues, which entrain circadian clock are light and temperature (Roenneberg and Foster, 1997; Sweeney and Hastings, 1960). Entrainment of the circadian clock is often studied using **phase response curves**.

1.3.1 Phase response curves (PRCs)

By giving light pulses to a circadian system in otherwise constant conditions it is possible to probe the sensitivity of the system throughout a circadian cycle. When light pulses are administrated in the "subjective morning" they have different effects than identical pulses in the subjective evening. Usually morning light pulses advance the phase of the clock and evening ones delay it. The phase shift is plotted as a function of the circadian time when the light pulse was delivered. Graphs obtained in this way are called phase response curves (PRC) (Fig. 3). The shape of a PRC can vary significantly according to the experimental conditions and the organism. PRCs reflect both the state of the oscillator or that of the light input pathway components (Roenneberg and Merrow, 1998; Fleissner and Fleissner, 1996; Roenneberg and Merrow, 2000).

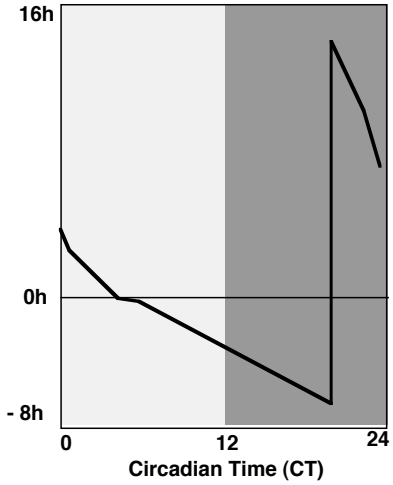

Figure 3. Phase response curve (PRC) is a graph of the time of day dependence of responses to an exogenous stimulus. A stimulus (e.g. light) is given in constant conditions and the amplitude of response (phase shift of the circadian rhythm) is presented as an advance (positive values) or a delay (negative values). The graph shown here is a *Neurospora* light PRC (redrawn from Dharmananda, 1980).

1.3.2 Circadian photosensory system

Photosensitive systems vary in their structure and are often specialized for function, but all share one common feature. They are able to detect changes in illumination. **Spatial change** (spatial contrast) carries information about location and shape of the object. To fulfill this function these photosensitive systems have high spatial resolution. In mammals, for instance, photoreceptor cell (rods and cones) are densely packed in the retina, providing the brain with a "high pixel density" image. To acquire precise temporal information, photoreceptors have to be sensitive to rapid changes in illumination (high temporal resolution). A retinal image in the turtle eye, for example, is renewable within 500 ms. **Motion** is change in stimulus over both space and time. Thus photoreceptor systems for motion detection require both spatial and temporal resolution (Zigmond, 1999).

Circadian photosensitive systems extract from the environment only the sort of information useful for assessment of day and night. They are insensitive to short-term changes in light intensity like a flash of lightning or the shadow of a cloud. Circadian photoreceptors act as an irradiance detector by integrating photons over the course of the

day. Research on different model systems has begun to unravel the mechanisms of circadian photoreception.

1.3.3 The *Gonyaulax* story

The photosynthetic dinoflagellate *Gonyaulax* provided evidence for the existence of two circadian oscillators in one cell, which are normally coupled together to regulate outputs (Roenneberg and Morse, 1993). In *Gonyaulax*, increasing the intensity of red light causes lengthening of the free-running period, whereas increasing blue light shortens it (Roenneberg and Hastings, 1988). This finding indicates that two distinct light input pathways feed into the entrainment of the coupled oscillators. It has been shown that allopurinol (flavoprotein inhibitor) blocks blue light input to the clock, suggesting that a flavoprotein could be serving as the photopigment (Deng and Roenneberg, 1997). Experiments with an electron transport inhibitor indicate that the *Gonyaulax* light input pathways also involve photosynthesis (Roenneberg and Taylor, 1994).

1.3.4 Circadian photoreception in *Arabidopsis*

As a good genetic model system, *Arabidopsis* was used to generate a panel of photoreceptor and clock mutants. *Arabidopsis* detect light signals using three main classes of photoreceptors: the ***cryptochromes*** (*cry*), the ***phytochromes*** (*phy*), and the ***phototropins*** (*nph*) (Quail, 2002). In *Arabidopsis*, both phytochromes and cryptochromes act as circadian photoreceptors (Fig. 4). *cry* and *phy* deficiencies cause period lengthening, indicating that both of them are, also required for circadian function (Somers et al., 1998a).

1.3.4.1 Cryptochromes

The cryptochromes are flavoproteins with two chromophores, pterin and FAD. FAD is placed in an amino terminal domain that is related to DNA photolyase (Briggs and Olney, 2001). Cryptochromes absorb in the blue and UV-A regions of the spectrum. In *Arabidopsis*, there are two cryptochromes, *cry1* and *cry2*. Both proteins contain a carboxy-terminal domain that is not found in photolyases and both are localized in the

nucleus (Guo et al., 1999; Kleiner et al., 1999). The photochemical mechanism of photon capture and transfer is likely to involve photooxidation. Cryptochromes most likely act posttranslationally by regulating proteosome mediated degradation of transcriptional activators. Light signals perceived by cryptochromes interrupt constitutive proteosomal HY5 protein degradation. The increased levels of HY5 protein activate transcription of downstream genes involved in photomorphogenesis (Chattopadhyay et al., 1998; Oyama et al., 1997).

1.3.4.2 Phytochromes

The phytochromes are dimeric chromoproteins consisting of two polypeptide subunits and a tetrapyrole chromophore. They are sensitive the red and far-red region of the spectrum. The carboxy-terminal domain has sequence similarity to prokaryotic two component histidine kinases and functions in dimerisation. In *Arabidopsis* five phytochromes, *phyA* to *phyE* (Briggs and Olney, 2001; Whitelam et al., 1998) have been described and all of them contain a carboxy-terminal PER-ARNT-SIM (PAS) domain. PAS protein domains are implicated in protein-protein interactions (Huang et al., 1993; Reisz-Porszasz et al., 1994) , which are also common to many clock and light input pathway components (Ballario and Macino, 1997; Briggs and Olney, 2001; Dunlap, 1999; Heintzen et al., 2001). The phytochromes are localized to the cytosol in their biologically inactive Pr form, but upon photoconversion to their active Pfr form they translocate into the nucleus. Phytochromes act as transcriptional regulators of photoresponsive promoters. A *phyA-cry* protein complex acts as a photoreceptor for red/blue light at low fluence (Ahmad and Cashmore, 1998). Phytochromes B, D and E serve as a receptors for high intensity red light (Fig. 4).

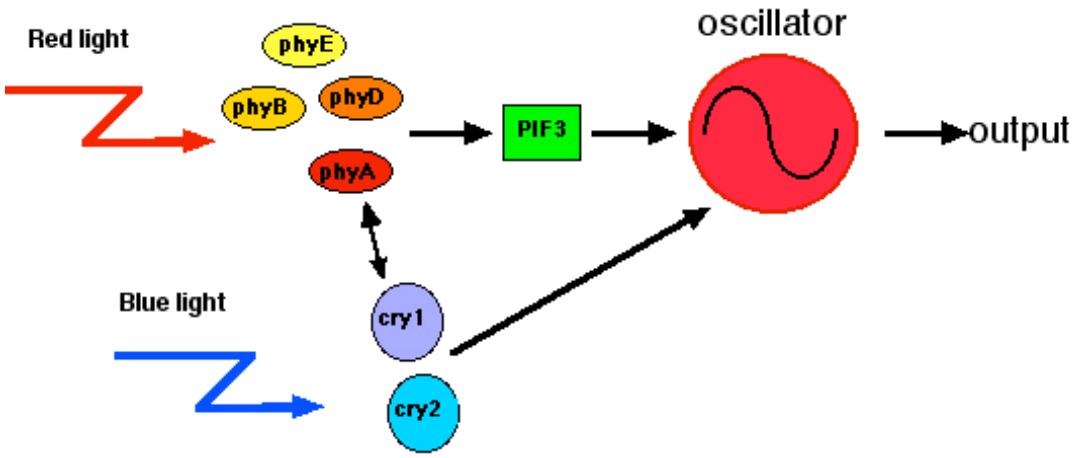

Figure 4. Light input to the clock in *Arabidopsis thaliana.* Both the red light photoreceptors *phytochromes* (*phy*), and the blue light receptors *cryptochromes* (*cry*), mediate input to the clock in higher plants. PHY A acts as a photoreceptor for low fluence rates of both red and blue light but shows a functional dependence on *cryptochrome1*. PHY act at the transcriptional level through promoter-bound PIF3 (Quail, 2002)

1.3.4.3 Resetting of the *Arabidopsis* clock with light

Arabidopsis clock components CCA1, LHY and TOC1 form a reciprocal feedback loop. CCA1 and LHY negatively regulate TOC1 expression through sequence specific binding to the TOC1 promoter, and TOC1 positively regulates CCA1 and LHY expression (Alabadi et al., 2001; Wang and Tobin, 1998). Entrainment of *Arabidopsis* clock occurs at the molecular level by two light induced processes: mRNA synthesis and protein-degradation and inactivation. PHYA and PHYB transiently induce *cca1* and *lhy* mRNA synthesis in response to light. Increased levels of CCA1 and LHY proteins reset the clock to dawn (Green and Tobin, 1999; Martinez-Garcia et al., 2000). CRY acts post-translationally to block constitutive degradation of HY5 protein. The increased levels of HY5 activate transcription of *cca1*, *lhy* and *toc1* genes and subsequent synthesis of protein products. Elevated levels of three main clock proteins CCA1, LHY and TOC1 reset the *Arabidopsis* clock.

1.3.5 Circadian Photoreception in mice

Complex organisms, like mice, have "organ clocks" with specialized cellular clocks working together. Tissues and organs are synchronized by the suprachiasmatic nucleus (SCN) in the hypothalamus. The suprachiasmatic nuclei (SCN) facilitates synchronization of all other cellular clocks in the organism by light (Zigmond, 1999). This small (in mice 1 mm in diameter), paired structure is positioned in the anterior hypothalamus, above the optic chiasm. The anatomical position of the SCN is optimal for receiving light entrainment signals through retino-hypothalamic tract (RHT). The mouse is a good molecular model system to address questions how a multilevel clock mechanism is entrained by light.

1.3.5.1 Specialized circadian photoreceptor cells in eye

Mammals use only their eyes for synchronization to the day-night cycles. In order to characterize circadian photoreceptive cells, rods and cones were selectively eliminated (Freedman et al., 1999; Lucas et al., 1999). These mice are still entrainable to light dark cycles indicating that mammals possess a circadian photoreception system distinct from the rod-cone based visual system. Experiments on retinal ganglion cells (RGCs) have shown that a small subset of RGCs are light sensitive (Berson et al., 2002; Hattar et al., 2002) (Fig. 5). This subset of RGCs express the putative photoreceptive protein melanopsin (Gooley et al., 2001; Hannibal et al., 2002; Hattar et al., 2002; Ruby et al., 2002b). Melanopsin containing RGCs project to the SCN, intergeniculate leaflet and olivary pretectal nucleus. Mutation studies revealed that melanopsin knockout mice are still light-responsive but they exhibit abnormal phase shifting in response to pulses of light (Panda et al., 2002; Ruby et al., 2002a). It has also been shown that the RGCs in melanopsin knockout mice are no longer light sensitive (Lucas et al., 2003). This means that melanopsin is probably one of several photoreceptive proteins involved in circadian photoreception in mammals. Additional candidates are cryptochromes *cry1* and *cry2*, which are both expressed in the mammalian retina (Gelder et al., 2003).

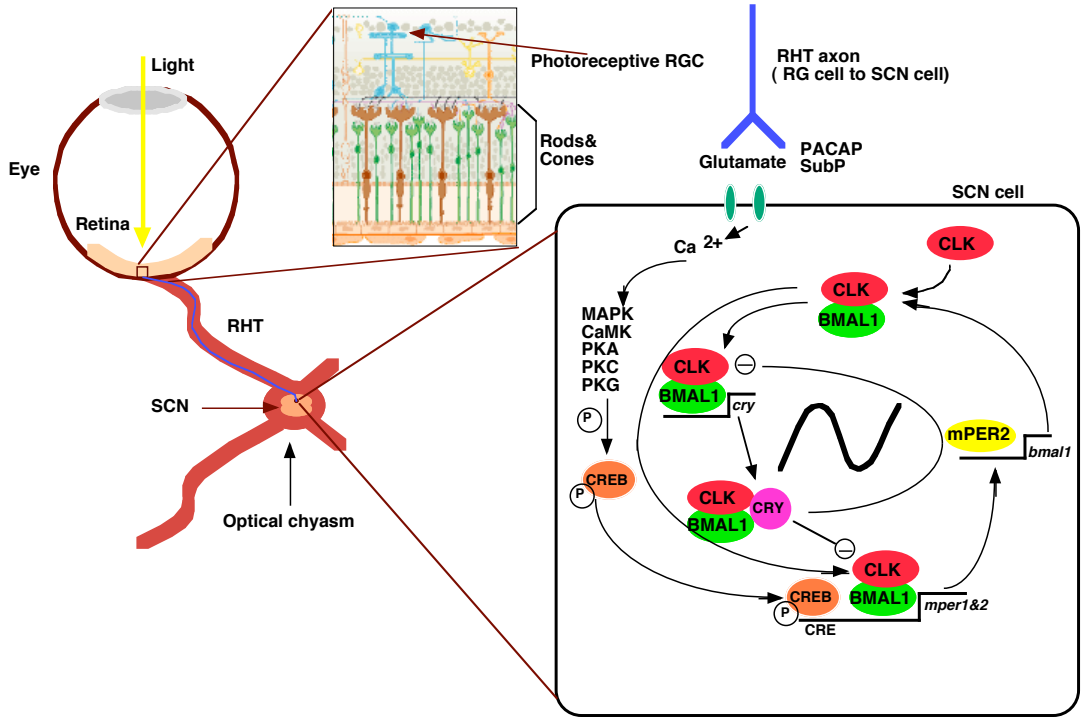

Figure 5. Model of circadian clockwork in mice. A "Master" circadian clock resides in the suprachiasmatic nucleus (SCN) which perceives light only via the retina. Circadian photoreception functions, in addition to rods and cones, *via* a small subset of retinal ganglion cells (RGCs). The light signal from RGCs is transduced to the SCN via retinohypothalamic tract (RHT) (redrawn from Menaker, 2003). Glutamate, released from terminals of the RHT activates a Ca^{2+} dependent signaling pathway leading to phosphorylation of CREB protein. Phosphorylated CREB activates *mper1* and *mper2*. *mper1-3, mcry1-2, bmal1-2* and *clk* are genetic components of the mammalian circadian system. They, are proposed to form transcriptional/translational feedback loops which generate circadian rhythmicity (Menaker, 2003; Shearman et al., 1997; Zylka et al., 1998).

1.3.5.2 Resetting of the clock within an SCN cell

Light causes glutamate release from the terminals of the RHT that innervate the SCN neurons. Glutamate receptors are present in the postsynaptic membranes of SCN neurons (Ding et al., 1998). Glutamate activates a Ca^{2+} dependent signaling pathway in a time of day specific manner (i.e. more robustly at same times of day than at others). Substance-P

(SubP) and pituitary adenylate-cyclase-activating-peptide (PACAP), released from RHT axons, modulate glutamate action. In the cytosol of SCN neurons, an activated set of kinases (CaMK, MAPK, PKA, PKC, PKG) phosphorylates cAMP-response-element-binding-protein (CREB) (Ginty et al., 1993). Phosphorylated CREB activates transcription of the clock genes *mper1* and *mper2* by direct interaction with a calcium/cAMP response element (CRE) in their promoters, what resets the clock at cellular level (Ding et al., 1997; Obrietan et al., 1998) (Fig. 5).

1.4 *Neurospora crassa*: A simple model system for clock and photobiology studies

1.4.1 The biology of *Neurospora crassa*

The filamentous fungus *Neurospora crassa* is an ascomycete. Depending on conditions it propagates asexually or reproduces sexually. *N. crassa* exists mainly as a haploid, and the diploid zygote immediately undergoes meiosis and generates haploid spores. The genus *Neurospora* has traditionally been found in moist, tropical and subtropical areas. Recent collection initiatives revealed that *Neurospora* habituate also many temperate zones as far North as Alaska. *Neurospora* is one of the first colonists in areas of burned-over vegetation. It can be also found growing indoors on food or food waste. *Neurospora* lives in a highly illuminated natural habitat and has developed a variety of light responses including mycelial carotenoid production (Harding and Turner, 1981), sexual structure formation and their phototropism (Degli-Innocenti and Russo, 1984; Harding and Melles, 1984), and gene expression (Arpaia et al., 1993; Collett et al., 2002; Crosthwaite et al., 1995; Li and Schmidhauser, 1995; Sommer et al., 1989).

1.4.2 Asexual propagation

In its asexual stage, *Neurospora* forms a mycelium (Fig. 6). A mycelium is made of syncytial hyphae, tubular filaments with multiple haploid nuclei. The asexual cycle also includes formation of macroconidia from aerial hyphae. The macroconidia (or simply conidia) have one to several haploid nuclei. Genetically different, haploid nuclei can

coexist in single spore or mycelia and such strains are called heterokaryotic. Macroconidia do not survive in nature for a long time, but due to their huge number they allow *Neurospora* to spread rapidly. Conidia germinate to form a hyphae, which grows by tip extension and branching to form a mycelium. In poor nutritional conditions, *Neurospora* produces uninucleate microconida.

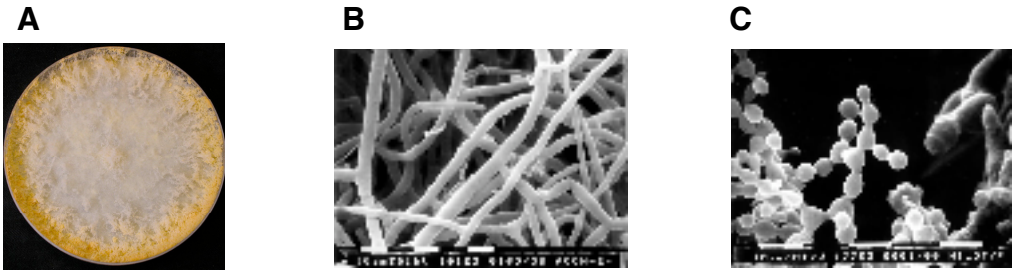

Figure 6. Growth and morphology of the *Neurospora crassa* during asexual propagation. (**A**) A few days after inoculation on solid media, the Petri dish is densely overgrown. In the center of the dish it is possible to see mainly vegetative mycelia, magnified in **B**. The edges of the culture feature conidia, shown magnified in **C**; (from FGSC, www.fgsc.net).

1.4.3 Sexual cycle

The sexual cycle of the *N. crassa* requires two mating types (a so called “big a” and a calld “small a”, by convention). Either strain may act as a "female" parent by forming a specialized multicellular knot of hyphae (protoperithecium) which contains the female gamete (ascogonium). Fertilization occurs via a specialized hyphae (trichogyne) which collects a conidium of the opposite mating type. Two gamete-nuclei (male and female) undergo simultaneous meiosis. At the same time the protoperithecium enlarges and forms a thick-walled, mature perithecium around ascogonium. Ascogenous hyphae form asci with eight sexual ascospores. Mature asci shoot ascospores away from the perithecium. Dormant ascospores can survive in the soil for long periods until activated by fire or chemicals.

1.5 Circadian Rhythms in *Neurospora crassa*

1.5.1 Conidiation is major output of circadian rhythm

Conidiation is regulated by the circadian system, as well as by environmental factors, including light. In constant darkness, conidia accumulate in discrete bands about once per 22 h, showing a free-running, circadian rhythm (Pittendrigh et al., 1959). In constant light, the consolidation of conidiation in discrete bands is absent, with conidia produced approximately continuously. In 24 h cycles of alternating light and dark, the conidia are produced within a precise temporal window (Chang and Nakashima, 1997; Merrow et al., 1999; Lakin-Thomas and Brody, 2000) that is systematically related to the cycle.

The circadian rhythm in *Neurospora* is routinely assayed as a conidiation rhythm on agar media. As hyphae grow across the substrate, once a day the clock signals the production of the easily observable fluffy orange conidia. This clearly discernable area is called a "band". The region between the bands is called "interband". The pattern of bands serves as a "fossil record" of the circadian rhythm. In practice, cultures for monitoring rhythms are grown on agar media in glass tubes (called "race tubes") filled with a solid growth medium (Fig. 7).

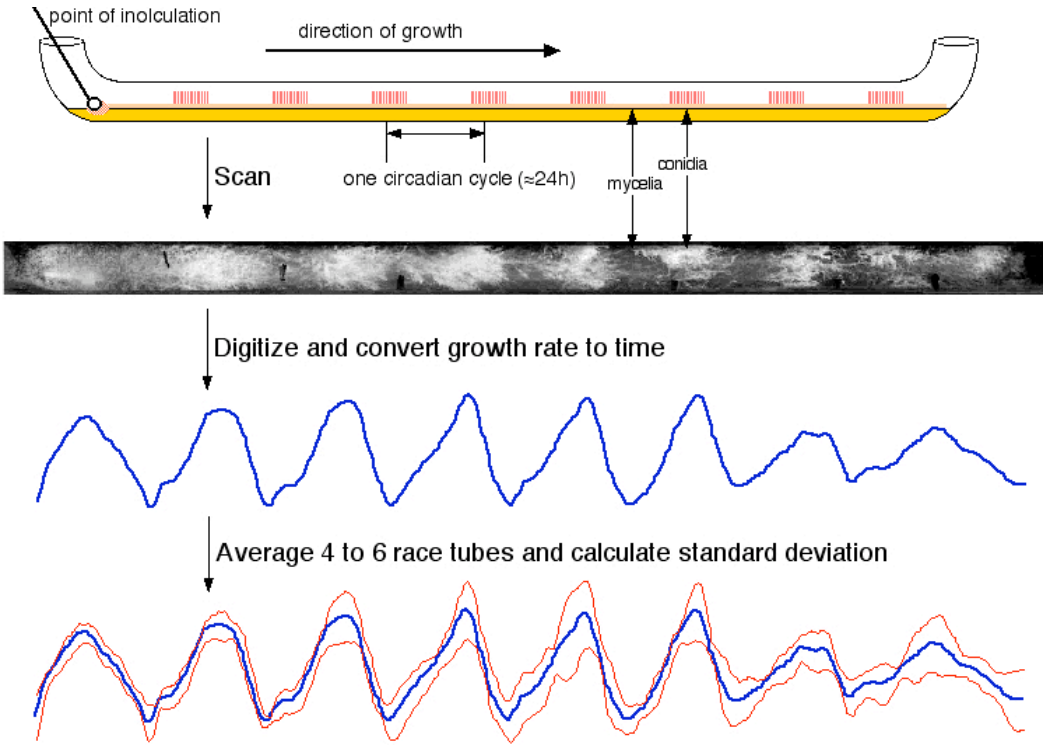

Figure 7. Race tube assay to determine the free running, circadian period of *Neurospora*. A race tube is hollow glass tube (40 or 60 cm long, up to 1.5 cm in diameter) bent at the ends and partially filled with a solid growth medium. It permits visualization of linear growth for a week to 10 days. Race tube experiments are used for describing clock controlled conidia formation. Race tubes are marked regularly to facilitate correlation of linear growth rate and conidial development with time and analyzed using the Chrono program (Roenneberg and Taylor, 2000).

1.5.2 Genetic analysis of the clock

Genetic analysis of the *Neurospora* circadian clock started with mutational analyses resulting in the description more than 30 mutant alleles with an influence on the clock (Feldman and Dunlap, 1983; Feldman and Hoyle, 1973; Lakin-Thomas et al., 1990; Loros and Dunlap, 2001). These clock mutants have been discovered mainly in screens for strains with period alterations. The first *Neurospora* clock gene *frequency* (*frq*) was found in a genetic screen for period mutants (Feldman and Hoyle, 1973). Subsequent screens yielded seven additional alleles of the same gene. The period lengths of the *frq* mutants were either shorter or longer than normal (21.5 h). Among the mutants was also

an arrhythmic strain (*frq*^{9}). Further characterization has shown that *frq*^{9} is a recessive, loss-of-function allele (Loros et al., 1986).

1.5.3 Genetic analysis of the light input pathway

Mutations in several genes affect light responsiveness in *Neurospora* (Linden et al., 1997). *White collar-1* and *white collar-2* (*wc-1* and *wc-2*) mutants have been reported to be impaired in light-regulated carotenogenesis. Subsequently, it has been shown that all other light responses are also abolished in these mutants (Ninnemann, 1991; Perkins et al., 1982b; Russo, 1988). To date, despite extensive screening, it was not possible to isolate other completely blind mutants. Thus, the hypothesis that one or both of these proteins are photoreceptors has been suggested (Harding and Shropshire, 1980). Subsequent work demonstrated that WC-1 and WC-2 mutants, are also clock mutants (Crosthwaite et al., 1997). Based on this experience, any light input mutant is potentially of interest to understand mechanisms of circadian rhythms in *Neurospora*.

Mutants called *riboflavin1* and *2* (*rib1* and *rib2*) exhibit reduced sensitivity for photosuppression of conidial banding due to flavin deficiency. This was the first evidence for the participation of flavin species in light reception in *Neurospora*.

1.5.4 The *Neurospora* genome suggests additional photoreceptors

The *Neurospora* genome is sequenced, annotated and available at: http://www-genome.wi.mit.edu/annotation/fungi/*Neurospora*/. It provides additional photoreceptor candidates, in addition to WC-1 and WC-2.

A protein with high homology to bacteriorhodopsin was identified (Bieszke et al., 1999a; Bieszke et al., 1999b). NOP-1 binds retinal and forms photochemically active pigment (Brown et al., 2001) but the physiological function of this fungal opsin is still not known.

The genome sequence also reveals a *cryptochrome* homologue and two homologues of bacterial phytochromes. Also, a homolog of the *Aspergillus nidulans* gene *velvet*, is present in *Neurospora*. In *Aspergillus*, this gene is involved in both red and blue signal transduction (Yager et al., 1998). The presence of three genes, which might be

involved in red light photoreception is surprising given that red light responses have not been described in *Neurospora* to date. These putative photoreceptors suggest a complexity of photobiology that has not yet been recognized in *Neurospora*.

1.6 Action spectra analysis

One of the experimental approaches to examine the nature of a photoreceptor molecule is the construction of action spectra. An action spectrum shows how much light of a given wavelength is required to obtain a given response. The level of response at a certain wavelength reflects the ability of the photoreceptor to absorb light at that wavelength. Thus, the action spectrum of a response represents the absorption spectrum of the photoreceptor molecule. Action spectra for different light regulated responses were made and all of them indicate that *Neurospora* receives near ultraviolet (UVA) and blue light (De Fabo et al., 1976; Dharmananda, 1980; Froehlich et al., 2002; Sargent and Briggs, 1967). Some of these action spectra are redrawn and shown in figure 8. For all of them, no wavelengths longer than 520 nm could stimulate any response. All of them show a maximum of activity at around 460 nm with sensitivity extending in the UVA region. This kind of action spectra indicates involvement of flavins or carotenoids as chromophores. However, photoreception in *N. crassa* is probably not based on carotenoids, because a triple albino mutant (*al-1*, *al-2*, *al-3*) which contains less then 0.5% of *wt* carotenoids exhibit normal sensitivity for other light responses (Russo, 1988). These findings taken together with decreased light sensitivity in mutants deficient in biosynthesis of riboflavin indicate flavin species as the best candidates for *Neurospora* photoreceptor chromophore.

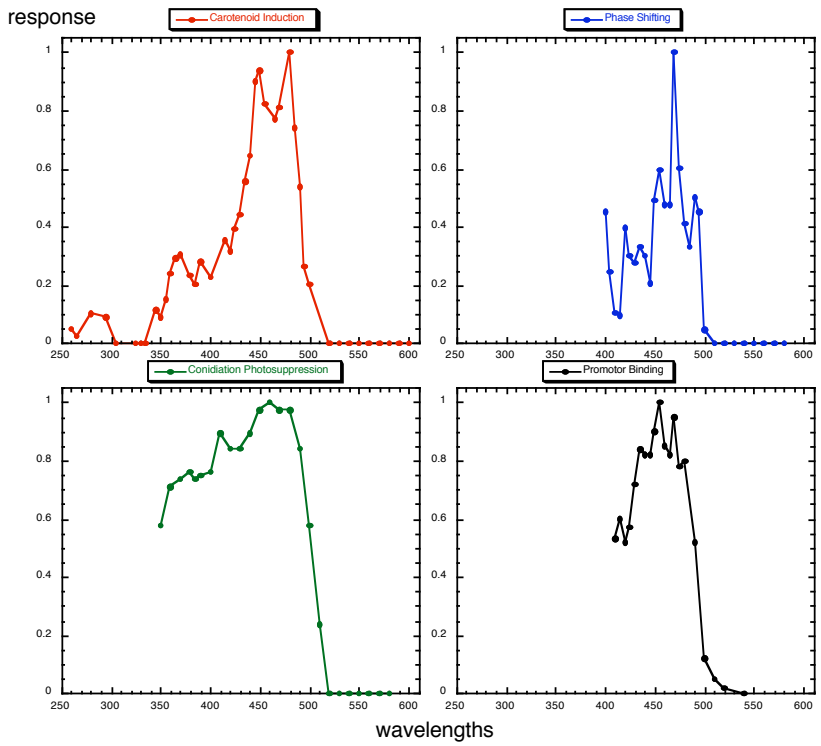

Figure 8. *Neurospora* is primarily sensitive to blue light. Published action spectra of different physiological and molecular light responses: (**A**) For the synthesis of mycelial carotenoids (De Fabo et al., 1976); (**B**) For the phase shifting of the free-running conidiation rhythm (Dharmananda, 1980); (**C**) For the photosuppression of self-sustained rhythmicity in conidial band formation (Sargent and Briggs, 1967); (**D**) For the *in vitro* light induced binding of the WC-1 protein to the promotor of the *frq* gene (Froehlich et al., 2003).

1.7 Molecular studies of the photoreception in *Neurospora*

1.7.1 White Collars

The White Collars (WC) proteins transduce the light signal, in part, by binding to light-regulated promoters and allowing transcription (Ballario et al., 1996; Linden and Macino, 1997). Functional links between light and circadian pathways are evidenced by the loss of circadian qualities (such as the ability to free-run using standard conditions) without either WC-1 or WC-2, on one hand, and the absence of light-regulated conidial band formation without FRQ, on the other (Chang and Nakashima, 1997; Lakin-Thomas and

Brody, 2000; Merrow et al., 1999). WC-1 and WC-2 form complexes with each other and with a FRQ protein (Fig. 9; Denault et al., 2001; Merrow et al., 2001; Talora et al., 1999).

The WC-1 protein contains a flavin binding motif called the light-oxygen-voltage domain (LOV) (Christie et al., 1999; He et al., 2002). WC-1 mutants with a deleted LOV domain have lost light induction of FRQ and the other light inducible genes (He et al., 2002; Lee et al., 2003). WC-1/WC-2 complex (WCC complex) purified from *Neurospora* tissue is associated with FAD suggesting that FAD binds *in vivo* to WC-1.

It has been also shown that the WC complex binds the promoter of the *frq* gene in a light dependent manner (Froehlich et al., 2002). Characterization of the binding according to light intensity and spectral qualities has shown good correlation with the spectral sensitivity of the circadian system (Fig. 8). These findings indicate that the WC-1 flavoprotein is a circadian photoreceptor in *Neurospora crassa*.

1.7.2 FRQ protein

Under free running conditions, *frq* mRNA and FRQ protein cycle in abundance, with a circadian period. The transcript peaks in the subjective mid-morning, with the FRQ protein lagging behind four to six hours (Garceau et al., 1997). *frq* expression is regulated through transcriptional and posttranscriptional control mechanisms: transcription is positively regulated by WC-1 and WC-2 proteins and the FRQ protein feeds back negatively on its own transcription (Aronson et al., 1994b; Crosthwaite et al., 1997). Nuclear localization of FRQ is essential for rhythmicity. FRQ enters the nucleus as it is made and represses accumulation of *frq* mRNA (Luo et al., 1998). Non-coding DNA strand of *frq* gene gets transcribed to, so called, antisense RNA. The full length, antisense transcript influences the timing of conidiation (Kramer et al., 2003).

FRQ is progressively phosphorylated throughout the day. Inhibition of phosphorylation results in a decreased rate of FRQ turnover and increases period length (Liu et al., 2000). Several kinases regulate stability of the FRQ protein and free-running period length (Görl et al., 2001; Liu et al., 2000; Yang et al., 2002). *frq* mRNA and protein are rapidly induced by light (Ballario et al., 1996; Crosthwaite et al., 1995). In

FRQ deficient mutants light entrainment of conidiation fails, indicating additional role for FRQ in the light input pathway (Merrow et al., 1999 and 2003).

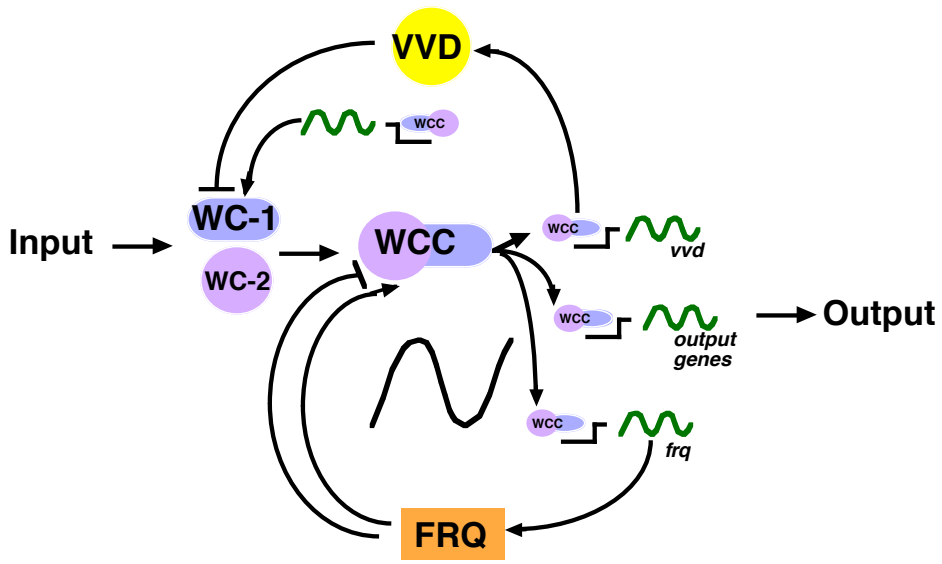

Figure 9. The molecular circadian clock mechanism in *Neurospora crassa*. FRQ, WC-1, WC-2, *vvd* and their gene products form interconnected transcription/translation feedback loops essential for circadian rhythmicity. The *Neurospora* rhythm generator receives light signals through the WHITE COLLAR protein complex (WCC), which increases *frq* transcription and resets the clock (details in text; redrawn from (Heintzen et al., 2001).

1.7.3 Resetting of the *Neurospora* clock by light

Transcriptional activation of *frq* and subsequent FRQ protein synthesis resets the *Neurospora* clock (Crosthwaite et al., 1995). A pulse of light given in the subjective morning (when *frq* mRNA levels are rising) advances the phase of the rhythm, whereas a pulse of light given late in the day (when *frq* mRNA level are falling) results in a phase delay. A saturating pulse of light given at any time of the subjective day increases *frq* mRNA and FRQ protein to maximal level and resets the circadian phase to mid-morning.

Another protein, WC-2 has an important role for circadian photoreception in *Neurospora*. WC-1 and WC-2 are transcription factors with a zinc-finger DNA binding domain (Ballario et al., 1996; Linden and Macino, 1997). WC-1 and WC-2 form a white

collar protein complex (WCC; Fig. 9), by hetero-dimerization via PER-ARNT-SIM (PAS) domains. A WCC is present both in dark and in light but after light induction, both WC-1 and WC-2 are phosphorylated. In constant light WC-1 is transiently phosphorylated in contrast to WC-2 which appears to be constitutively phosphorylated (Schwerdtfeger and Linden, 2001; Talora et al., 1999). Results by Froehlich et al. (2002) have shown that WCC binds to the *frq* promoter in both light and dark, and following light exposure it activates transcription. Light-dependent phosphorylation of WC-1 and the induction of light regulated genes correlates (Schwerdtfeger and Linden, 2001; Talora et al., 1999), indicating that the WCC transition from inactive to transcriptionally active form occurs most likely via the process of phosphorylation.

1.7.4 Photoadaptation and circadian photoreception

Photoadaptation is a process in which the initial response to light is downregulated over a time. This phenomenon is well known for visual photoreception (Zigmond, 1999). In higher plants, photoadaptation in the phytochrome signaling pathway have been described, but none of the regulatory components has been found (Bowler et al., 1994). In *Neurospora*, adaptation of light regulated genes under constant illumination is well documented (Arpaia et al., 1993, 1999; Lauter and Yanofsky, 1993; Talora et al., 1999). Work on the *vivid* (*vvd*) mutant provides deeper insights into the mechanism of photoadaptation. The *vvd* mutant was identified because of its bright orange color, indicating a defect in light regulation of carotenogenesis (Perkins et al., 1997; Perkins et al., 1982a).

The VVD protein contains a PAS domain and thus has similarity to other proteins involved in light reception and regulation of circadian rhythmicity. *vvd* mRNA and protein are rapidly and transiently induced by light and VVD protein down regulates its own transcription levels (Heintzen et al., 2001). In continuous light the *vvd* mutant exhibits sustained expression of light regulated genes and constitutive phosphorylation of WC-1 (Heintzen et al., 2001; Schwerdtfeger and Linden, 2001; Shrode et al., 2001). Given that the *vvd* knock-out mutant retains self-sustained rhythmicity (free-running period remains the same 23.5 h) VVD cannot be considered as element of the rhythm generator. However, PRC analysis revealed that loss of VVD alters the phase of

entrainment of the clock; conidiation rhythms are delayed up to 4 h as compared to wild-type. Thus functional photoadaptation mechanism is not critical for circadian photorecption but it is involved in determining circadian phase.

1.8 Open questions

Despite the progress in understanding light signal transduction in *Neurospora*, many issues about the molecular mechanism of circadian photoreception remain unanswered. The previously described lack of light-regulated conidiation indicates an important role for the *frq* in the light signal transduction mechanism. This finding opens the question how the FRQ protein, as a clock element, impacts on the light input pathway.

The *wc-1* and *wc-2* mutants failed to show all known light-induced physiological responses. Therefore, *wc-1* and *wc-2* were suggested to have critical role in light signal transduction. Interestingly, *wc-1* and *wc-2* are also required for self-sustained circadian rhythmicity. But the question how the *wc-1* and *wc-2* gene products fulfill these complex functions remains open.

2 RESULTS

2.1 Molecular and genetic regulation of the light input pathway in *Neurospora crassa*

The *wc-1* and *wc-2* genes are required for *Neurospora* light responses (Ballario and Macino, 1997; Linden and Macino, 1997; Talora et al., 1999) including the light induction of the *frq* RNA. FRQ protein (FRQ) has been established as central component of the rhythm generator (Dunlap, 1999). However FRQ deficient strains are entrainable in temperature cycles, whereas light entrainment fails (Merrow et al., 1999). This finding indicates an additional role for FRQ in the light input pathway to regulation of conidiation. In order to understand how light signaling functions in *Neurospora, wc-1* and *frq* and their regulation were studied.

2.1.1 Rhythmicity in DD: FRQ and WC-1

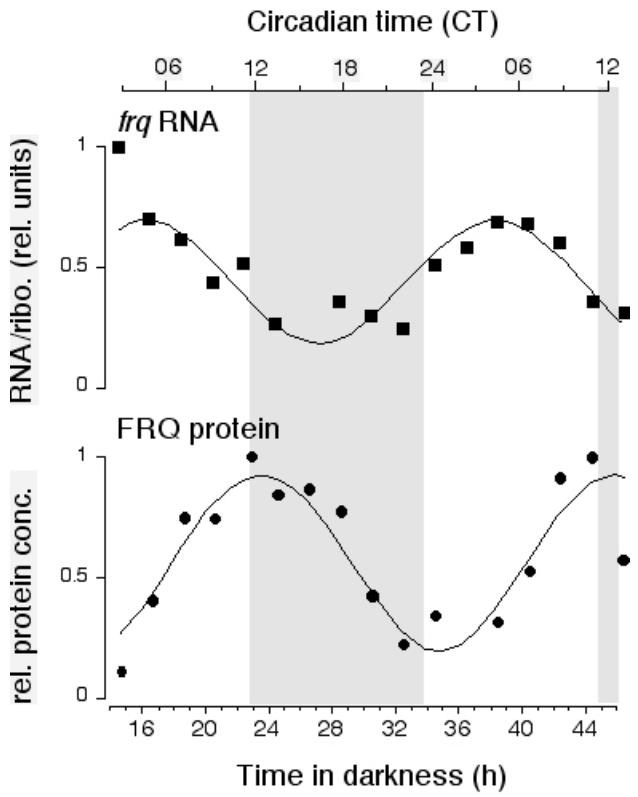

Figure 10. *frq* RNA and protein are rhythmic in constant darkness with a circa 24h period. Samples were harvested at 2 h intervals from cultures grown in darkness at 25 °C. Specific RNA signals were normalized to ribosomal RNA to determine relative units (rel. units). Specific protein signals were normalized to amido-black stained blots to yield relative protein concentration (rel. protein conc.). In these rhythmic time series, the highest value was set to 1. See Methods section for curve fits. The initial light to dark transfer of the tissue corresponds to dusk and is designated circadian time (CT) 12. See Methods section for determination of CT. Gray areas indicate subjective night and open areas subjective day (Aronson et al., 1994b; Garceau et al., 1997; as published in Merrow et al. 2001).

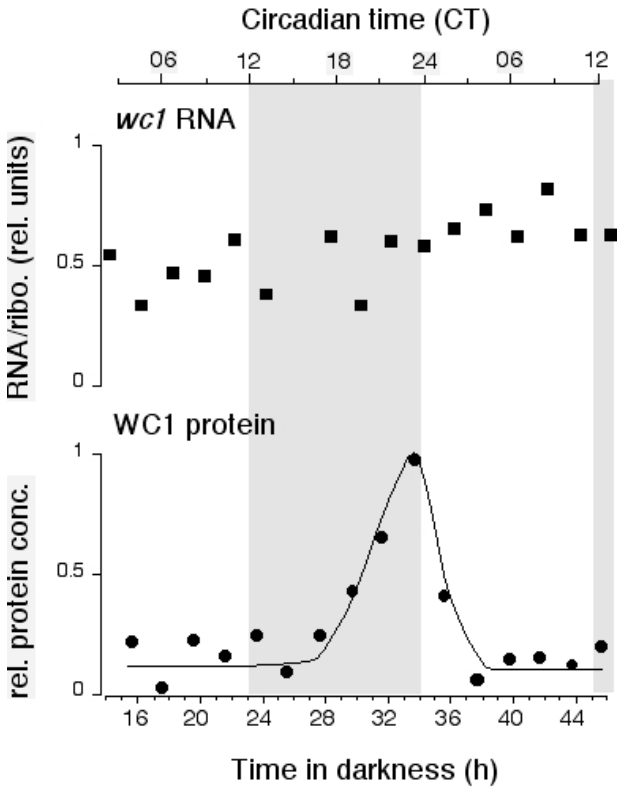

Figure 11. WC-1 protein is rhythmic in constant darkness. Samples were harvested at 2h intervals. Specific RNA signals were normalized to ribosomal RNA and presented as relative units (RNA/ribo. relative units). Specific protein signals were normalized to amido black stained blots to yield relative protein concentration (rel. protein conc.). The average value was set equal to 0.5 in the top panel and 1.0 in the bottom one. See Methods section for curve fit. The initial light to dark transfer of the tissue corresponds to dusk and is designated circadian time (CT) 12. Gray areas indicate subjective nigh; open areas, subjective day. Arhythmic RNA givies rise to rhythmic protein (Lee et al., 2000; as published in Merrow at al. 2001).

frq RNA and protein are rhythmic in constant darkness (DD) (Aronson et al., 1994b; Garceau et al., 1997). The period of the oscillation is about 24 h. If the phase of the molecular oscillation is shifted (with light and temperature) the phase of the conidiation rhythm also changes (Fig. 10; Crosthwaite et al., 1995).

wc-1 RNA and protein (WC-1) levels are analyzed under the same conditions. The RNA levels of *wc-1* were variable, but not circadianly regulated (Fig. 11; Lee et al., 2000). WC–1 protein levels, however, changed with circadian time (Fig. 11). The phase of the oscillations for FRQ and WC-1 (Fig. 10 and 11) is different by 12 h (half of the

period). Maximum WC–1 levels coincide with the FRQ minimum. The differences between *frq* and *wc–1* RNA and protein profiles in constant conditions show that their regulation is distinct.

The observation that variable but circadianly regulated *wc-1* transcript levels give rise to rhythmic WC-1 protein indicates posttranscriptional regulation of *wc-1* expression (see section 2.2 for further investigation of this observation).

2.1.2 Regulation of *frq* and *wc-1* is interdependent: WC-1 regulates *frq* and FRQ regulates *wc-1*

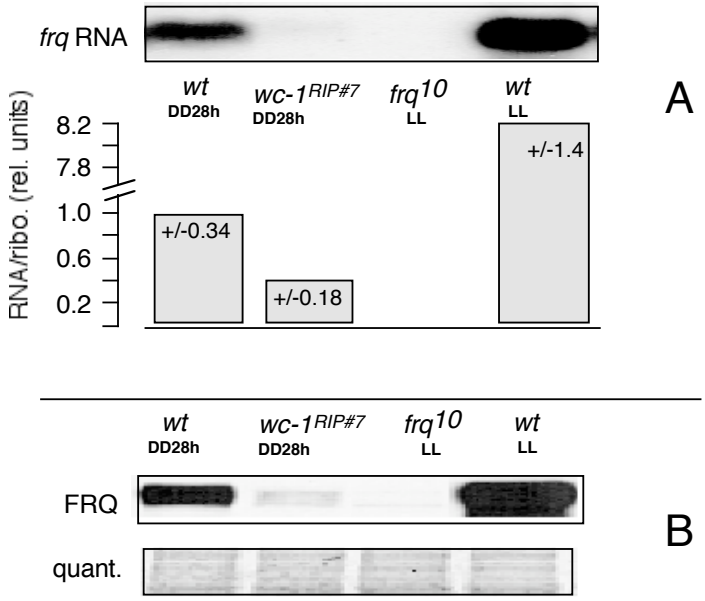

Figure 12. WC-1 protein regulates the expression of *frq*. Mycelial pads from *wt*, *wc-1*$^{RIP\#7}$, *frq*^{10} and *frq*^{9} were incubated in darkness for 28h and then RNA and protein extracts were prepared. (**A**) *frq* RNA was detected by Northern-blotting (upper panel), quantified and normalized (lower panel) to ribosomal RNA levels. The columns in the graphs represent averages of four experiments (S.D. are given at the top of each bar). The controls *frq*^{10} and *frq*^{9} show no *frq* RNA or elevated levels respectively. (**B**) FRQ protein is reduced in *wc-1*$^{RIP\#7}$. FRQ protein was detected by Western-blotting. To control for equal loading of the gel, the membrane was stained with amido black (lower panel). The controls, *frq*^{10} and *wt*, were cultured in LL (constant light) and show either no FRQ protein or elevated levels, respectively (Crosthwaite et al., 1997; as published in Merrow at al. 2001).

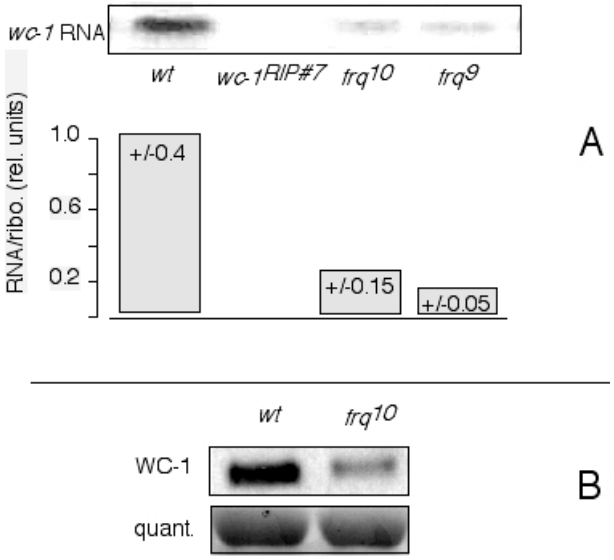

Figure 13. FRQ protein regulates expression of *wc-1*. Mycelial pads from *wt, frq*^{10} and *frq*^{9} were incubated in darkness for 28h and then RNA and protein extracts were prepared. (**A**) *wc-1* RNA was detected by Northern-blotting (upper panel), quantified and normalized (lower panel) to ribosomal RNA levels. The columns in the graphs represent averages of four experiments (S.D. are given at the top of each bar). The control *wc–1* $^{rip\#7}$ shows no *wc-1* RNA. (**B**) WC-1 protein is reduced in *frq*^{10} (Also published in (Lee et al., 2000). WC-1 protein was detected by Western-blotting. To control for equal loading of the gel, the membrane was processed as described in Fig. 12. The control *wt* shows the level of WC-1 protein at DD 28 (as published in Merrow at al. 2001).

To elucidate the role of FRQ in light entrainment of circadian rhythms, its expression is analyzed in *white collar* mutants. It was already known that *frq* mRNA and protein levels are low in *wc–1* and *wc–2* mutants (Crosthwaite et al., 1997). Here, this finding is confirmed with a *wc–1*$^{RIP\#7}$ strain (see also methods section for strain description). In DD, *frq* RNA and FRQ levels were substantially lower in *wc–1*$^{RIP\#7}$ than in a *wt* strain (Fig. 12). Subsequently, Froehlich et al. (2002) and all showed direct binding of WC-1 to the FRQ promoter. These observations show that expression of *frq* is under control of the WC–1 protein.

wc–1 RNA levels are determined in *frq*^{10} (a *frq* knock-out strain, see Materials and Methods for description), showing levels lower than those normally observed in *wt* grown in DD; WC–1 protein levels were similarly reduced (Fig. 13) (Lee et al., 2000). Thus, FRQ is required to maintain DD levels of *wc–1* mRNA and WC-1 protein.

In *Drosophila,* activators of clock genes depend on 'downstream' gene products for their expression (Bae et al., 1998; Glossop et al., 1999). The positive effects of FRQ on *wc-1* expression plus rhythmicity of WC–1 (Lee et al., 2000) suggest a similar interdependent regulation between *frq* and the *wc* genes and gene products.

2.1.3 *frq* and the light signaling pathway

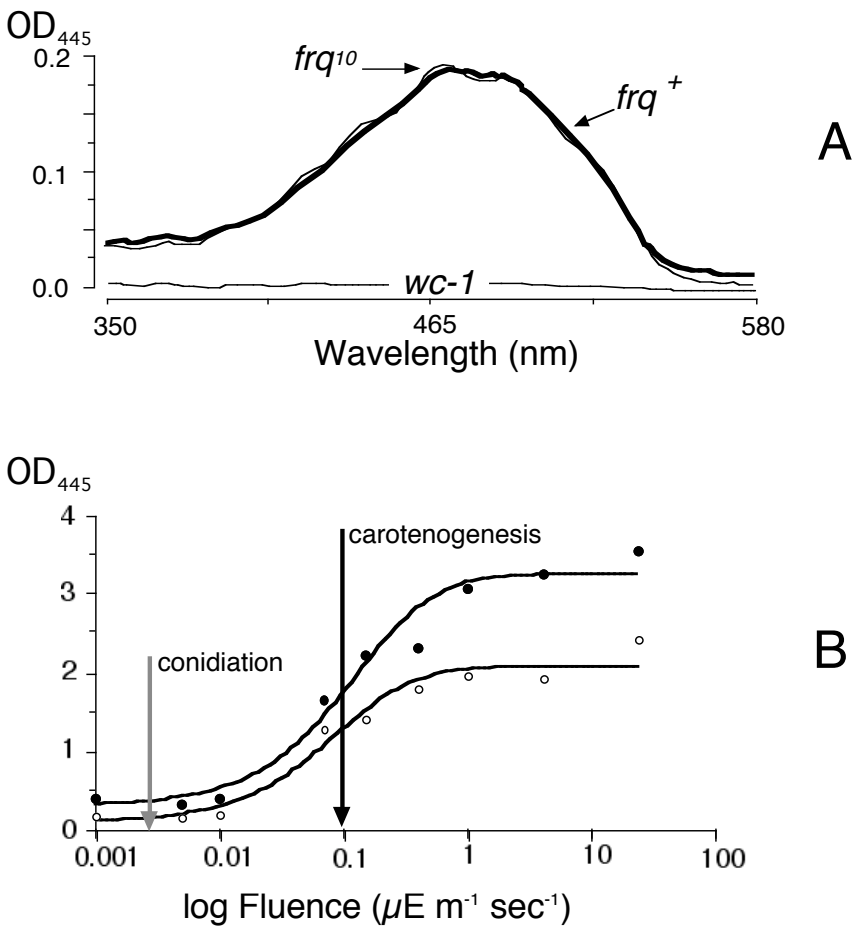

Figure 14. Carotenoids are light-induced in the *frq* knockout mutant, but the overall levels are lower. (**A**) The absorption spectrum of carotenoid extracts in frq^{10} and *wt* are the same. Carotenoids were induced in *wt* (thick line), frq^{10} (thin line), and $wc\text{-}1^{RIP\#7}$ with 4 μE $m^{-2}sec^{-1}$ of light for 5 h. Light dependent carotenogenesis is entirely absent in $wc\text{-}1^{RIP\#7}$ mutant but remained qualitatively intact in frq^{10} mutant. The wt extract was diluted twofold relative to the other samples. (**B**) Light induction of carotenoids was compared in frq^{10} and *wt* by titrating fluence. The fluence sensitivity for carotenogenesis is independent of FRQ protein but overall levels are lower. The black arrow indicates fluence rate at which half-maximal light induction of carotenoids occurs for both strains. For comparison, the gray arrow indicates the fluence threshold for light dependent conidial band formation in *wt* (Merrow et al., 1999; Roenneberg and Merrow, 2001; as published in Merrow et al., 2001).

No light impairments have been described for FRQ deficient mutants prior to the reports showing that they failu to synchronize to LD cycles (Lakin-Thomas and Brody, 2000; Merrow et al., 1999). To further understand the blindness of *frq* mutants molecular and physiological readouts were used.

Light induced mycelial carotenogenesis (De Fabo et al., 1976) was used to determine if frq^{10} shows a deficiency in light responsiveness at the level of another light regulated output. Fig. 14A shows that this light response remained qualitatively intact in frq^{10}: the absorption spectrum of hexane extracted, light induced tissue was the same in frq^{10} and in *wt*. Note that light dependent carotenoid synthesis is entirely absent in the *wc–1* mutants (Harding and Turner, 1981; Linden et al., 1999).

When fluence response curves for light induction of carotenogenesis in *wt* and frq^{10} were compared, the amplitude of the saturation response in frq^{10} was about half that of *wt* (Fig. 14B). The sensitivity of both strains (fluence rate at half-maximal response, black arrow) was, however, identical, suggesting that the same photoreceptor regulates carotenogenesis in both *wt* and frq^{10}.

frq mutants are unresponsive to light at the conidiation level but their blindness is selective because they do produce light–induced carotenoids. This indicates a bifurcation in the *Neurospora* light input pathway at genetic level, which reflects either existence of distinct photoreceptors or branching of signaling pathways. A bifuraction in the light input pathway is also supported by fluence titration of conidiation and carotenogenesis as readouts: conidia formation is regulated by light at levels of 2-5 $nE/m^2/s$ (gray arrow, Fig. 14B; Sargent and Briggs, 1967), whereas light induction of carotenogenesis needs ~20X more (black arrow, Fig. 14B). For this case, two distinct photoreceptor can be hypothesized.

2.1.4 Circadian regulation of light signaling

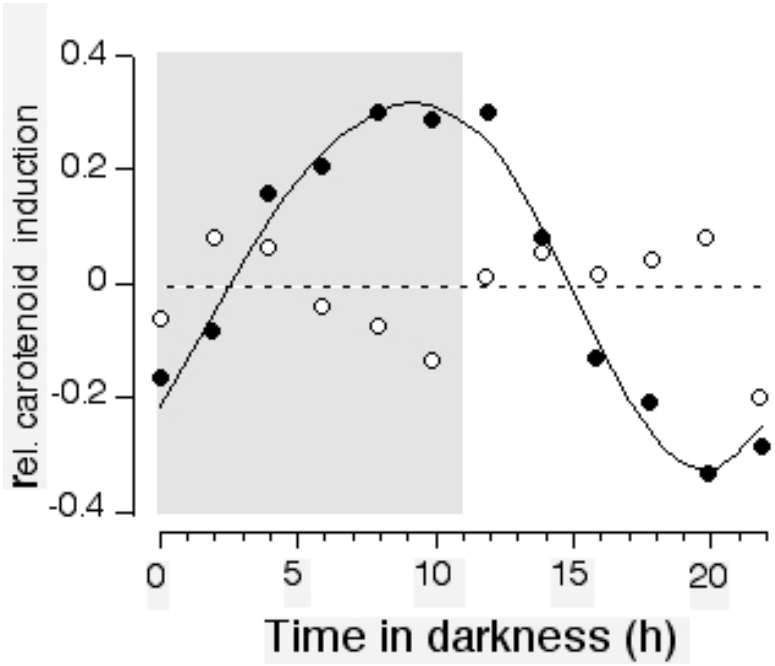

Figure 15. The amplitude of light-induced carotenogenesis is circadianly regulated. *wt* (filled circles) and *frq*^{10} (open circles) mycelia were transferred from light to dark. After the indicated time in darkness, samples were exposed to light for 5 h to induce carotenogenesis. Gray areas indicate subjective night and open areas are subjective day (as published in Merrow at al., 2001).

It is shown that WC-1 levels change over time in constant dark conditions (Fig. 11). To test if the level of WC-1 influences light-responses over the course of a day, the amplitude of light induced carotenogenesis was determined at different circadian times. Increased amount of carotenoids were light induced at the end of the subjective night compare to the subjective day. Notably, the circadian modulation of light induced of carotenogenesis is absent in *frq*^{10} (Fig. 15). This finding indicates that light-dependent accumulation of carotenoids is regulated by the circadian system.

2.2 Posttranscriptional control of *wc-1* expression

Some molecular components of the *Neurospora* clock and light input pathway oscillate with a circa 24 h period (Fig. 10 and 11). Both *frq* mRNA and FRQ protein are rhythmic in constant darkness. Under the same conditions, although *wc-1* mRNA levels are variable, they do not oscillate with a circadian period. However WC-1 protein shows circadian regulation (Fig. 11; Lee et al., 2000). It is known that eukaryotic mRNAs can interact with proteins that stimulate or inhibit its expression in the cytoplasm (Dreyfuss et al., 1996; Stripecke et al., 1994). This suggests a posttranscriptional regulatory process that might also be involved in regulation of WC-1 expression.

2.2.1 Identification of putative protein binding sites in *wc-1* UTRs

A ccatgggttaagcaacgacacccacggtccctcaatgtgatcacccgacccggcccttcctggcgcaccacctttagcacacctat
actacgaccaaatcctaaga**agagaggagagagaggagagagaggagagagagagagag**cttcttagctaagagc
ttgtttctattgtcaacccattacgaatcgcttggggcgaccgatgcagccaccatg

B agagagaggagagagaggagagagaggagagagagagagag

C tgcctgcagtggaagtcggtgaccatactgacccccagcaacaactacaagatcaaggcccgctgtcagactcataggctggg
acaacaacaacaaaaacaacaacaacaacaagaaggagaacaacaacaacacaaagaacatagtagtacgagtcta
ccgtcccagaggcaacggttacac

D caacaacaacaaaaacaacaacaacaacaa

Figure 16. Inspection of 3' and 5' *wc-1* UTRs suggests translational regulatory binding sites. (**A**) Sequence of cloned fragment from 5' UTR region of *wc-1* mRNA used as a probe for gel shift assay. Predicted binding site is in bold print and underlined. (**B**) The sequence of the predicted binding site. Inspection reveals nanomer repeats. (**C**) Sequence from the 3' UTR region of *wc-1* mRNA used as a probe for mobility gel shift assay. The predicted binding site is bold and underlined. (**D**) The putative binding site from the 3' UTR contains triplet tandem repeats.

Fragments in the 5' or 3' UTR which contain repetitive elements are potential targets for RNA-binding proteins involved in translational regulation or mRNA-stability control respectively (Casey et al., 1988; Dandekar and Hentze, 1995; Ostareck-Lederer et al.,

1994). Sequence analysis of 5' and 3' untranslated regions (UTRs) of *wc-1* mRNA revealed several repetitive elements (Fig. 16A, C). *wc-1* mRNA has four tandem-repeats of a slightly varied nonamer motif in its 5'-UTR (Fig. 16 A, B) and B). Furthermore, in the 3'-UTR there are nine tandem-repeats of a short, pyrimidine-rich, motif (Fig. 16 B and C). To detect RNA-binding protein complexes specific for *wc-1* 5' or 3' UTR, a RNA gel shift assay is established. Putative protein-binding sites with flanking regions were cloned into pBSK II (Fig. 16 A, C) and these plasmids are used to produce the ^{32}P labeled RNA probes (see Methods section).

2.2.2 Proteins bind to 5' and 3' UTRs of *wc-1* mRNA

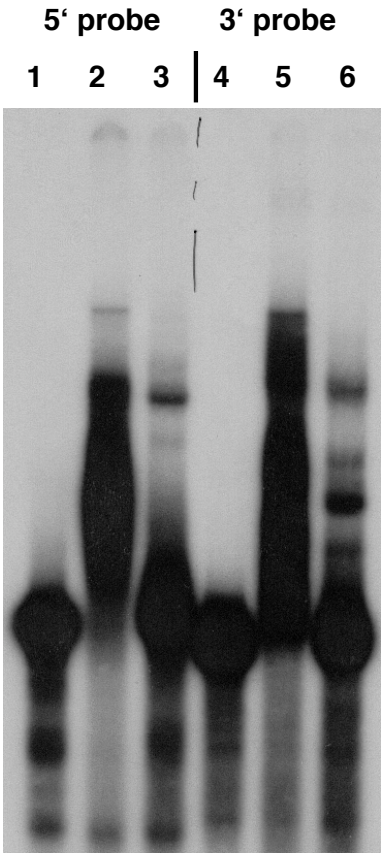

Figure 17. Gel shift analysis of 5' and 3' *wc-1* UTRs reveals RNA binding proteins. *Neurospora* protein extracts were examined for binding to ^{32}P labeled 5' or 3' UTR of *wc-1* mRNA. Radioactively labeled controls (no protein extract) run without shifting (lanes 1 and 4). Radioactive probe incubated with protein extracts in lanes 2 and 5 indicate the formation of numerous RNA-protein complexes. Addition of high amounts of nonspecific competitor (polyG) prevented the formation of the majority, but not all, of the complexes (lanes 3 and 6). This indicates that some proteins bind specifically to the RNA probes.

Extracts from light grown mycelial tissue were examined for the presence of proteins capable of binding the 5' UTR and 3' UTR probes (Fig. 17). Control reactions (Fig. 17, lanes 1 and 4) contain only ^{32}P-labeled 5'UTR and 3'UTR RNA probe, respectively. Both controls show no formation of high molecular weight complexes.When ^{32}P-labeled RNA 5' or 3'probes is co-incubated with the protein extracts from light grown mycelia (Fig.

17, lanes 2 and 5), all of the RNA probe present in these reactions is shifted to a higher molecular weight. The addition of unlabeled competitor, polyguanilic acid (polyG), prevented the formation of some but not all of the complexes (Fig. 17, lanes 3 and 6). This indicates that some of the observed complexes represent nonspecific reactions, whereas others appear to have specificity for the 5'UTR and 3'UTR sequences. Identification of complexes insensitive to competition with nonspecific inhibitor suggests that this assay is good tool to further characterize the specificity of RNA-protein interactions.

2.2.3 Examining specificity of protein-UTR complexes

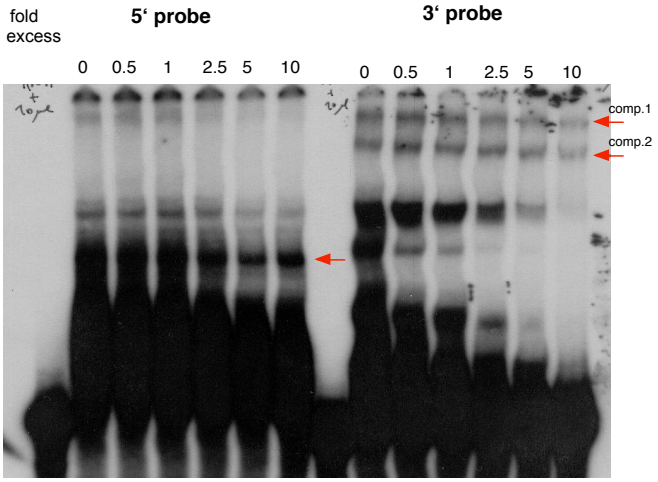

Figure 18. RNA-protein complexes show a high level of specificity. The specificity of UTR-protein complex formation was examined by including an increasing amount of non-specific cold RNA in the binding reactions. The fold of excess of cold competitor is given above each lane. The red arrows indicate complexes resistant to "cooling" with nonspecific RNA, i.e. these complexes represent specific interaction using the 5' UTR. It is possible to see one specific complex (arrow). With the 3' UTR, two complexes are noted (comp. 1 and comp. 2)

The specificity of the protein interactions with the 3' and 5' UTRs of *wc-1* RNA is further examined by including increasing amounts of nonspecific cold RNA in the binding reactions (Fig. 18). The reactions contain protein extract, ^{32}P-labeled RNA 5' or 3' probes, polyguanilic acid and increasing amounts of unlabeled nonspecific RNA.

Some RNA-protein complexes are more resistant to competition than others, indicating their higher specificity. Using the 5' UTR, one RNA-protein complex detected (Fig. 18). Within the 3' UTR, two RNA-protein complexes are seen (Fig. 18): the slower migrating complex is named complex 1 (comp. 1) and faster migrating complex 2 (comp. 2).

All three complexes are resistant to a 10 fold molar excess of cold nonspecific RNA what suggests their high specificity.

2.2.4 Circadian regulation of complex formation is not observable

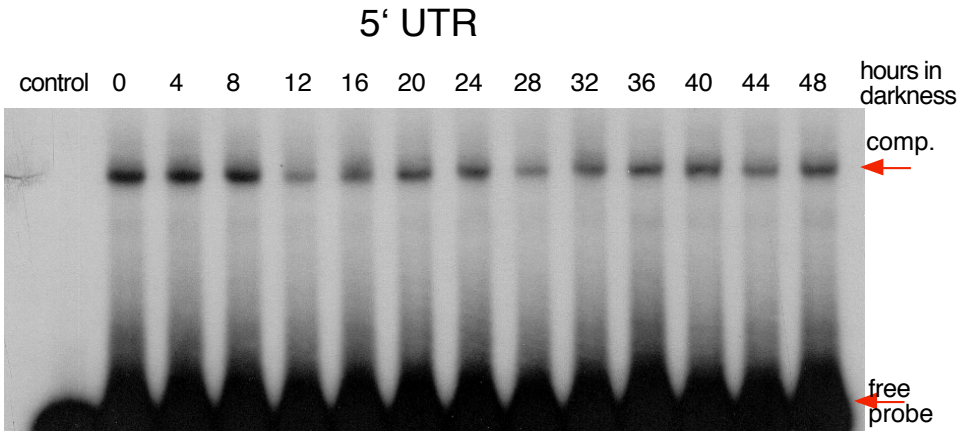

Figure 19. Complex formation in the 5' UTR is not regulated by the circadian system. A circadian time course of 5'UTR complex formation is shown. For the gel shift assay, cell extracts were prepared from age–matched mycelial pads, inoculated and grown for one day in the light and the transferred to darkness. Tissue was harvested in darkness at the time points indicated above each lane. The first lane (control) was loaded only with unbound RNA probe (lower red arrow). The upper arrow indicates the specific RNA-protein complexes.

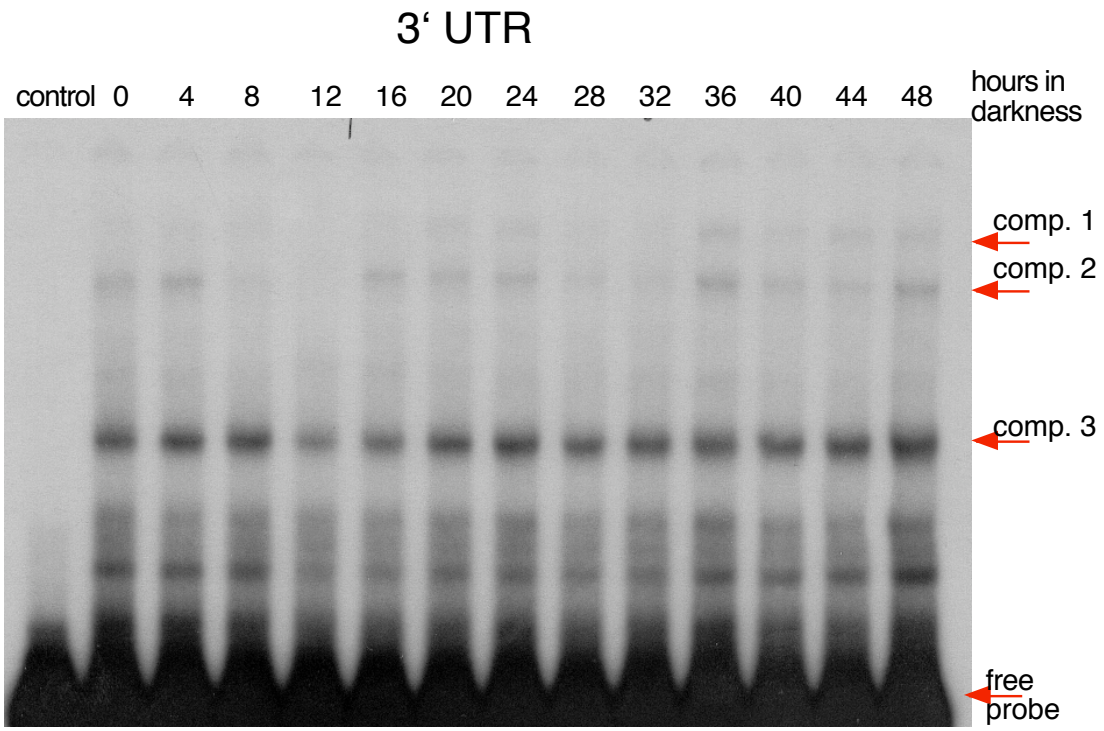

Figure 20. Complex formation in the 3’ UTR is not regulated by the circadian system. Circadian time course of 3’UTR complex formation. Protein extracts were prepared from age matched mycelial pads, which were inoculated and grown for one day in the light and then transferred to darkness. Harvests were done in darkness at the time points indicated above each lane. The first lane (control) was loaded with unbound RNA probe (lower red arrow). Using the 3’ end of *wc-1* mRNA it is possible to detect three complexes (comp. 1, comp. 2 and comp. 3, indicated with arrows).

The finding that constant *wc-1* mRNA gives rise to the circadianly rhythmic protein indicates posttranscriptional regulation. Identification of specific *wc-1* mRNA-binding proteins suggests their involvement in this regulation. One regulatory mechanism could be circadianly regulated RNA binding. To evaluate this, it was tested whether the complex formation of the 5’ and 3’ UTR is circadianly rhythmic. Protein extracts were prepared from mycelial pads, inoculated and grown for one day in constant light and then transferred to darkness. Samples were harvested at 4 h intervals. The entire circadian time course represents two days. To enhance specific complex formation in the binding reaction, a 100-fold molar excess of nonspecific competitor (polyG) was added. The control lane was loaded with only radioactive probe and nonspecific competitor. The

amount of 5' UTR radioactive probe shifted to high molecular weight complexes is variable but the pattern is not clearly circadian (Fig. 19). The same protein extracts were used to examine 3' UTR complex formation. In this case, it is also not possible to detect circadian regulation of complexes (Fig. 20). These data suggest that the circadian translation regulation does not occur through the identified complexes. Subsequently it was shown that protein extracts from dark grown *Neurospora* cultures retain light sensitivity (Froehlich et al., 2002). Ideally, these experiments should have been repeated under the safe lights.

2.2.5 Light regulates UTR complex formation

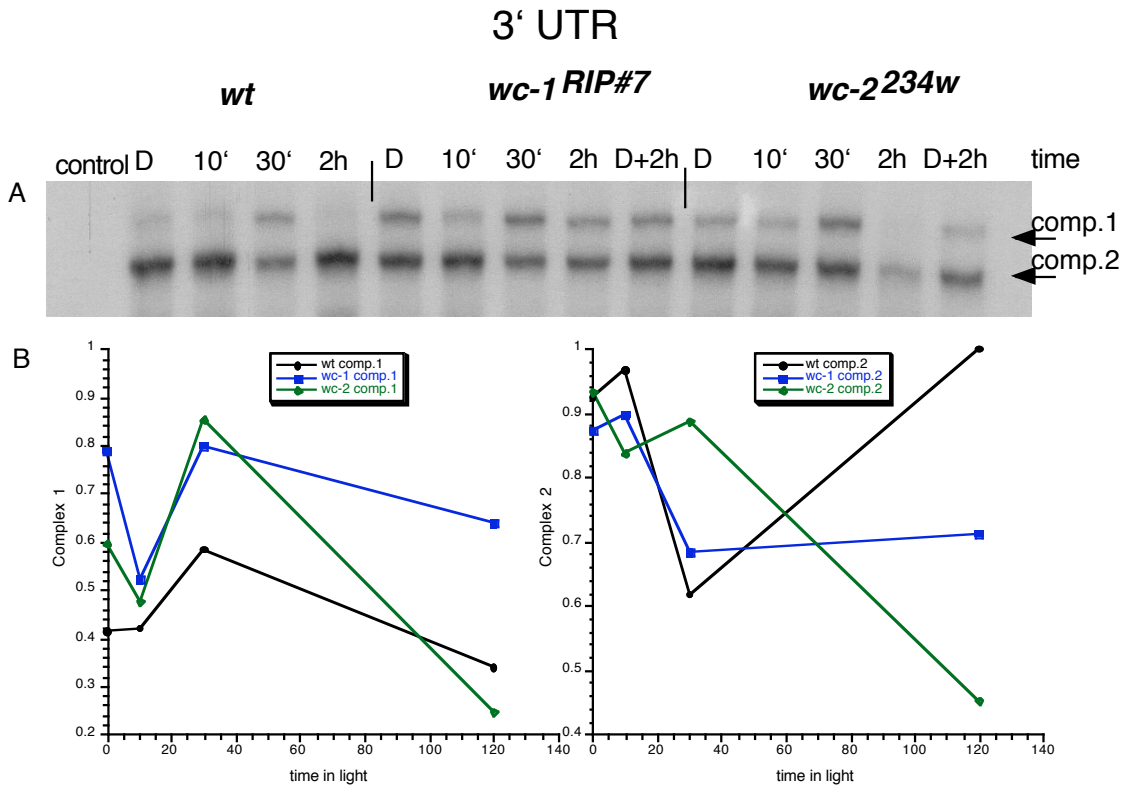

Figure 21. Light regulates formation of the complex at the 3’ UTR of *wc-1* RNA. Gel-shift assay was performed with protein extracts made from mycelial pads which were grown in darkness and then transferred to light. (**A**) Lanes labeled only with D contain proteins extracted from mycelia harvested shortly before lights on. Lanes labeled “D+2h” contain proteins from mycelia incubated for an additional two hours in darkness. Pads were harvested after 10 min, 30 min and 2 h in light. First lane (control) was loaded only with radioactive RNA probe. Three different strains were used *wt*, *wc-1* $^{RIP\#7}$, and *wc-2*^{234w}. (**B**) Quantifications of complex 1 and complex 2 intensities.

Light regulation of 3’ UTR complex formation was also investigated (Fig. 21). For this experiment *wt* strain and the blind strains *wc-1*$^{RIP\#7}$ and *wc-2*^{234w} were used. Mycelial pads were incubated in DD and then exposed to saturating light (20 μE m^{-2}sec^{1}). Samples were harvested over two hours. Control tissue was harvested before lights came on (lane D).

Wc-1 and *wc-2* strains have an additional control, namely a sample that was held in and harvested at the end of the experiment (lane D+2h).

In the *wt* strain, complex 1 in darkness (lane D) and 10 min (lane 10') after lights on is not detectable. After 30 min in light formation of complex 1 is clearly visible and after 2 h the complex is disassociated. This transient profile of complex formation resembles other molecular light responses in *Neurospora* (e.g. transient profile of WC-1 phosphorylation or mRNA induction). Complex 2 is more abundant than complex 1 over entire 2h time course. The minimum of complex 2 formation coincides with the maximum of complex 1, indicating that their regulation is distinct.

Wc strains have different shift-pattern compared to *wt*. Complex 1 and complex 2 are present in both *wc-1* and *wc-2* strains over the entire light induction time course. The amount of probe shifted to complex1 and complex 2 in both *wc-1* and *wc-2* mutants is variable, but not light regulated. This observation suggests that light dependent complex 1 and complex 2 formation is under the control of WC-1 and WC-2 proteins.

2.3 Light-regulated behavior in *white collar* mutants

An important step in characterization of the circadian light input pathway is identification of circadian photoreceptors. Currently there are several candidates. Finding that *frq* mutants fail to synchronize to LD cycles (Merrow et al., 1999) proposes FRQ for this role. *wc* mutants are recognized as blind for all photoresponses on the physiological, as well as on the molecular, level (Arpaia et al., 1993; Crosthwaite et al., 1995; Harding and Turner, 1981). However, assays for light regulated conidiation in *wc* mutants were based only on release from constant light to free-running conditions (Crosthwaite et al., 1997). This assay has limited value because it was performed using standard race tube conditions where the *wc* mutants are arrhythmic. In this study, the *wc* mutants were reinvestigated with a circadian entrainment protocol, which does not require self-sustained rhythmicity.

2.3.1 *white collar* mutants synchronize conidiation in response to light

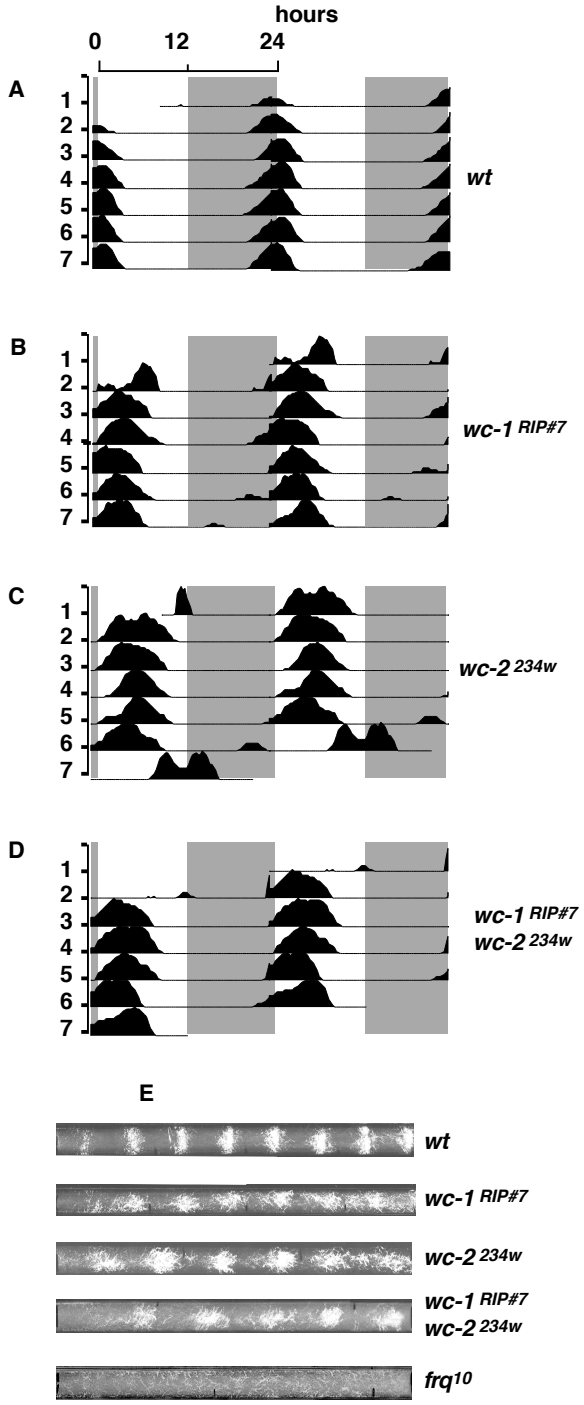

Figure 22. Conidiation in *wc-1* and *wc-2* deficient strains is synchronized in LD cycles. Data from a week of 12:12 LD cycles (12 h light 12 h dark) are double plotted (two days per line, repeating the day graphed on the right side on the left side of the next line down). The dark period is indicated by gray shading. The peaks on the graphs represent consolidation of conidiation, and the corresponding *Neurospora* race tubes are shown in (**E**). A. wild type (*wt*); B. $wc\text{–}1^{RIP\#7}$ (Talora et al., 1999) C. $wc\text{–}2^{234W}$ (Linden & Macino 1997); D. $wc\text{–}1^{RIP\#7}wc\text{–}2^{234W}$ double mutant; E. Race tubes for the above graphs and also for frq^{10} (only a race tube is shown for this strain, as it fails to synchronize conidiation to light'; Merrow et al., 1999). Fluence rates for **A**–**C** are 4 μE m^{-2} sec^{-1}, for D and E, 35 μE m^{-2} sec^{-1}. The race tube shown for wt runs for longer than the 7 days shown on the graph; the loss of synchrony seen in the last day of graph (**C**) reflects early removal of the race tubes from experimental conditions (as published in Dragovic et al. 2002).

In the experiments described here, a robust, light–regulated physiology is seen for both *wc* mutants, with conidia production consolidated to a discrete phase of the LD cycle (Fig. 22B–C), qualitatively similar to the wild type strain (Fig. 22A). In the *wt* the phase angle of conidiation (measured relative to onset of the conidial band) occurs in the middle of the night. The phase of conidiation in the mutant strains is, however, delayed relative to wild type. In $wc\text{–}1^{RIP\#7}$, the onset of conidiation is delayed for ~2.5 h. In $wc\text{–}2^{234W}$, the phase of conidiation is delayed even further, for 3 h.

$Wc\text{–}1^{RIP\#7}$ is blind for most of the same outputs as $wc\text{–}2^{234W}$. Several scenarios accommodate these observations, including the possibility that one or both protein products act as photoreceptors. Given the observation that either of the single mutants can synchronize conidiation to light, a double mutant, $wc\text{–}1^{RIP\#7}wc\text{–}2^{234W}$, was generated and submitted to 24 h LD cycles. Like the single mutants, the double mutant strain consolidates conidia production in the light phase (Fig. 22 D and E), with a phase similar to the single mutants (delayed by 2.8 h relative to *wild type*).

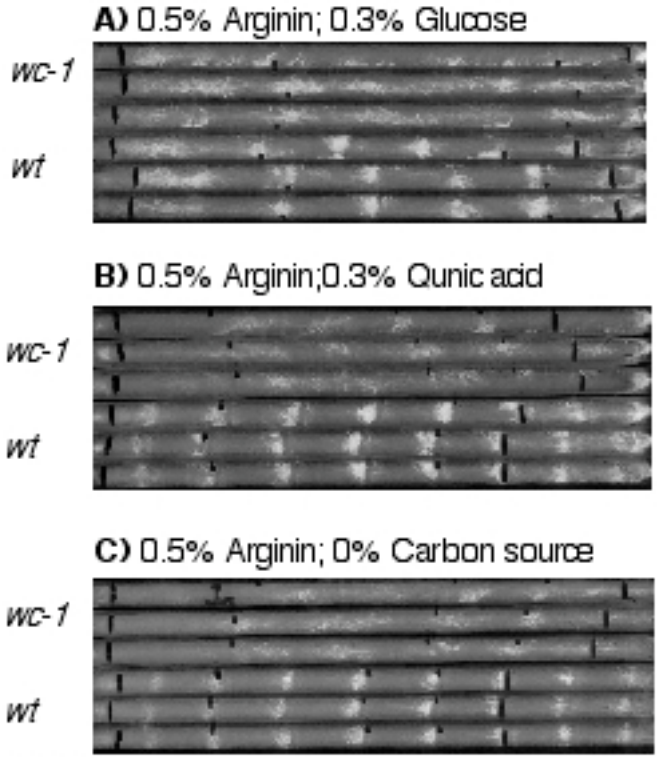

Figure 23. Appearance of conidial bands in different media. Race tubes from a 12:12 LD cycle are shown. Both *wt* and *wc-1*$^{RIP\#7}$ mutant consolidate conidiation in response to L:D cycles on different media. All three media contain 1X Vogel's salts, 0.5% Arginin but the carbon source is different : 0.3% Glucose (**A**), 0.3% Qunic acid (**B**) or no carbon source (**C**).

Nutrition has been shown to play a role in light reception (Nakashima and Fujimura, 1982; Sokolovsky et al., 1992) and clock mutants do not have the nutritional compensation that wild type strains have (Loros and Feldman, 1986). Therefore, several media formulations were compared for appearance of conidial bands in the mutant strains. Media containing either glucose, quinic acid (a carbon source encountered in nature by *Neurospora*) or no carbon source was tested. Although responses to light are clearly seen in cycles run under all three conditions, the bands were clearest on media with quinic acid or with no carbon source (Fig. 23). The bands produced by the mutant strains increase in density over the course of the week–long race tube experiment, similar to what is seen for the free–running rhythm in FRQ–less strains (Loros et al., 1986). Thus, long race tubes were used to improve data acquisition possibilities.

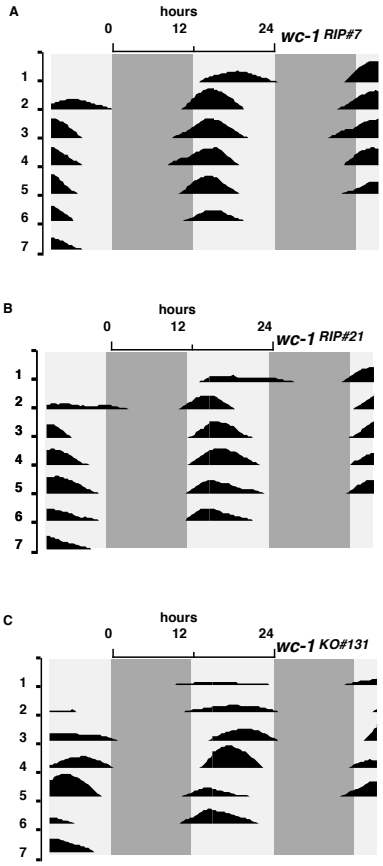

Figure 24. Conidiation in various *wc-1* mutants is synchronized in LD cycles. Data from a week of 24 h LD cycles, are double plotted. The dark period is indicated by gray shading. The peaks on the graphs represent consolidation of conidiation. The fluence rate for all race tubes was 35 μE m^{-2} sec^{-1}. (**A**) *wc–1*$^{RIP\#7}$ strain with RIPed promotor (see Methods) and 5' end of ORF (Talora et al., 1999) ; (**B**) *wc–1*$^{RIP\#21}$, RIP of entire ORF (He at al. 2002); (**C**) In the *wc–1*$^{KO\#131}$ the *wc-1* ORF is replaced by the *hph* gene (Lee at al., 2002).

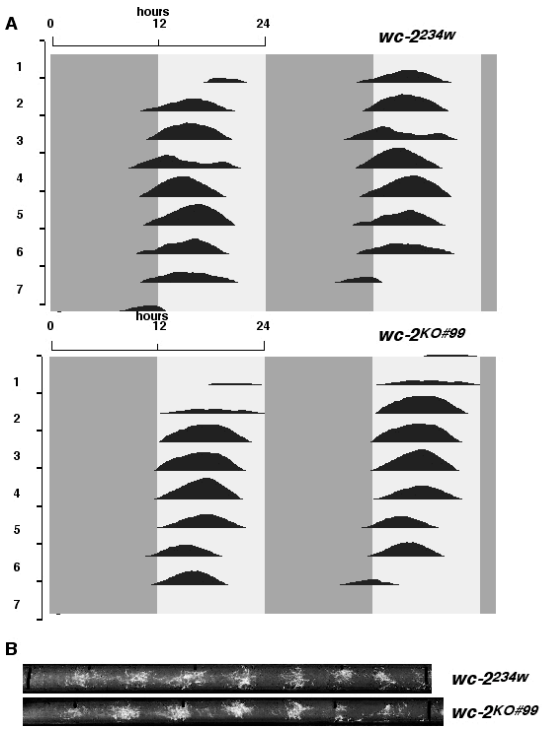

Figure 25. Conidiation in various *wc-2* deficient strains is synchronized in LD cycles. The fluence rate for all race tubes was 20 μE m^{-2} sec^{-1} (75% cool fluorescent white light Osram L36 and 25% was UVA light Osram L80 solarium light bulb). The wc–2^{234w} strain is point mutant that results in the production of a truncated protein (234*w*; FGSC number 3187*)*; In the *wc*–$2^{KO\#99}$ the *wc-2* ORF is replaced by a *hph* gene (Collett et al., 2002). (**A**) Data from a week of 24 h LD cycles are double plotted. (**B**) Race tubes corresponding to double-plotted data.

To distinguish if light-regulated conidiation is a general property of *wc-1* deficient strains, additional *wc* mutants were assayed for entrainment. We have employed two *wc–1* strains from independent sources. *wc–*$1^{RIP\#21}$ is mutant with a non-functional *wc-1* allele, generated by the introduction of stop codons throught the entire ORF by RIP (Y. Liu personal communication and He et al., 2002; Fig. 24B). *wc–*$1^{KO\#131}$ was made by replacing the *wc-1* ORF-segment encoding amino acids 59-1133 with the gene for hygromycin resistance (*hph*, hygromycin B phosphotransferase; Lee et al., 2003). The *wc–*$1^{RIP\#21}$ and *wc–*$1^{KO\#131}$ strains (Fig. 24B and 24C) also consolidate conidiation in the light phase with the phase delayed by 2-3 h relative to *wc-*$1^{RIP\#7}$. The light source was cool fluorescent light (75%) enriched for UVA wavelengths with solarium light (25%, see also legend for Fig. 24 and Methods).

Additional *wc-2* mutants were also assayed for entrainment in light cycles. *wc–2*^{234w} mutant (FGSC#3817) is a point mutant with premature stop codon, creating a truncated protein of 356 amino acids. Given the presence of a truncated WC–2 protein, and despite the lack of light–induced carotenoids, the light response in the *wc-2*^{234w} mutant could be due to residual activity deriving from the N terminus of the protein. To confirm that the light–induced behavior of the *wc-2*^{234w} mutant does not derive from this protein fragment, a complete *wc–2* knockout *wc-2*$^{KO\#99}$ (Collett et al., 2002) was tested in the same experiments and found to regulate conidiation according to the LD cycle (Fig 25). Race tubes (Fig 25A) were analyzed and data are double plotted in Fig. 25B. In the *wc–2*$^{KO\#99}$ strain, the phase is delayed by 3-4 h relative to *wc-2*^{234w}.

2.3.2 Fluence titration of light induced conidiation in *wc* mutant strains

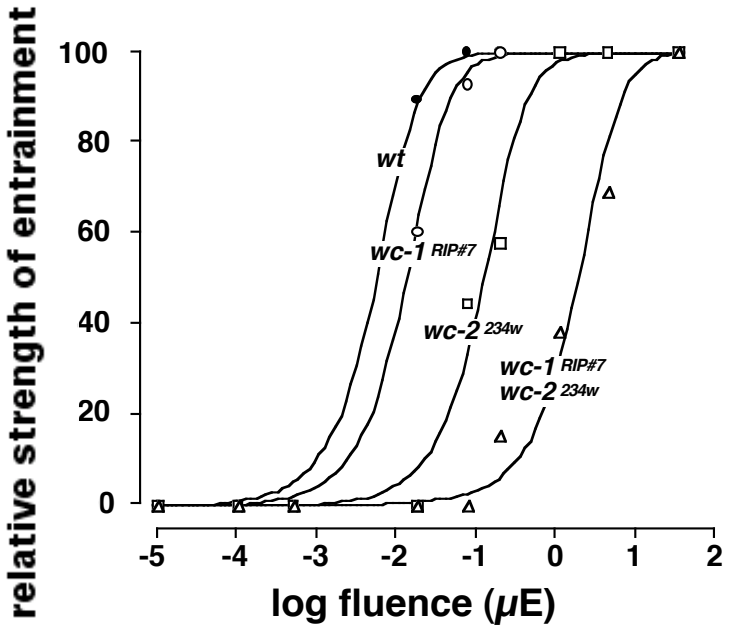

Figure 26. *Wc* strains are less sensitive to light than *wt* for entrainment of conidiation. Race tubes were held in 24 h LD cycles with titrated fluence rates. The relative strength of entrainments (see methods) for different fluence rates is plotted for each strain (as published in Dragovic et al., 2002).

The sensitivity of light regulated conidiation was determined by titration of fluence rate. The fluence threshold for 50% synchronization of the *wt* strain (Fig. 26) is in good agreement with previously published data (Merrow et al., 1999). The *wc-1*$^{RIP\#7}$ mutant is also efficiently synchronized, though it requires about twice as much light as wild type. Synchronization of the *wc-2*^{234w} mutant required 20–fold more light than wild type, while the double mutant, *wc-2*^{234w} *wc-1*$^{RIP\#7}$, is approximately 200 times less light sensitive than wild type. Although the fluence titration was not repeated with the *wc-1*^{ko} strain, it is clear that these mutants require higher fluences for entrainment. This finding suggests that mutants use distinct molecular mechanisms for light regulation of conidiation.

2.3.3 A self–sustained circadian rhythm in the wc mutants

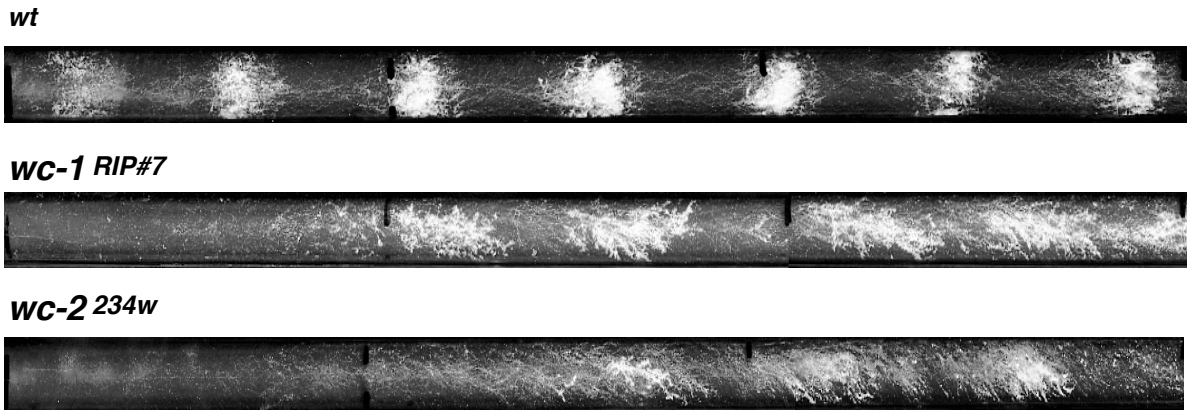

Figure 27. A self-sustained, circa 24 h rhythm of conidiation in the *wc* mutants. Race tubes incubated in constant darkness show a free-running conidiation rhyrhm, indicating a remaining clock machinery in the absence of the central feedback loop (as published in Dragovic et al., 2002).

Although the *wc* mutants were repeatedly shown to lack self-sustained circadian rhythmicity (Crosthwaite et al., 1997; Ninnemann, 1991; Russo, 1988), the issue was revised using conditions that were optimized for LD, entraining cycles. Interestingly the null *frq* mutants exhibit free-running rhythms, but only on long race tubes (Aronson et al., 1994a; Loros et al., 1986). Here, the *wc* mutants were assayed for free-running circadian rhythm. When the *wc* mutants were grown in constant darkness without glucose and on long race tubes, they developed a self-sustained rhythm in conidia formation (Fig. 27). Under these conditions, the period is longer than for *wt*. Specifically, the tubes from a single experiment yielded periods of 21.5, 22.2, 23.3 and 29.3 h for *wc-1*$^{RIP\#7}$, with S.D.s of 1.6, 2.8, 2.6, 2.4 h, respectively. In comparison, two *wild type* control race tubes had periods of 22.9+/-1.2 and 22.8+/-1.7 h. The race tubes for *wc-2*^{234w} had periods of 24.8, 30.5, 33.8 and 34.7 h with S.D.s of 1.3, 5.7, 0.5 and 1.2 h. In general, the mutant race tubes had three to four conidial bands used for these calculations, while the *wild type* had seven to eight. These data reveal only a partial loss of circadian function in the *wc* mutants-while self-sustainment is still intact, precision appears to be lost.

2.4 Molecular characterization of a series of white collar alleles

Given that there is physiological evidence for a light response in *wc* mutants (circadian entrainment shown section 2.3), There may also be light-regulated molecular responses. Because FRQ is light inducible, and that induction was correlates with phase shifting of conidiation (Crosthwaite et al., 1997) the ability of the different *wc* strains to activate light induced synthesis of FRQ protein was investigated.

2.4.1 Light induction of FRQ protein in different *wc* background

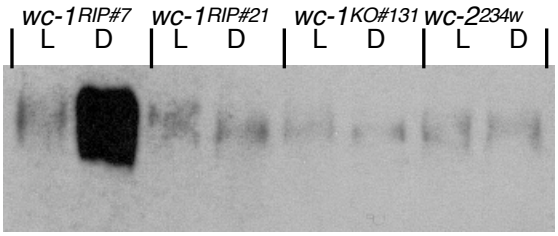

Figure 28. FRQ protein expression profiles are different in various *white collar* mutants. Mycelial tissue was grown for 28 h in darkness and then transferred to light for an additional 4 h ('L' lanes). Dark controls ('D' lanes) were harvested at DD32. The light intensity was 35μE m^{-2} sec^{-1}; cool fluorescent white light bulbs were used (as published in Dragovic et al., 2002).

Mycelial pads of four *wc* alleles (see methods) were grown in darkness and then transferred to light (Fig. 28). Uninduced controls were held in darkness. All samples were harvested after 4 h. Western analysis of the samples showed that different *wc* mutants have different FRQ protein expression profiles (Fig. 28). In darkness (lanes labeled with D) FRQ protein is detected in all *wc* mutants. Following a dark-to-light transfer, FRQ levels remain low in *wc-1*$^{RIP\#21}$, *wc-1*$^{KO\#131}$ and wc-2 ^{234w} strains. The *wc–1*$^{RIP\#7}$ background levels of FRQ protein were high in light induced sample (lanes labeled with L). This observation suggested one of two possibilities:

1. *wc-1*$^{RIP\#7}$ mutant is contaminated with *wt* strain

2. The *wc-1*$^{RIP\#7}$ mutant produces a residual WC-1 protein, sufficient to mediate light induction of FRQ protein.

2.4.2 Verification of the *wc* strains

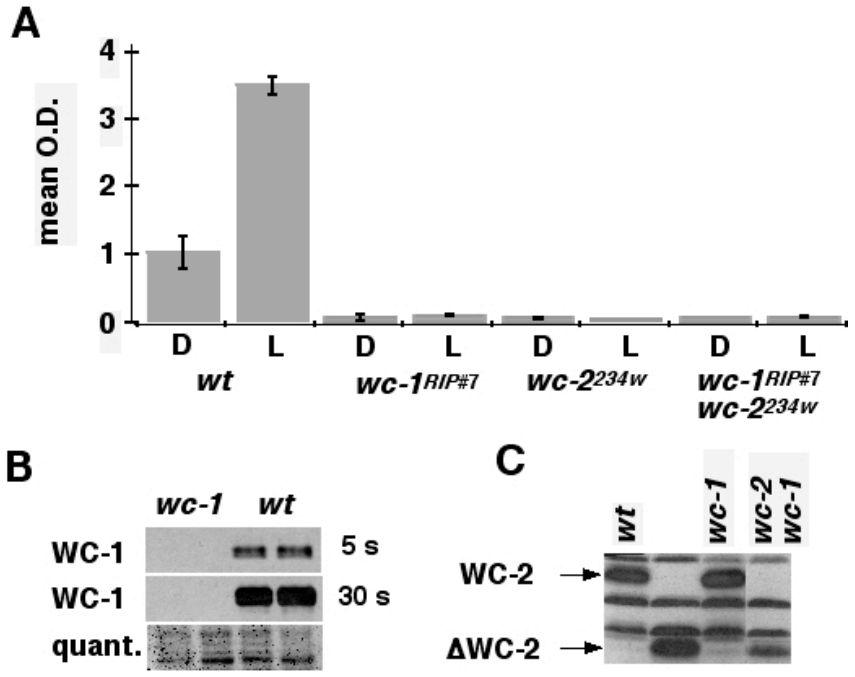

Figure 29. Identity of the wc strains at the physiological and molecular levels. (**A**) Light–induced mycelial carotenogenesis fails in the *wc* mutant strains both in darkness (D) and in response to light (L). (**B**) A western blot for WC–1 protein shows no detectable protein in the *wc-1*$^{RIP\#7}$ mutant (two left lanes), compared to *wt* (two right lanes, *wt*) (Talora et al., 1999), excluding the possibility that the mutant is contaminated with the *wt* strain. The top panel is a 5 s exposure, the middle panel is overexposed (30 s). The blot was stained with Ponceau S for quantification purposes (bottom panel). (**C**) A western blot for WC–2 protein, with arrows on the right, showing the full length protein in comparison with the truncated form (ΔWC–2; strain *wc-2*^{234w}; Linden and Macino, 1997). The background bands indicate even loading of the wells (as published in Dragovic et al., 2002).

Additional experiments were performed to rule out possibility of contamination. These tests compare light-induced carotenogenesis in *wc-1*$^{RIP\#7}$, *wc-2* ^{234w} and *wc-1*$^{RIP\#7}$ *wc-2* ^{234w} (double) mutant, strains which were entrained in LD cycles (section 2.3). The *wc* mutants

tested here fail to generate carotenoids in mycelial tissue both in constant darkness and in response to light (Fig. 29A), whereas the wild type strain responds to light strongly, increasing basal mycelial carotenoids by over 3-fold. The mutant strains were also evaluated for the presence of either WC–1 or WC–2 protein. No WC–1 protein was found in the mutant strain (Fig. 29 B). The results shown in figure 29 C confirm the absence of a full length WC-2 protein in the *wc-2* ^{234w} mutant, while the truncated, smaller form is detectable. Given the presence of a truncated WC–2 protein, and despite the lack of light–induced carotenoids, the *wc-2* ^{234w} mutant could have residual activity deriving from the N-terminus of the protein. Double *wc-1*$^{\mathrm{RIP\#7}}$ *wc-2* ^{234w} mutant strain was verified in two ways: namely, failure to produce light–induced carotenoids (Fig. 29 A), and production of a truncated WC-2 protein (Fig. 29 C).

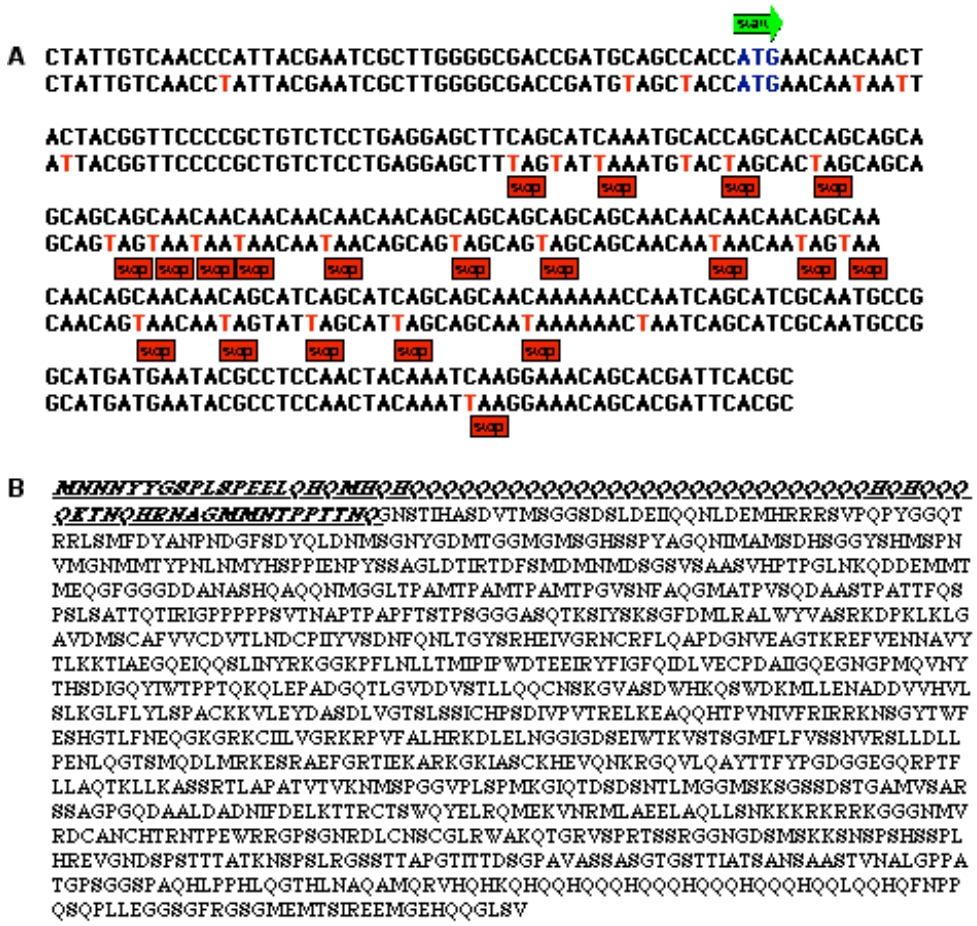

Figure 30. Sequence of the mutations in *wc-1*$^{RIP\#7}$. (**A**) Nucleotide sequence of *wt* (top) and *wc-1*$^{RIP\#7}$ mutant (bottom) between –48 and +255. Numerous stop codons (red rectangles) have been introduced after the transcriptional start site (indicated with green arrow) with RIPing method (Talora et al., 1999). (**B**) Amino acid sequence of the WC-1 protein. The N-terminus of the protein that is ripped in the *wc-1* mutant is underlined and italicized. Utilization of a downstream ATG as an alternative translation start site would yield a truncated protein lacking the glutamine-rich domain (Cheng et al., 2003; Lee et al., 2003; as published in Dragovic et al., 2002).

To further characterize the *wc-1*$^{RIP\#7}$ mutation, genomic DNA corresponding to the 5' end of the gene ws sequenced. Analysis indicates that more that 20 stop codons have been introduced in the 5' region of the ORF (Fig. 30 A). In the event that any RNA is

produced from the RIPed promoter, translation would stop after 15 aa, resulting in a peptide devoid of its signature transcription factor sequences and protein dimerization domains. Translation could reinitiate downstream of the last stop codon, resulting in a low levels of WC-1 protein lacking the N-terminal glutamine-rich region (Fig. 30 B). This theoretical possibility was tested unsuccessfully using western blotting. If a truncated protein is produced, the levels are lower than the limit of detection of our protocol.

2.4.3 Molecular dissection of light input mechanisms

Although the *wc-1*$^{\text{RIP\#7}}$ and *wc-1*$^{234\text{w}}$ strain synchronize conidiation in response to light, carotenogenesis is completely abolished. In these genetic backgrounds, it is possible to if the WC proteins are required for light induction of different genes with respect to the regulation conidiation and carotenogenesis. Thus, the *wc* mutants provide an opportunity to dissect mechanisms of photoreception at the molecular level.

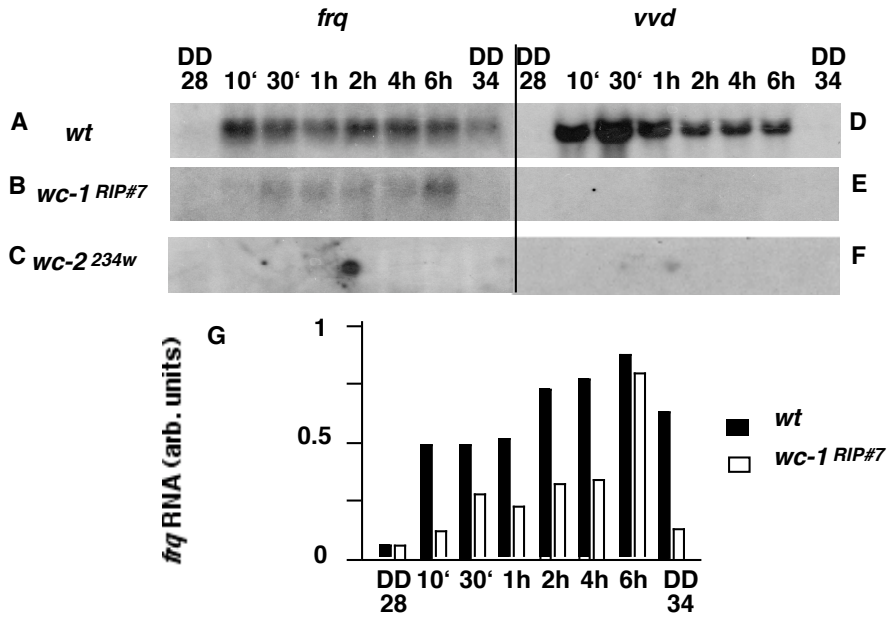

Figure 31. *wc-1*$^{RIP\#7}$ and *wc-2*^{234w} mutants show different profiles of light induced mRNAs. mRNA levels were determined by Northern blot analysis. Panels **A**, **B** and **C** depict *frq* RNA levels; **D**, **E** and **F** show those for *vvd*. **A** and **D** are samples from wild type cultures; **B** and **E** from *wc-1*$^{RIP\#7}$; **C** and **F** from *wc-2*^{234w} (Linden and Macino, 1997; Talora et al., 1999), where the panels are overexposed. Loading of RNA was controlled by probing for ribosomal RNA (not shown), and these values were used for quantification. **G** is a quantification of *frq* RNA induction as shown in panels **A** and **B**. The harvest times are indicated, up to 6 h after lights–on, with DD28 and DD34 representing the dark controls harvested at the beginning and the end of the light exposure (as published in Dragovic et al. 2001).

Several molecular events have been described with respect to the regulation of conidiation by light (Corrochano et al., 1995; Crosthwaite et al., 1995; Heintzen et al., 2001; Li and Schmidhauser, 1995). These include rapid induction of *frq* and *vvd* RNA and protein (see Figs. 31 A and D, respectively). To elucidate the molecular pathways involved in light–induced conidial band formation, these outputs were investigated in the mutant strains. In the *wc-1*$^{RIP\#7}$mutant, *frq* RNA is induced within 10 min of light exposure and remains elevated for the entire 6 h of light incubation (Fig. 31 B and G). The kinetics of induction are, in general, similar to those seen for *wt* (Fig. 31 A and G). The low basal levels of *frq* RNA in the *wc-1*$^{RIP\#7}$ strain are especially apparent at the DD34 time point, a time at which the circadian system in the wild type strain is

promoting increased *frq* RNA levels. This is consistent with previous reports, and reflects the co–dependent regulation of these molecules by each other (Crosthwaite et al., 1997; Lee et al., 2000; Merrow et al., 2001). By the end of the 6 h light incubation, the amount of *frq* RNA in the *wc-1*$^{RIP\#7}$ and wild type strains is approximately equal, indicating that over the course of an extended incubation in light, *frq* RNA levels in *wc–1*$^{RIP\#7}$can approach those in the wild type strain. In contrast to the results with the *wc-1*$^{RIP\#7}$strain, neither *frq* RNA (Fig. 31 C) nor FRQ protein (Fig. 32 B) are induced by light in the *wc*–2^{234w} strain. Thus, induction of *frq*, per se, is apparently not required for entrainment of conidiation. The large difference in light sensitivity of *wc-1*$^{RIP\#7}$ and *wc-2*^{234w} may reflect the *frq* induction.

Neither of the *wc* mutant strains yielded light–induced *vvd* RNA (Fig. 31 E and F), consistent with previous reports of the failure of light–induced gene expression in the *wc* mutants (Arpaia et al., 1993; Li and Schmidhauser, 1995; Sommer et al., 1989).

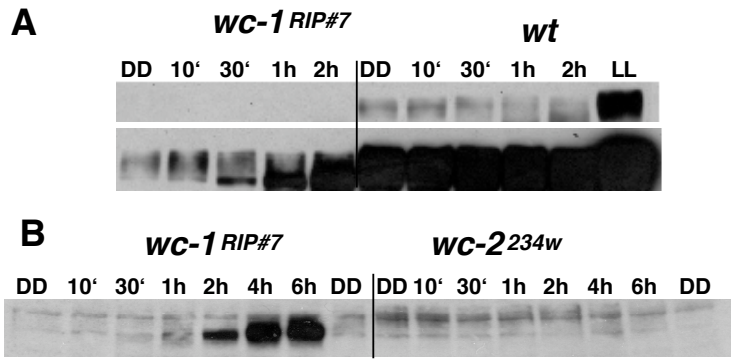

Figure 32. Light-induced FRQ protein in the *wt*, *wc-1* and *wc-2* mutant strains. (**A**) FRQ in *wc-1*$^{RIP\#7}$and wild type protein extracts in short (top panel, 1 s) and long (bottom panel, 30 s) exposures of Western blots. Control samples (DD) were harvested at DD28; Positive control (LL) is from wild type mycelia, grown in constant light. Harvest times are indicated at the top, starting from lights on at DD28. (**B**) FRQ protein is induced following light exposure in the *wc–1*$^{RIP\#7}$, but not the *wc–2*^{234w}, strain, as shown here in an extended film exposure (30 s). Control samples at left and right of both *wc–1*$^{RIP\#7}$ and *wc–2*^{234w} series were harvested at DD28 and DD34, the beginning and the end of each light incubation. Harvest times are indicated at the top, starting from lights on at DD28 (as published in Dragovic et al., 2002).

The kinetics of light–induced FRQ protein production in *wc-1*$^{RIP\#7}$ (Fig. 32 A) parallels the wild type strain, first appearing within 30 min, with substantial amounts accumulating within 2 h (Fig. 32 A and B). The qualitative aspects of FRQ protein induction are also similar when the two strains are compared: the high molecular weight form that is prevalent at DD28, is replaced after 2 h of light with newly made, low molecular weight (poorly phosphorylated) protein.

2.4.4 Presence of FRQ but not quantitative or qualitative changes are required for the regulation of conidiation by light

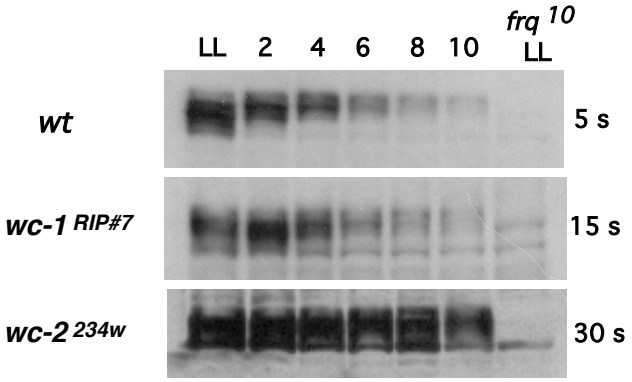

Figure 33. Regulation of conidiation does not require cycling of FRQ. Mycelia were grown in LL and then harvested for up to 10 h (indicated at top) following release into DD; proteins were extracted for Western blotting. The *wt*, *wc-1*$^{RIP\#7}$ and *wc-2*^{234w} strains are compared for FRQ protein. Exposure lengths are 5 s, 15 s and 60 s, from top to bottom. Control samples are *frq*^{10} grown in LL and are in the right lanes of all three panels. The difference in appearance of background bands derives from alternative development protocols, which were used on the bottom panel to decrease background levels for long exposures (as published in Dragovic et al., 2002).

Previously we have showed that FRQ, is required for regulation of conidiation by light (Merrow et al., 2001). Although not induced by light in *wc-2*^{234w} low levels of *frq* and FRQ are observed (Collett et al., 2002; Crosthwaite et al., 1997; Merrow et al., 2001), a pre–condition which apparently allows the light–regulated conidiation shown here (Fig. 22 C and D). But there might be quantitative or qualitative changes in FRQ that occur over an extended light incubation, e.g., in the 12 h of light used in these cycles, that facilitate band formation, versus the 6 h of light used in the light induction experiments of figures 3 and 4. To investigate this possibility, FRQ protein was evaluated in mycelia from cultures that were transferred to darkness after an extended light incubation (approx. 44 h, Fig. 33). In both *wc–1* $^{RIP\#7}$ and wild type, FRQ accumulates to relatively high levels in constant light and degrades away in darkness. In the *wc–2*^{234w} mutant, no

quantitative or qualitative change in FRQ levels is seen. Thus, the regulation of conidiation by light, while dependent on FRQ, does not require its apparent modification.

2.4.5 Fluence titration of light induction of FRQ protein

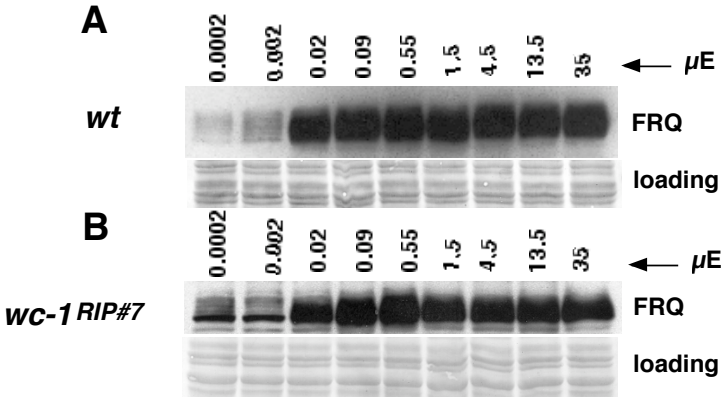

Figure 34. Sensitivity of light induction of FRQ in *wt* and *wc-1*$^{RIP\#7}$ is similar. Levels of light-induced FRQ protein were determined following a 4 h light incubation, beginning at DD28. The fluence rate was titrated, and wild type (**A**) versus *wc–1*$^{RIP\#7}$ (**B**) strains are compared (as published in Dragovic et al., 2002). In both strains full induction occurs with 20 nE/m^2/s.

The sensitivity of light induction of FRQ protein is determined in the *wt* and *wc–1*$^{RIP\#7}$ mutant strains (Figs. 34 A and B). FRQ induction is seen in *wt*, with as little as 0.002 μE m^{-2} sec^{-1} of light, and in both strains almost full induction occurs with 0.02 μE m^{-2} sec^{-1}. The sensitivity of light–induction of FRQ in both *wt* and *wc-1*$^{RIP\#7}$ correlates well with synchronization of conidiation by light (Fig. 26).

We have defined two branches of a light input pathway at the genetic level by demonstrating that light regulated conidiation persists in *wc* mutants blind for carotenogenesis and other light responses (Merrow et al., 2001). We also find that there are differences between the *wc–1* $^{RIP\#7}$ and other *wc-1* mutants in light induced gene expression. In the *wc–1* $^{RIP\#7}$ background, these responses can be divided in two groups: one in which the response was completely abolished (*vvd* mRNA induction) and another in which the light induction is altered but is still significant (*frq*). The reduced induction of *frq* mRNA and protein could reflect a low-dosage effect of the truncated WC-1

protein. Also, deletion of the Q (glutamine)-rich N-terminal domain could be important for achieving a full activation profile. If *Neurosora* has additional photoreceptors, their function could be elucidated in a *wc–1* $^{RIP\#7}$ background what would allow their dissection at functional and molecular levels.

2.5 Identification of light induced genes in *wc-2* mutant

To characterize function of WC-2 in light signal transduction, microarray analysis was performed with *wc-2*^{234w} mutant. Microarray slides contained double-spotted probes for 1343 *N. crassa* genes (Lewis et al.,2002). Slides were generously provided by D.B. Pedersen, Texas A&M University, College Station, TX 77843. EST libraries used for probe synthesis originated from the Neurospora Genome Project at the University of New Mexico (http://www.unm.edu/~ngp/).

The slides were hybridized with labeled cDNA probes made from *wc-2*^{234w} dark-grown mycelial cultures as well as cultures exposed to constant light for 2h. 28 genes (represented by 28 pairs of probe spots) showed at least a two-fold increase in mRNA levels following exposure to light (Tab. 1). BLAST analysis (see figure legend, Table 1) of the EST sequences revealed nine already known *N. crassa* genes (Tab. 1 column 'BLAST match'). Two of these genes (*ccg-2* and *ccg-6*) were previously identified as light-inducible in *wt* strains.

Light induction of several transcripts observed in microarray analysis (Tab.1) was tested independently by quantitative real time PCR. Some of the already known light inducible transcripts were included in the analysis as controls. Furthermore, their light induction was tested in three different genetic backgrounds, *wt*, *wc-1*^{KO131} and *wc-2*$^{KO\#9}$. Light inducibility of some transcripts observed in microarray analysis could also be seen by quantitative real time PCR. However, this observation was made only in *wt* background. There was no light induction observed of any of the transcripts tested in the *wc-1*^{KO131} or *wc-2*$^{KO\#9}$ mutants. However the analysis of the light inducible genes in *wc-1* and *wc-2* mutant background was limited to a small number of genes. Microarray analysis which include all known *Neurospora* genes will provide more information about light regulated gene expression in *wc* mutants.

Table 1. Microarray analysis revealed light induced genes in *wc-2*^{234w} mutant strain. Relative mRNA levels in dark grown cultures were compared to cultures exposed to light for 2h (see also Methods 4.4.7). Light induced genes showing a minimum two-fold change in relative mRNA levels following light induction are shown.

EST name[1]	BLAST match[2]/ predicted ORF[3]
1. NCC1A11	no significant BLAST matches
2. NCC4A08	no significant BLAST matches
3. NCC5F05	*Botrytis cinerea* strain T4 cDNA library
4. NC5E3	*N. crassa* clock controlled gene 2(hydrophobin); *ccg–2* / NCU08457.1
5. NC3C3	*N.crassa,* glyceraldehyde-3-phosphate dehydrogenase / NCU56397.1
6. NCC4G5	*N. crassa* clock-controlled gene-6; *ccg-6* / NCU46086
7. NCM1A3	no significant BLAST matches
8. NCM1A7	no significant BLAST matches
9. NCM1C3	*N. crassa*, hypothetical protein / NCU09152.1
10. NCM2B5	no significant BLAST matches
11. NCM2B8	no significant BLAST matches
12. NCM2C7	no significant BLAST matches
13. NCM3B6	no significant BLAST matches
14. NCM1D5	*Mortierella verticillata* translation elongation factor 1-alpha
15. NCP2E3	no significant BLAST matches
16. NCP2B5	*Sordaria macrospora* partial ppg2 gene for pheromone precusor gene
17. NCP2D4	*N. crassa* OR231A beta-isopropylmalate dehydrogenase (leu-1) / NCU01061
18. NCP4A11	*N. crassa* histones H3 and H4 / NCU01635.1 and NCU01634.1
19. NCSC1E10	no significant BLAST matches
20. NCSM1C1	*N. crassa* Ca/CaM-dependent kinase / NCU09123.1
21. NCSM1C8	no significant BLAST matches
22. NCSP1B1	no significant BLAST matches
23. NCSP6A4	*N. crassa* Woronin body major protein gene hex-1
24. NCSP6E7	*N. crassa* plasma membrane ATPase gene / NCU08332.1
25. NCSP6F6	Aspergillus fumigatus GTPase Rho1 gene
26. NCSP6F9	Botrytis cinerea strain T4 cDNA library
27. NCSP6G3	*Drosophila melanogaster* CDC42 protein
28. NCW10A1	no significant BLAST matches

[1]Expressed Sequence Taqs (ESTs) libraries were provided by the Neurospora Genome Project at the University of New Mexico (http://www.unm.edu/~ngp/).

[2]The BLAST matches represent the most homologous gene/DNA sequence as determined at NCBI database (minimum e-value $1e^{-5}$).

[3]The predicted ORFs are from the Neurospora Sequencing Project, Whitehead Institute:

(http://www-genome.wi.mit.edu/annotation/fungi/neurospora/)

Table 2. Quantitative real time PCR analysis of mRNA light induction for different genes in different genetic backgrounds (*wt*, *wc-1*^{KO131} and *wc-2*$^{KO\#99}$).

#	[1]EST / *gene name*	mRNA light induction in *wt*	mRNA light induction in *wc-1*	mRNA light induction in *wc-2*
1	NC5E3	induced; fold ≈2	not	not
2	NM1C3	mRNA not detectable	mRNA not detectable	mRNA not detectable
3	NC1A11	not	not	not
4	SM1C8	induced; fold ≈2	not	not
5	NM2B8	induced; fold ≈6	not	not
6	NM1B8	not	not	not
7	W17G3	induced; fold ≈1000	not	not
8	*actin*	not	not	not
	26s ribosomal RNA	not	not	not
9	*cry*	induced; fold ≈500	not	not
10	*phy4*	downregulation; fold ≈3	not	not
11	*phy5*	induced; fold≈4	not	not
12	*nop-1*	not	not	not
13	*mus-25*	not	not	not
14	*mus-11*	not	not	not
15	*phr* (photolyase)	induced;fold≈70	not	not
16	Ca-CaM kinase	no	not	not
17	*con-6*	induced; fold≈60	not	not
18	*con-10*	induced; fold≈500	not	not
19	*hex-1*	not	not	not
20	*vvd*	induced; fold≈150	not	not
21	*wc-1*	induced; fold≈5	not	not
22	*bli-3*	induced; fold≈16	not	not
23	*bli-4*	induced; fold≈50	not	not

24	*frq*	induced; fold≈15	not	not
25	*al-1*	induced; fold ≈2000	not	not

[1]EST=Expressed Sequence Tags; fold=fold of mRNA light induction; downregulation=mRNA levels were downregulated in response to light.

2.6 Action spectrum for FRQ protein induction

A first step for determining the nature of a non-WC photoreceptor is constructing an action spectrum. An action spectrum shows how much light of a certain wavelength is required for a given biological response. To be used by the organism, photons must first be absorbed by the photoreceptor. The action spectrum describes the specific wavelengths that the photoreceptor molecule absorbs the best. These observations can provide suggestions as to which chromophores are involved in *Neurospora* photoreception. Several action spectra have been made using different physiological outputs as a readout (De Fabo et al., 1976; Dharmananda, 1980; Sargent and Briggs, 1967) and all of these point to flavin as a chromophore. An action spectrum was constructed by using FRQ induction as readout.

2.6.1 Equal Intensity action spectrum

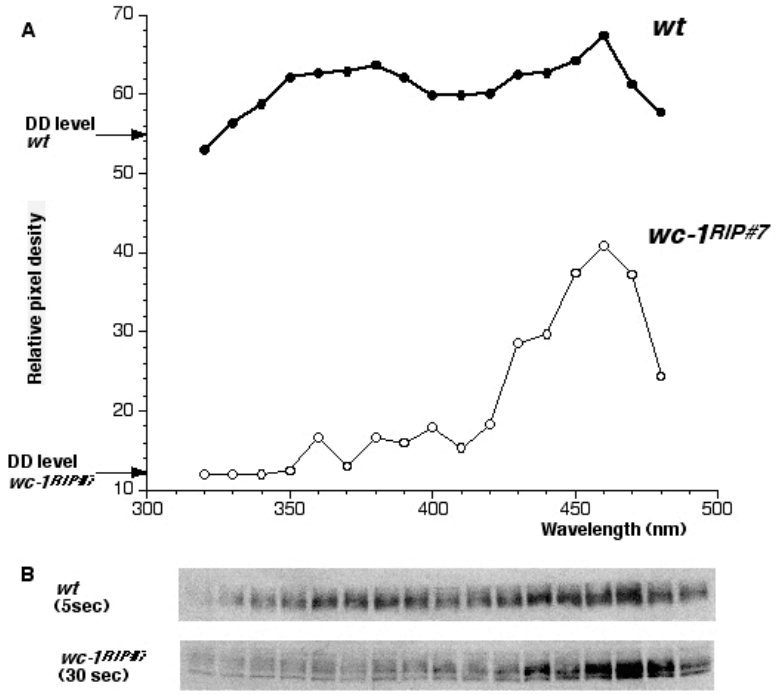

Figure 35. FRQ is induced by blue and near ultraviolet light. (**A**) Equal-intensity action spectra for light induction of FRQ protein. Pads of dark-grown tissue were exposed to the same fluence of light at wavelengths varying from 330 to 480 nm. Light induced FRQ protein was quantified by western blot analysis. The *wt* strain shows two peaks in sensitivity, one at 460nm and a broader one at 350-380nm. The *wc-1*$^{RIP\#7}$ mutant shows differences in spectral sensitivity, with only one peak at 460 nm. Overall levels of FRQ proteins are lower in the *wc-1*$^{RIP\#7}$ strain. (**B**) Two different exposures of western blots (short for *wt*, long for *wc-1*$^{RIP\#7}$) are presented.

Fig. 35 A shows the results of the equal-intensity action spectrum for FRQ light induction. In Fig. 35 B Western blots for wt and *wc-1*$^{RIP\#7}$ are shown. Due to lower overall levels of FRQ longer exposure has been shown for *wc-1*$^{RIP\#7}$. For this action spectrum, the same total amount of light was given to the samples at each wavelength tested (17 wavelengths varying from 330 to 480 nm, in steps of 10 nm). The light source

for all action spectra experiments is monochromatic light produced by a commercial monochromator with 5 nm bandwidth (see Appendix). Mycelial pads were exposed to subsaturation amount of light at 1μmol photons/m^2 (50 nE m^{-2} sec^{-1} for 20 seconds). It was important to dose light to levels which elicit approximately 50% of maximal FRQ induction. Following the light pulse, tissue was subjected to an additional incubation (4h in darkness to allow FRQ accumulation) and mycelial pads were frozen in liquid nitrogen. FRQ was quantified using western blotting (see Methods). Densitometric analysis of the FRQ signal in *wt* (Fig. 35) shows two peaks in sensitivity, one at 460nm and a broader one at 350-380 nm. The *wc-1*$^{RIP\#7}$ mutant has a distinct action spectrum, with only one peak at 460 nm. Difference in action spectra indicates that more than one photoreceptor regulate FRQ light induction. Fig. 36B shows two of the Western blots that were used for densitometric analysis.

2.6.2 Range of reciprocity for FRQ protein light induction

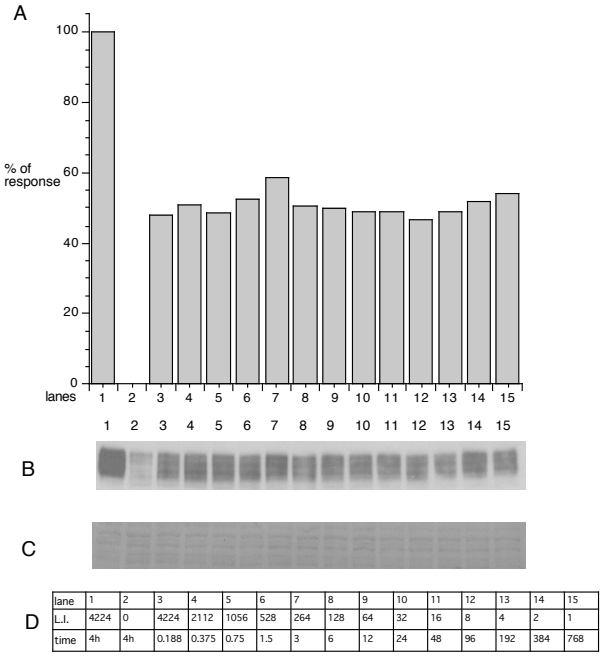

lane	1	2	3	4	5	6	7	8	9	10	11	12	13	14	15
L.I.	4224	0	4224	2112	1056	528	264	128	64	32	16	8	4	2	1
time	4h	4h	0.188	0.375	0.75	1.5	3	6	12	24	48	96	192	384	768

Figure 36. The photoreceptor for FRQ induction integrates photons over a broad range of light intensities and durations. Mycelial pads were grown for 28 h in the dark and then exposed to different light intensities for different durations. The light source was blue, monochromatic light (460 nm). (**A**) Quantification of FRQ protein after light induction: Lane 1 shows the saturated light response. Mycelial pads were induced at 4.2 μE /m^2/s for 4h. Lane 2 is the D28 control (no light). Bars 3-15 represent FRQ induced with different combinations of light intensity and duration that yield identical photon exposure (768 nE/m^2). (**B**) Western blot for the data graphed in (**A**). (**C**) Ponceau-S stained membrane for normalization. (**D**) Table with light intensities (L.I. in nE /m^2/s) and durations of light inductions (in seconds except where indicated).

In action spectra experiments, different amounts of light are given to different samples. When either intensity or time are varied, the 'reciprocity law' must be tested. Reciprocity occurs when the product remains constant over a range of durations and light intensities.

The range of reciprocity for FRQ induction by light at 460 nm is shown in figure 36 A: lane 1 shows the saturation light response (presented as 100%) subtracted for FRQ

level in darkness at DD28 (lane 2). Lanes 3-15 show that 50% of FRQ induction is elicited with different combinations of duration and light intensity resulting in equal doses of photons. Combinations of light intensiy (L.I. in nE m^{-2} sec^{-1}) and durations of light pulses are presented in figure 36 D and show that reciprocity holds over a very broad range. 0.8 μM of photons were delivered from over 0.188 seconds to more than 10 minutes at light intensities from 1 to 4224 nE m^{-2} sec^{-1}. Light induced FRQ was equivalent over this entire range. Using this information, an action spectrum can be constructed by varying time of exposure at constant intensity.

2.6.3 Dose response curves

A

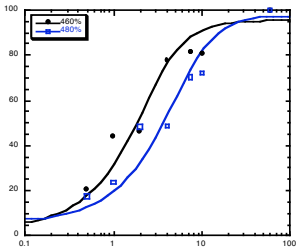

Fluence titration N°1: 480nm		
	Value	Error
m1	97.789	4.2873
m2	6.7917	1.2055
m3	0.38667	0.28787
Chisq	520.14	NA
R	0.98515	NA

Fluence titration N°2: 460nm		
	Value	Error
m1	95.4	3.47
m2	3.1122	0.53646
m3	0.09083	0.12862
Chisq	448.65	NA
R	0.98778	NA

B

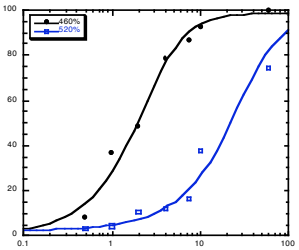

Fluence titration N°2: 460nm		
	Value	Error
m1	98.861	1.9487
m2	3.2817	0.29306
m3	-0.01798	0.066906
Chisq	138.54	NA
R	0.99664	NA

Fluence titration N°2: 520nm		
	Value	Error
m1	97.697	3.6082
m2	38.55	6.9691
m3	0.88953	0.92709
Chisq	253.39	NA
R	0.99243	NA

C

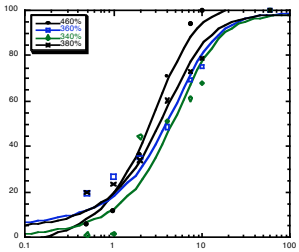

Fluence titration N°3: 460nm		
	Value	Error
m1	98.408	2.8416
m2	6.0222	0.66124
m3	0.23558	0.15342
Chisq	203.77	NA
R	0.99442	NA

Fluence titration N°3: 360nm		
	Value	Error
m1	99.003	3.1959
m2	7.4893	0.95513
m3	0.41829	0.22772
Chisq	282.76	NA
R	0.99196	NA

Fluence titration N°3: 380nm		
	Value	Error
m1	103	2.6251
m2	4.3738	0.45795
m3	-0.15235	0.098348
Chisq	223.96	NA
R	0.99522	NA

Fluence titration N°3: 340nm		
	Value	Error
m1	98.349	5.1882
m2	7.9203	1.5354
m3	0.038095	0.33957
Chisq	735.91	NA
R	0.98121	NA

D

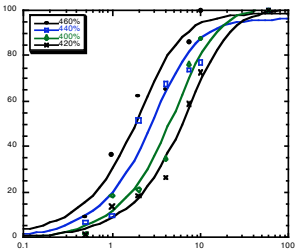

Fluence titration N°4: 460nm		
	Value	Error
m1	98.778	3.1784
m2	3.1166	0.46124
m3	0.0043073	0.10662
Chisq	376.23	NA
R	0.9909	NA

Fluence titration N°4: 440nm		
	Value	Error
m1	96.282	4.0782
m2	4.5213	0.80129
m3	-0.042661	0.17591
Chisq	534.28	NA
R	0.98661	NA

Fluence titration N°4: 420nm		
	Value	Error
m1	100.94	2.2091
m2	10.755	0.8256
m3	-0.06237	0.11715
Chisq	127.66	NA
R	0.99678	NA

Fluence titration N°4: 400nm		
	Value	Error
m1	101.76	3.2633
m2	7.6863	0.89185
m3	-0.10869	0.19316
Chisq	292.56	NA
R	0.99308	NA

E

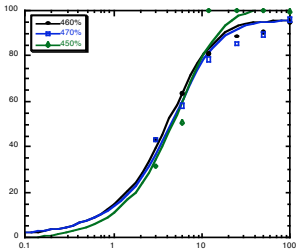

Fluence titration N°5: 460nm		
	Value	Error
m1	98.206	1.4351
m2	6.7492	0.54243
m3	0.042922	0.13923
Chisq	108.17	NA
R	0.99717	NA

Fluence titration N°5: 470nm		
	Value	Error
m1	95.953	1.8847
m2	7.492	0.78496
m3	0.092663	0.20224
Chisq	182.17	NA
R	0.99519	NA

Fluence titration N°5: 450nm		
	Value	Error
m1	102.19	2.7031
m2	8.131	1.1022
m3	-0.11356	0.27894
Chisq	387.76	NA
R	0.99181	NA

F Equation:
y=m1*(((m0+m3)/m2)/(1+((m0+m3)/m2)^ 2)^ 0.5)

Figure 37. Dose response curves for FRQ induction by monochromatic light. Light pulses were given to mycelial cultures and amount of induced FRQ protein was determined. Light was varied by wavelength and duration, not intensity. The distance from the light source was also constant. Eight mycelial pads were used for each wavelength, each for different duration. The FRQ signal is plotted as a function of the length of the light pulse; All dose response curves were fittedusing the formula shown under F (see also methods section). Tables show factors (m1-m3) which define specific curve fits at each wavelength. Each graph (**A-E**) represents one experiment and each dose response curve within a graph represents one wavelength. The 50% response level was calculated with same the equation (**F**) by designating y as 0.5 *y* and calculating value the valu of m_0 (see also Methods section).

An action spectrum of FRQ induction was constructed based on dose response curves. This kind of action spectrum usually provides more reliable information about the chromophore involved in given light response. Dose response curves (DRC) are shown in figure 37. Graphs A-E show the amount of light-induced FRQ protein versus total amount of monochromatic light. The amount of FRQ protein is normalized to 100% (saturation). The DRCs were determined for 11 wavelengths, between 320 and 520 with steps of 20 nm. Eleven wavelengths were assayed in five independent experiments. To normalize for differences between experiments, a dose response curve at 460 nm was generated each time. The amount of light was titrated by regulating the duration of light pulse. Eight mycelial pads were used per one wavelength; one pad was used per wavelength. The intensity of light was constant for all pads (250 $nE/cm^2/sec$) and the duration of light pulses was controlled by a commercial electronic "shutter" system (see appendix). The amount of FRQ protein was estimated with western analysis, as described previously (see also methods section).

The results show a clear, dose-response relationship between the amount of monochromatic light and FRQ protein induction. Data from each of the 11 wavelengths (Fig. 37 A-E) was fit using three parameter sigmoidal curve. The curves are all highly significant (lowest correlation coefficient R was 0.981). The half-maximal responses were calculated from the fitted DRCs (where y = 0.5; see also Methods section).

2.6.4 Action spectrum for FRQ protein induction

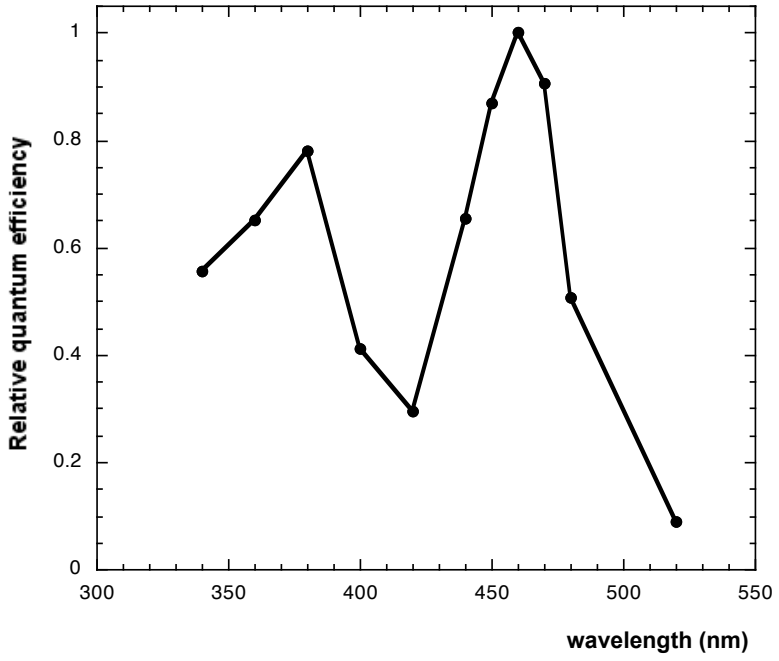

Figure 38. Action spectrum of FRQ protein induction in *wt*. The Y axis represents the relative quantum efficiency for induction of FRQ protein at different wavelengths of light, calculated based on the amount of light necessary to induce FRQ protein to 50% of maximal level. The determination is shown for 11 wavelengths.

The DRCs were used to derive an action spectrum. This spectrum is calculated from the absolute amount of photons that elicit 50% saturation of the light-induced FRQ protein for each of the 11 wavelengths in the *wt* strain. The half saturation values were derived from the DRCs shown in Fig. 37. The action spectrum was plotted as relative quantum efficiency varsus wavelength (Fig. 38). The action spectra data points are connected with lines, i.e. no curve-fit has been used. This action spectrum defines the photoreceptor for FRQ light induction as a blue and near UV (UVA) photoreceptor. The sensitivity extends below 320 nm and has a cut-off above 520 nm. This action spectrum also indicates FAD

(Faeder and Siegel, 1973) as the chromophore which mediates light dependent FRQ protein induction.

2.7 Novel photoreceptor candidates

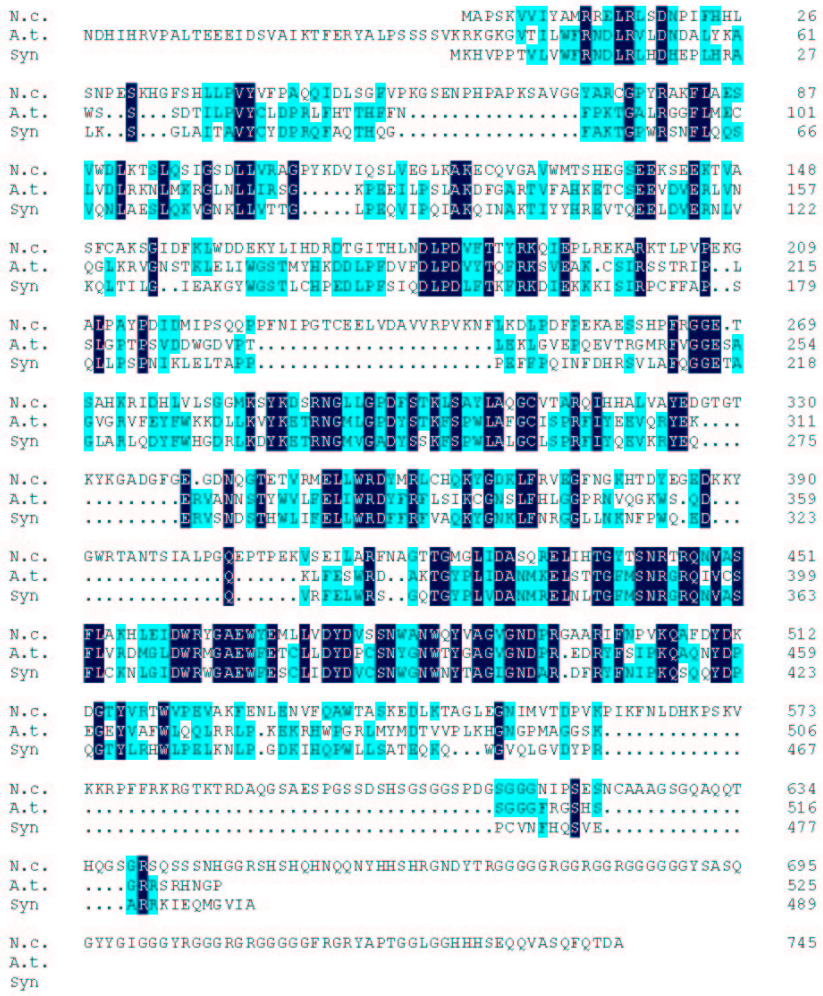

Figure 39. *Neurospora's* cryptochrome is homologous to *cryptochromes* from the DASH family. The sequence of cryptochrome DASH (Brudler et al., 2003), from *Synechocystis sp*. PCC68803 (Syn) and *A. thaliana* (A.t.) were aligned to the *N. crassa* (N.c.) *cryptochrome*. Amino acid residues of *Synechocystis cryptochrome*, which have been described to bind FAD, are conserved in the other two cryptochromes. Black shading represent identical amino acids and gray similar amino acids.

A BLAST search of the recently annotated Neurospora genome (http://www–genome.wi.mit.edu/annotation/fungi/neurospora) revealed the presence of three new potential photoreceptors: one chryptochrome (NCU00582.1) and two

phytochromes (NCU05790.1 and NCU04834.1). In flies and plants, cryptochromes are known as components of circadian light input (Ceriani et al., 1999; Somers et al., 1998b). Plants use also phytochromes as circadian photoreceptors (Quail, 2002).

Cryptochromes share sequence homology and the cofactor (FAD) with the DNA-repair enzymes photolyases. Cryptochromes however, lack the ability to revert UV light-induced pyrimidine dimers. Prior to its functional analysis, the putative cryptochrome (NCU00582.1) was blasted (Protein-Protein BLAST search on NCBI), showing high sequence identity to one *Arabidopsis* and *Synechocystis* cryptochrome, two members of newly established DASH-cryptochrome family (*Drosophila, Arabidopsis, Synechocystis and Homo*, (Brudler et al., 2003). Alignment of these three proteins is shown in Fig. 39. Three cryptochromes have 29% overall identity. Importantly, four amino acid residues (Ser249, Lys251, Phe252 and Gln359 in *Synechocystis cryptochrome*), which are in van der Waals contact with the FAD, are also conserved in *Neurospora cryptochrome* suggesting its ability to bind FAD. To function as a photolyase, the *Neurospora cryptochrome* would require Asn at position 325 and Met at position 433. In all three shown *cryptochromes* these residues are replaced with other amino acids (Brudler et al., 2003). This alignment indicates that *Neurospora cryptochrome* functions as a photoreceptor with FAD as chromophore rather than as an additional photolyase.

Genes with annotation numbers NCU05790.1 (in this study called *phy5*) and NCU04834.1 (called here *phy4*) are both highly homologuous to the bacteriophytochrome from *Pseudomonas putida* (E=$2e^{-31}$; seq.identitiy=40% and E=$2e^{-31}$; seq.identitiy=27% respectively). A BLASTp search also revealed a high level of homology to two bacteriophytochromes from *Agrobacterium tumefaciens* (labeled in alignment as bacteriophytochromes with capital and small letters), *Tolypotrix spp.* and *Nostoc*. In *Agrobacterium tumefaciens* two Bphs have the capacity to simultaneously sense red and far-red light (Bhoo et al., 2001; Karniol and Vierstra, 2003) indicating that *Neurospora's phys* could function as red-light photoreceptors. To date, no red light responses have been demonstrated in *Neurospora*. Amino acid sequence alignment of GAF domain (Montgomery and Lagarias, 2002) conserved among *phytochrome*-like proteins of *Neurospora, Agrobacterium, Tolypotrix , Nostoc* and *Synechocystis* is shown in figure 40. GAF domains are ligand binding domains first indentified in vertebrate

cGMP- specific phospohodiesterases. Phytochrome GAF domains (known also as BLD) bind *bilin* molecules (Montgomery and Lagarias, 2002).

```
Synechocystis_sp    HMANA.............................................   142

Ncphy5              IGMATKIQTQFSEAATVPDLLETIVSIVKEVTRFHRVMVYQFDRDYNGTV   366
Ncphy4              FDIMSQVQEQLANAPNLEKFLKILVGIVKELTGFHRVMIYQFDSSFNGKV   528
BACTERIOPHYTOCHR    YPLVRSFVASLQVASSIEDLLQQTVLQLKRITGFGRVKAYRFDAEGNGQV   186
bacteriophytochr    ........KYLNSAPSLEDALFRTAQLVSSISGHDRTLIYDFGLDWSGHV   167
Tolypothrix_sp._    ......SINQLEKTTNLRDFCQIIVQEVRKVTGFDRVMLYKFDDDGHGSV   186
Nostoc_sp._PCC_7    ......AMLKLQGTATTTEISQILAQEVRKITGFDRVMVYRFDEQWNGKV   186
Synechocystis_sp    ......ALNRLRQQANLRDFYDVIVEEVRRMTGFDRVMLYRFDENNHGDV   186

Ncphy5              VAELMDPKASNDVYRGLHFPASDIPPQARKLYMINKVRVLFDRSQRTSRL   416
Ncphy4              VTELVDPMQTRDLYKGLHFPATDIPSQARELYKLNKVRLLYDRDVESARI   578
BACTERIOPHYTOCHR    LAEVVDPGYPS..YAGLCFPAADIPRQARELYRVNRIRVIEDANYQPSPL   234
bacteriophytochr    VAEAGS..GALPSYLGLRFPAGDIPPQARQLYTINRLRMIPDVDYKPVPI   215
Tolypothrix_sp._    IAEEKL..DSMEPYLGLHYPESDIPKPARKLFASNFIRLIPDAHAEPVQI   234
Nostoc_sp._PCC_7    IAEVKP..EYLTSYLGLNYPASDIPQQARKLYSQNWLRLIPDAKYQPVPI   234
Synechocystis_sp    IAEDKR..DDMEPYLGLHYPESDIPQPARRLFIHNPIRVIPDVYGVAVPL   234

Ncphy5              IGRDVSDMDVPLDLTHAYLRAMSPVHLKYLSNMGVRSSMSMSLESDGKLW   466
Ncphy4              VCRTPEDLETPLDMTHSYLRAMSPIHLKYLANMAVRSSMSISINAFGDLW   628
BACTERIOPHYTOCHR    LPATNPRTGKPLDMSFAALRSVSPVHLQYMRNMGTLASMSLSIVVDGQLW   284
bacteriophytochr    RPEVNAETGAVLDMSFSQLRSVSPVHLEYMRNMGTAASMSVSIVVNGALW   265
Tolypothrix_sp._    LPINHPQSQQPIDLTNSILRTAANCHLEYLHNMGVGASLTISLIKDGKLW   284
Nostoc_sp._PCC_7    VPINNPLNDQPLDLSRSVLRSVSPLHIEYMQNMGVTASMSISIMKNQKLW   284
Synechocystis_sp    TPAVNPSTNRAVDLTESILRSAYHCHLTYLKNMGVGASLTISLIKDGHLW   284

Ncphy5              GLIVCHSYGPAATRVPFSIRELSFFVGLAASTCLQKLLNSE....RLQAH   512
Ncphy4              GLVSCHSYGPKGMRVSFPIRKMCRLIGDTASRNIER.........LSYAS   669
BACTERIOPHYTOCHR    GLISCHHQQPRPVDLRT..RTACELLASVLSLQIESRESHASTRKLLTLR   332
bacteriophytochr    GLIACHHATPH..SVSLAVREACDFAAQLLSMRIAMEQSSQDASRRVELG   313
Tolypothrix_sp._    GLIACHHQTPK..YVSYEFRKACEFLGRVIFTEISTREETEDYDYRMNLA   332
Nostoc_sp._PCC_7    GLIACHHQSPK..YIPYEIRSACEFLGQMTSVEMSAKEDSEDTEDKIQVK   332
Synechocystis_sp    GLIACHHQTPK..VIPFELRKACEFFGRVVFSNISAQEDTETFDYRVQLA   332
```

Figure 40. Neurospora's phytochromes (labeled *phy4 and phy5*) display sequence homology to phytochromes from bacteria. Black shading represents identical amino acids and gray shows similar amino acids. In this alignmen the t conserved GAF domain is shown from: *N. crassa* (Ncphy5 and Ncphy4), *Agrobacterium tumefaciens* (bacteriophytochr and BACTERIOPHYTOCHR), *Tolypotrix* , *Nostoc* and *Synechocystis*.

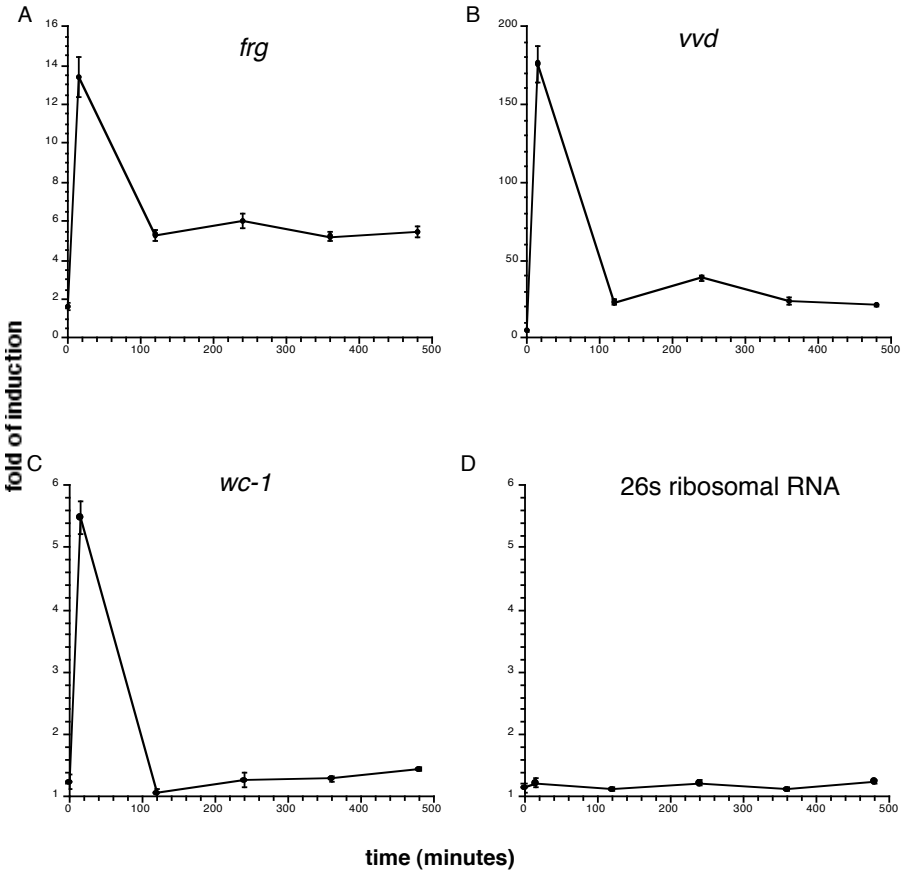

Figure 41. mRNA of the genes involved in the light input pathway is rapidly regulated with light. *wt* mycelial pads were incubated in dark and then transferred to light. The first sample (0') is the dark control. Total RNA was extracted and used as a template for cDNA synthesis and analysed with Real Time PCR analysis. (**A**) *frq* mRNA is rapidly induced by light followed by adaptation. Levels remain elevated under constant illumination. (**B**) *vvd* mRNA shows similar kind of regulation as *frq* mRNA, but the fold of induction is for two orders of magnitude higher. (**C**) *wc-1* mRNA is light induced with an amplitude lower that that of *frq*. It gets adapted rapidly and once adapted remains low in constant light. For normalization of loading, Ct values for 26s ribosomal RNA were used (see also Methods section). **(D)** Constant levels of 26s ribosomal RNA. Error bars represent the standard deviation of three replicate reactions. Mycelial pads were incubated in dark and then transferred to light. Total mRNA A)frq B)vvd C) wc-1 D)ribo. Y-axis (fold mRNA induction) for all three light induced genes represents different fold of induction.

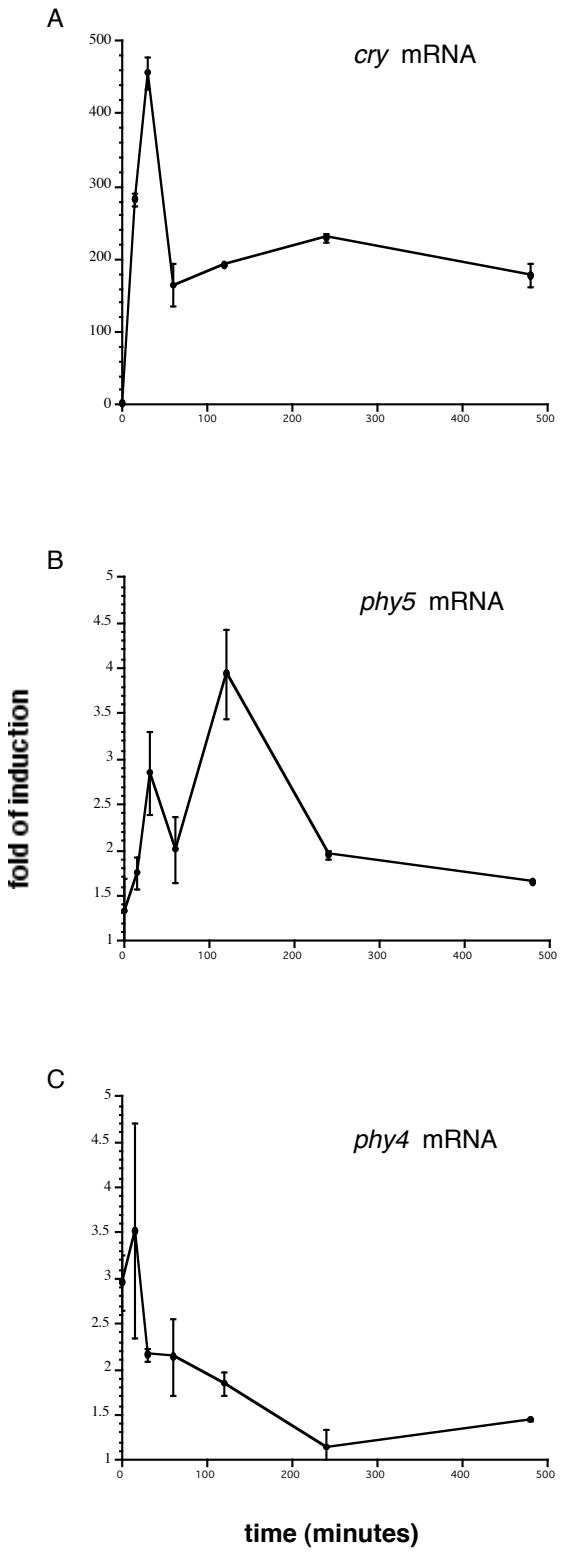
A
cry mRNA
500
400
300
200
100
0
0
100
200
300
400
500
B
phy5 mRNA
fold of induction
5
4.5
4
3.5
3
2.5
2
1.5
1
C
phy4 mRNA
time (minutes)

Figure 42. *cry*, *phy4* and *phy5* mRNA are regulated with light. Mycelial tissue was incubated in dark and then transferred to light. mRNA levels were analyzed with RTPCR. For normalization of loading, Ct values for 26s ribosomal RNA were used. (**A**) *cry* mRNA is rapidly induced by light followed by adaptation. (**B**) *phy4* mRNA degrades in response to light. (**C**) *phy5* mRNA has a slower kinetic of light induction than *cry* or *con-6* mRNA. Also, the amplitude is two orders of magnitude lower (Y-axis represents different fold of induction).

Rapid light-induction of mRNA followed by adaptation is a characteristic regulation of many genes involved in light transduction in *Neurospora*. In figure 41, profiles of light induced mRNA for *frq*, *vvd* and *wc-1*genes are shown. Quantitative real-time PCR analysis (RT PCR; see methods section) was used. Results are comparable to results obtained earlier with Northern analysis (Crosthwaite et al., 1995; Heintzen et al., 2001).

To characterize novel photoreceptor candidates, we started by assessing the light induction of their mRNAs. Key genes in the light signaling pathways (*frq* and*wc-1*) are regulated by light. A similar regulation picture for candidate photoreceptors would give suggestion about their function. Samples were inoculated and kept for about 15 h in the light. For the next two days they were incubated in darkness. The first sample was harvested in darkness and the others were kept in light for the indicated times before harvesting. Total RNAs were isolated and subjected to RT PCR analysis.

The data in figure 42 are presented as 'fold induction' of mRNA by light (*y* axis). We used *con-6* as a positive control. *con-6* mRNA shows 200 fold induction and characteristic adaptation of induction after two hours in constant light (this profile is highly consistent with profiles obtained by Northern analysis; (White and Yanofsky, 1993). We then tested mRNAs of *cry* and two *phys* for light induction. Figure 42 B shows a rapid, almost 500 fold light induction of *cry* mRNA. An adaptation profile is also present and rapid, so that already after 1 hour, mRNA reaches a lower, stationary level. The adapted level of *cry* mRNA is elevated in sustained light relative to levels in darkness. This profile of induction is similar to those for *frq* and *vvd* (Fig. 41). Figure 42 C shows also changes in the level of *phy4* mRNA levels after light induction. Levels of *phy4* mRNA slowly decrease after light exposure, reaching a minimum after 4 h. This is a novel light regulated RNA profile. *phy5* mRNA is light induced with an amplitude lower than that of *cry*. The induction has different kinetics similar to those shown for *ccg-2*

(Bell-Pedersen et al., 1996). It reaches maximum after 2 h and gets adapted slowly, after about 4 h. Once adapted in constant light *phy5* mRNA remains low.

3 DISCUSSION

3.1 Regulation of the light input pathway in *N. crassa*

frq was identified in mutant screens as a clock gene, essential for self-sustained rhythmicity (Feldman and Hoyle, 1973). Research since then has led to the hypothesis that *frq* is the central component of the *Neurospora* rhythm generator (Aronson et al., 1994; Dunlap, 1999). However, results from Merrow et al. (1999) have shown that *frq*-less mutants can be entrained in temperature cycles, suggesting the existence of an FRQ independent oscillatory machinery. Furthermore, FRQ deficient mutants are not entrainable in light-dark (LD) cycles, leading to the conclusion that FRQ has a role in a light input pathway regulating conidiation. To get deeper insight into this novel role of FRQ we focused our research on regulation of *frq* and *wc–1* gene expression.

3.1.1 Levels of WC-1 protein are circadianly regulated

WC-1 protein has been established as a critical component of the light input pathway (Harding and Shropshire, 1980; Russo, 1988; Linden and Macino, 1997). Subsequent work has shown that WC-1 deficient mutants are also arrhythmic, defining *wc-1* as an essential clock gene (Crosthwaite et al., 1997). mRNA and protein of the clock gene *frq* are circadianly rhythmic in constant darkness (DD) (Aronson et al., 1994b; Garceau et al., 1997) (Fig. 10). Analysis of *wc-1* expression under the same conditions revealed variable but not rhythmic *wc-1* mRNA levels (Fig. 11), although WC-1 protein does oscillate (Fig. 11). The maximum of WC-1 levels coincides with the FRQ protein minimum, indicating that their regulation is different. As they are both known to be induced by light, one hypothesis might hold that they are reglated similarly. Level of WC-1 protein rise around the middle of the subjective night and peak at dawn (Fig. 11). Similar results have been published by Lee et al. (2000). What could be biological importance of such timing? Recent studies showed that WC-1 functions as both a general and a circadian photoreceptor (Froehlich et al., 2002; He et al., 2002). High levels of photoreceptor at dawn would increase light sensitivity and triggering of light responses to maximal levels. Interestingly, two other circadian photoreceptors, CRY in *Drosophila* (Emery et al., 1998) and PHY B in plants (Bognar et al., 1999) show similar

characteristics. Besides their function as general photoreceptors they also serve as circadian photoreceptors and their levels are circadianly regulated. It seems plausible that circadian regulation of the systems photoreceptors is a general mechanism involved in the light input to the clock.

The unexpected finding that arrhythmic *wc-1* mRNA gives raise to the rhythmic protein indicates involvement of posttranscriptional regulatory mechanisms. This is discussed in chapter 3.3.

3.1.2 Interdependent regulation of FRQ and WC-1

The suggested role of WC-1 as photoreceptor and the light-regulation of *frq* mRNA synthesis implies that WC-1 controles *frq* expression. Indeed, *frq* mRNA is low in WC-1 deficient mutants (Fig. 12)(Crosthwaite et al., 1997). There is also evidence for reciprocal regulation: basal (DD) levels of *wc-1* mRNA and protein in FRQ deficient strains are lower than those observed in *wt* (Fig. 13). Thus, putting *frq* regulation simply downstream of the WC-1 would be incorrect because FRQ regulates WC-1 levels.

A negative-feedback loop model was proposed for the *Neurospora* clock almost a decade ago (Aronson et al., 1994b): the *frq* gene is transcribed and, upon translation, protein negatively feedbacks on self-transcription. Positive regulation of the *wc-1* gene by FRQ proteins shown in this study (Dragovic et al., 2002) indicates that at least one additional positive-feedback loop is involved in *Neurospora* clock mechanism. Via this positive feedback loop FRQ may positively regulate its own levels: FRQ protein transcriptionaly activates *wc-1*, WC-1 protein level increases what leads to an increase of FRQ levels. This hypothesis is in good agreement with the model presented by Lee et al. (2000). But the question remains how do these two feedback loops generate circa 24 h rhythmicity?

3.1.3 Circadian regulation of light responses

The fact that WC-1 and FRQ levels oscillate in DD, suggests that the strength of light responses depends on circadian time. Indeed, gene regulation from photoreceptor mRNA induction to induction of enzymes is dependent on the time of subjective day (Merrow et al., 2001). What are the roles of FRQ and WC-1 in circadian regulation of light

responsiveness? FRQ seems to be critical element because circadian modulation of carotenogenesis is absent in *frq*-null strain, despite intact carotenoid induction by light. Circadianly regulated FRQ protein may transduce the circadian modulation of light responses by regulating WC-1 levels. This hypothesis is in good agreement with fact that WC-1 protein levels and the capacity to induce carotenoids with light (Fig. 12 and 15) both peak at the same time of day i.e. shortly before subjective dawn.

Thus, circadian regulation of light signaling is evident at numerous levels, from some of the earliest known events of light detection to enzymatically regulated, downstream outputs.

3.2 Novel photoreceptors in *Neurospora*

3.2.1 *wc* mutants respond to light

The *wc* mutants have repeatedly been found to be non–responsive to light, leading to the conclusion that they are completely blind (Ballario et al., 1996; Cheng et al., 2001a; Cheng et al., 2001b; Linden and Macino, 1997; Schwerdtfeger and Linden, 2001; Sommer et al., 1989). Here, I report that the *wc* mutants, readily synchronize conidial band formation at light levels that are far below those encountered in natural daytime conditions (Figs. 22 - 25). The key to this observation was the use of entrainment protocols (24 h light:dark cycles). Previous assays examining the effects of light on conidiation in the *wc* mutants, e.g., (Crosthwaite et al., 1997) used only constant light or constant darkness in combination with media containing high levels of carbon source. In other experiments, a light pulse delivered in otherwise constant darkness revealed a response to light that could not be evaluated because conditions did not favor self-sustained rhythms (Crosthwaite et al., 1997; Ninnemann, 1991). The entrainment protocols used here clearly demonstrate a novel light input pathway in *Neurospora*. The first observation was obtained using *wc-1* RIP strain ($wc\text{–}1^{RIP\#7}$) and a *wc-2* point mutant ($wc\text{–}2^{234w}$; see Methods). Subsequent experiments on knock-out mutants confirms that the entrainment occurs in the complete absence of WC-1 or WC-2 proteins (Fig. 24 and 25). The description of a robust, light regulated output supports the existence of a photoreceptor, which is neither WC-1 nor WC-2. Finding that the *wc-1* knock-out mutant

is entrainable by light does not eliminate WC-1 protein as a photoreceptor candidate, but rather introduces the possibility of a additional one (Fig. 43).

Multiple photoreceptors in *Neurospora* have been already suggested (Dharmananda, 1980) based on multiple peaks and discrepancies of action spectra when using different read-outs, namely phase shifting vs. light–induced carotenogenesis (De Fabo et al., 1976). This study provides the first genetic evidence for this hypothesis. Two branches of a light input pathway are defined at the genetic level by demonstrating that light regulated conidiation persists in *wc* mutants blind for carotenogenesis and other light responses (this thesis and Merrow et al., 2001). In this thesis is shown that there are differences between the *wc–1* $^{RIP\#7}$ and other *wc-1* mutants in light induced gene expression. In the *wc–1* $^{RIP\#7}$ background, these responses can be divided in two groups: one in which the response was completely abolished (*vvd* mRNA induction) and another in which the light induction is altered but is still significant (*frq*). The reduced induction of *frq* mRNA and protein could reflect a low-dosage effect of the truncated WC-1 protein. Also, deletion of the Q (glutamine)-rich N-terminal domain could be important for achieving a full activation profile. If *Neurosora* has additional photoreceptors, their function could be elucidated in a *wc–1* $^{RIP\#7}$ background what would allow their dissection at functional and molecular level.

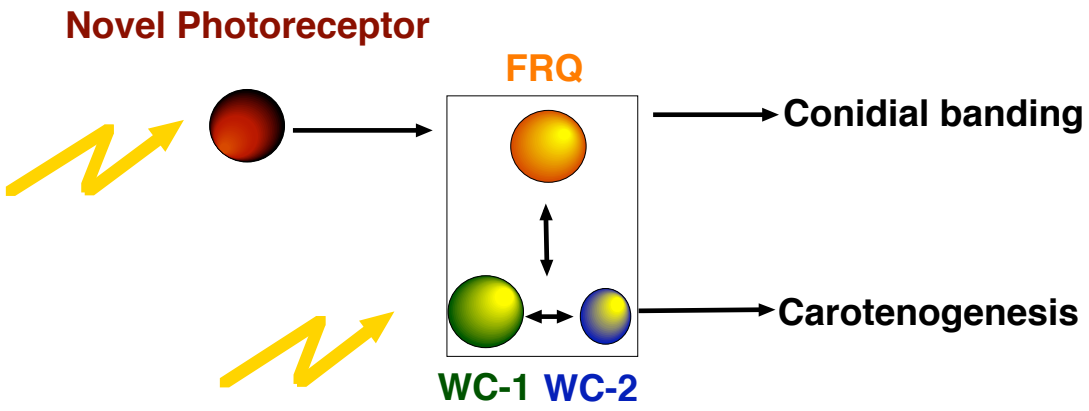

Figure. 43 Model of light input pathway based on genetic and molecular evidence for a novel photoreceptor in *Neurospora*. Carotenogenesis requires both WC proteins, while regulation of conidiation is completely abolished without FRQ. All three proteins are part of a complex that modulates their gene expression (for details about protein complexes see: Crosthwaite *et al.,* 1997; Lee *et al.,* 2000; Merrow *et al.,* 2001; Cheng *et al.*, 2002; Goerl *et al.,* 2002;). Symbols: Filled circles, protein products; lightning, exogenous light; rectangle, protein complex formation.

3.2.2 What are the photoreceptors in *Neurospora*?

Based on functional comparisons with the WC-1 protein, FRQ might be proposed for this role. This is unlikely, given that FRQ has no signature sequences that indicate photoreceptor function (McClung et al., 1989). It is more likely that a novel photoreceptor is involved in circadian photoreception in *Neurospora*.

Multiple circadian photoreceptors have been already described in other models. In *Arabidopsis*, two Cryptochromes and three Phytochromes function as circadian photoreceptors. Moreover they overlap in their circadian function (Quail, 2002). The entrainment of circadian rhythms by blue/UVA light is influenced by input from both CRY1 as well as phytochromes. Another class of flavoproteins, phototropins (NPHs) is required for the phototropic response to light and so far it has not been shown that they have an influence on circadian rhythms (Christie et al., 1998). WC-1 has the highest homology to the phototropins (Froehlich et al., 2002; He et al., 2002).

The *Neurospora* genome project has recently revealed the presence of homologues of *cryptochrome* and *phytochromes* photoreceptors. The photoreceptor

candidate NCU00582.1 has shown a high level of homology to members of the DASH family of cryptochromes (Brudler et al., 2003). Almost all members of this family have already been well established as circadian photoreceptors indicating that *Neurospora* cryptochrome could function similarly. Cryptochromes are evolutionary closely related to photolyases and these two groups show a high level of homology. The protein sequence of NCU00582.1 (called here "*cry* homologue") is clearly distinguishable from photolyases. In DASH *cry*, the cavity for binding the thymine dimer becomes wider and shallower than in photolyases through replacement of specific amino acids (Fig. 39) (Brudler et al., 2003). The consequences of these replacements should be lower affinity for pirimidine dimers and loss of photolyase activity. Moreover, the gene for the *Neurospora* photolyse is already known and the protein product repairs UV-induced DNA damage. *Neurospora cry* shares all 15 aa residues of *Arabidopsis cry* (another member of the DASH family) involved in FAD binding but only 5 of 12 residues involved in 8-HDF binding (Fig 39) and (Tamada et al., 1997). This suggests that the second *Neurospora* chromophore may be distinct or even absent in *Neurospor*a *cry*, although the structures retain sufficient space for either second chromophore to bind. It is also possible that a second chromophore is still present but the mechanism of photon capture and transfer to flavin is different than in photolyases. Based on the predicted protein structure of *Neurospora's cry* and other cryptochromes and given that structural requirements for photolyase activity are well known, it is likely that the NCU00582.1 protein retains photoreceptor features but cannot repair photodimers.

In working towards a preliminary model for how *frq*, *wc–1*, *wc–2*, *cry* and the *phys* interact, the regulation by light was determined for the new photoreceptor candidates. *cry* mRNA is strongly (≈500X) induced in response to a light pulse (Fig. 42) It reaches peak within 30 minutes and adapts within 1 hour. Relative to its levels in darkness *cry* mRNA is elevated in constant light (≈150X). Of the two phytochrome homologues only, *Phy5* mRNA is activated at the level of transcription. The profile is, however, very different from *cry* mRNA. The kinetics is slower and full induction takes around two hours. *Neurospora* light regulated genes can be divided into early light regulated genes with an peak at 20-30 minutes after onset of light and late regulated genes with maximum mRNA accumulation after 45 to 120 min (Lewis et al.,2002)

(Sommer et al., 1989). *cry* and already known components of light input in *Neurospora frq, wc-1 and vvd* (Fig. 41) belong to the fast light-regulated genes. The *Neurospora cry* may be novel circadian photoreceptor, based on regulatory and sequence features.

3.2.3 Dual light input pathway in *N. crassa*

Separate light input pathways for carotenogenesis and conidiation can be genetically defined by demonstrating that light–regulated conidiation persists in the otherwise blind, *wc* mutant strains. WC-1 protein is required for a subset of light-regulated physiological responses (e.g., carotenogenesis), but another output (e.g., conidiation) can be regulated with light without WC-1 or WC-2. The existence of a dual light input pathway is additionally supported by the fact that carotenogenesis and conidiation have vastly different light sensitivities (Fig. 14). However it would be wrong to say that conidiation is completely intact in the *wc* mutants. One consequence of WC deficiency is a strong sensitivity defects (Fig. 26). FRQ deficient strains can produce light induced carotenoids but the amplitude of the response is about half of *wt* (Fig. 14). These findings indicate that two light input pathways, to some extent, share same components, namely WC-1, WC-2 and FRQ.

Additional evidence for multiple light input pathways can be seen in differences between the $wc\text{–}1^{RIP\#7}$and $wc\text{–}1^{KO\#99}$strains in light-induced gene expression. *frq* mRNA and protein are light induced in the $wc\text{–}1^{RIP\#7}$ strain (Fig. 28) but not in the $wc\text{-}1^{KO\#131}$ or $wc\text{–}1^{RIP\#21}$ background. In contrast to *frq*, *vvd* mRNA is not induced in either *wc-1* mutants. Given that $wc\text{–}1^{RIP\#7}$ produces low level of WC-1 protein, *vvd* and *frq* genes probably have different requirements for WC-1 protein. Unlike *frq, vvd* requires higher amounts of WC–1 to activate light-regulated transcription (Fig. 31). One explanation is that the residual WC-1 protein present in $wc\text{–}1^{RIP\#7}$ strain is sufficient to achieve conidiation-related function but not sufficient to fulfill its role in the carotenogenesis pathway. This hypothesis indicates that VVD is part of the carotenogenesis pathway, which is is in good agreement with physiological data. The most conspicuous feature of a *vvd* mutation is the abnormally high carotenoid accumulation, but VVD also modulates the effects of light input to the circadian system. These effects are likely mediated by

disrupting adaptation of the response under prolonged light exposure (Heintzen et al., 2001; Schwerdtfeger and Linden, 2001; Shrode et al., 2001).

3.2.4 FRQ role in regulation of conidiation and carotenogenesis

As previously shown, FRQ deficient strains cannot synchronize conidiation in light-dark cycles. To test whether FRQ is required only for the conidiation pathway or also for other light regulated outputs, light inducible carotenogenesis was used as readout. Results showed that *frq*-null strain still synthesize carotenoids upon light induction, although overall accumulation is about half of *wt* (Fig. 14). This strongly suggests that FRQ modulates both conidiation and carotenogenesis. But while one light-regulated response (synchronized conidiation) is completely absent, the other one (carotenogenesis) shows modest deficits.

The response strength of light–induced carotenogenesis is greater with FRQ than without (Fig. 14) and the fluence rate threshold is unchanged in either case, i.e., there is no sensitivity defect. Thus, in the carotenogenesis pathway, FRQ functions as a response amplifier without changing sensitivity. How can a non-photoreceptive molecule fulfill this function? The amplitude of the light-induced carotenogenesis may be simply regulated by the amount of the photoreceptor (WC–1); FRQ could indirectly, by increasing levels of photoreceptor, increase the amplitude of the response.

In the case of conidiation, fluence titration reveals different levels of sensitivity defects in the different *wc* mutants (Fig. 26). Despite undetectable levels (less than few % relative to *wt*) of WC-1 protein, the $wc\text{–}1^{RIP\#7}$ strain still approaches wild type sensitivity. The same strain is able to generate approximately 50% of light induced light induced FRQ protein levels relative to the *wt* (Fig. 32). Intrinsically, strains with the lowest sensitivities for light regulated conidiation ($wc-2^{234w}$) and double mutant $wc\text{–}1^{RIP\#7}wc\text{–}2^{234w}$) have the least FRQ (about 5% of wild type levels). These experiments suggest an additional role for the FRQ protein as a sensitivity amplifier. Function of FRQ as sensitivity amplifier is probably mediated by binding to self and WC proteins andd regulating WC-1 protein levels (Crosthwaite *et al.,* 1997; Lee *et al.,* 2000; Merrow *et al.,* 2001; Cheng *et al.*, 2002; Goerl *et al.,* 2002). However, photoreception for conidiation is a composite of FRQ, WC-1, WC-2 and the function of a novel photoreceptor.

Information about this as yet unidentified photoreceptor will supplement our knowledge about the FRQ role in conidiation light input pathway.

3.2.5 A self-sustained circadian rhythm in the *wc* mutants

Another deficiency reported for the *wc* strains is their lack of circadian rhythmicity (Crosthwaite et al., 1997). However, given that *frq* deficient mutants, are rhythmic under restricted conditions (Aronson et al., 1994a; Loros et al., 1986), we tested the *wc* mutants for self–sustained rhythmicity with the media and race tubes used in the light dark, entrainment protocols. In constant darkness, both $wc\text{–}1^{RIP\#7}$ and $wc\text{–}2^{234w}$ mutants exhibit a self–sustained circadian rhythm. As reported for the *frq* mutants, the rhythmicity lacks circadian qualities, in this case precision, and the period tends to be longer than wild type. This observation is helpful in modeling the circadian system; there is circadian machinery beyond the *frq*/*wc* transcription-translation feedback loop that oscillates with a circadian period. This circadian machinery lacks many circadian qualities, which the transcription-translation feedback loop may contribute to the intact system.

3.2.6 Action spectrum of FRQ protein induction

Action spectra for different light responses revealed that light perception in *Neurospora* occurs only in the near ultraviolet (UVA) and blue part of the spectrum (De Fabo et al., 1976; Dharmananda, 1980; Sargent and Briggs, 1967). Genetic and biochemical evidence for the participation of flavin species in blue-light perception came from the studies of different mutants and light induced absorbance changes of tissue (Ballario et al., 1996; Linden and Macino, 1997; Linden et al., 1997; Ninnemann, 1979; Paietta and Sargent, 1981). Recent studies reported by He et al., (2003) present convincing evidence that the WC-1 protein binds FAD and functions as blue/UVA photoreceptor. To test whether WC-1 is the photoreceptor which regulates *frq*, an action spectrum of FRQ protein induction was made.

The equal-intensity action spectrum (Fig. 35) and the dose-response-curves based action spectrum (Fig. 36-38) reveal the same results for the *wt* strain. Two peaks in sensitivity can be observed, one at 380 nm and second at 460 nm. This is in good

agreement with previously published action spectra that describe photoreceptors for photosuppression of conidiation (Sargent and Briggs, 1967), phase shifting (Dharmananda, 1980) and light regulated complex formation with the *frq* promotor (Froehlich et al., 2002). All three action spectra reveal a peak in sensitivity around 450-470 nm, with no response to wavelengths above 520 nm and with sensitivity extending in to the UVA region. When the WC complex is purified from *Neurospora* tissue, it exhibited two excitation peaks at 370 and 450 nm which are characteristic of flavins (He et al., 2002). The action spectra provide functional evidence that the phototransduction mechanism involved in regulation of *frq* expresion is mediated by flavin species (Fig. 38) (Froehlich et al., 2002).

In contrast to conidiation only one action spectrum has been done to functionally characterize photoreceptor(s) that regulate carotenogenesis. The action spectrum for carotenoid induction (Fig. 8) (De Fabo et al., 1976) shows a major peak at 460 nm and second lower peak (≈25% of major peak) at 370nm. These data contrast the action spectrum of FRQ induction, indicating that different photoreceptor(s) could be involved in regulation of carotenogenesis and conidiation. The same hypothesis was previously suggested by Dharmananda (1980).

An equal-intensity action spectrum of FRQ induction revealed differences between *wt* and the *wc-1*$^{RIP\#7}$ mutant (Fig 35). In the *wt* strain it is possible to observe two peaks in activity one at 380nm and a second at 460nm. In the *wc-1*$^{RIP\#7}$ mutant only one peak is detectable, at 460 nm. Although the equal-intensity action spectrum cannot be taken as a definite spectral characterization of FRQ induction in *wc-1*$^{RIP\#7}$, the idea that FRQ induction is regulated with more than one photoreceptor looks plausible.

3.3 Posttranscriptional regulation of *wc-1* expression

Involvement of posttranscriptional regulation in *wc-1* expression is indicated by the observation that constant *wc-1* transcript give rise to rhythmic WC-1 protein (Fig. 11) (Lee et al., 2000). Data presented in this study (chapter 2.2) shown that the *wc-1* mRNA is amenable to regulation by RNA-protein interactions. Gel-shift studies revealed several protein complexes, which specifically interact with the 5' and 3' untranslated regions

(UTRs) of the *wc-1* mRNA (Fig. 17 and 18). Formation of one RNA-protein complex in the 5' UTR region and two in the 3' UTR was detected (Fig. 17 and 18). Gel-shift assay was further used to investigate circadian and light regulation of mRNA-protein complexes formation at both 5' and 3' UTRs.

3.3.1 Regulation of translation efficiency by binding to the 5' UTR

It is already known that formation of mRNA-protein complexes in the 5' UTR could control translation initiation. The best described example of this mechanism is the regulation of mRNAs encoding proteins involved in iron metabolism. Iron regulatory protein (IRP) binds to an RNA element (iron responsive element, IRE) in the 5' UTR of mRNA for ferritin and represses the translation of the downstream open reading frame by steric blockage of the ribosomal entry (Goossen et al., 1990; Hentze et al., 1990; Walden et al., 1988). In view of the analogy with the IRE-IRP system and the 5' UTR location of the *wc-1* mRNA-protein complex formation, the effect of the RNA-binding protein on *wc-1* activity could be translational repression (Fig. 44). To confirm this hypothesis would be necessary to delete binding site and test molecular and physiological consequences *in vivo*.

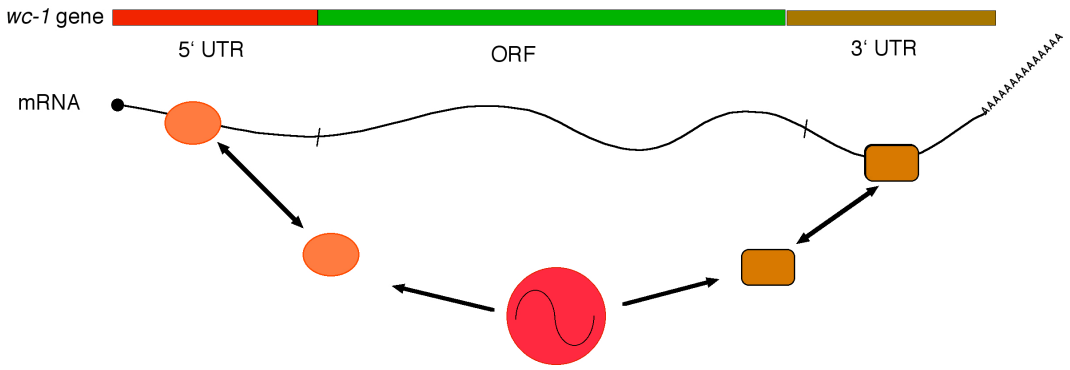

Figure 44. A model for mRNA binding proteins in the *Neurospora* clock mechanism. Unknown proteins bind specifically RNA sequences in 5' and 3' untranslated (UTR) regions of *wc-1* mRNA influencing translational efficiency or stability of mRNA. Without changes at the transcriptional level, WC-1 proteins can oscillate over the course of the day.

3.3.2 Adaptation in constant light and regulation of mRNA stability by binding to the 3' UTR

Profiles of light induction at the mRNA level have been described for many *Neurospora* genes (Linden et al., 1999). This phenomenon cannot be explained simply with regulation at the transcriptional level. If endogenous promoters would remain active in continuous light, mRNA abundance would continuously rise throughout the time course and reach a steady state. Thus, it is unlikely for mRNA levels to reach a peak and then fall to basal levels in the continuous presence of the stimulus unless the same stimulus also triggers promoter repression or a specific degradation pathway later in the time course. Elements involved in mRNA destabilization could be present anywhere in the mRNA, but majority of these sequences are situated in the 3'-UTRs (Hentze and Kulozik, 1999; Preiss and Hentze, 1999).

In this study it is shown that few protein complexes bind specifically to the 3' UTR of *wc-1* mRNA (Fig. 17, 18 and 20) and some of them are regulated with light (Fig. 21). Function of shown protein complexes binding to the 3' UTR of *wc-1* mRNA remain to be defined, but one hypothesis involves them in regulation of *wc-1* mRNA stability. This would not be first example for the involvement of such a postrancriptional mechanism in

the clock. It has been shown that stability of mRNA plays a regulatory role within the mammalian and the *Drosophila* circadian oscillator as well. In continuous light *mPer1* levels show transient profile of mRNA induction, suggesting the involvement of mRNA degradation (Edery, 1999; Kim et al., 2002; Stanewsky et al., 2002; Wilsbacher and Takahashi, 1998).

4 MATERIALS AND METHODS

4.1 Physiological Methods

4.1.1 Strain maintenance

Bench-stocks of *Neurospora* are maintained in glass tubes as conidial cultures on solid media (Vogel's minimal media supplemented with 2% glucose as carbon source, see Appendix). Cultures were kept at room temperature in a closed cabinet to avoid drafts. 4-5 days after inoculation, conidia can be used to inoculate other slants, flasks, race tubes and liquid cultures. Conidia production stops after 7 -10 days, but they usually stay viable at room temperature for a year or longer. Older cultures will take longer to germinate than young ones.

4.1.2 Media supplements

Metabolic mutants (auxotrophs) like *his-* or *aro-* require additional supplements for growth. Mutant selection or maintenance of heterokaryotic strains requires the addition of selective agents to the growth media. For routine laboratory work, it was convenient to maintain concentrated stock solutions of supplements that can be easily added to the media. To avoid autoclaving, supplement stock solutions were filter sterilized and stored at –20°C so that they can be added before or after autoclaving. A list of recommended concentrations for supplements is in the Appendix.

4.1.3 Stock management

7-10 days old cultures on slants (same as for bench-stocks) were closed with cotton plugs, sealed with Parafilm and frozen at –20°C. Conidia prepared in this way can survive at least a few years. Stocks of *Neurospora* should not be maintained by serial inoculations since this might lead to the accumulation of mutations.

4.1.4 Lab practice

All *Neurospora* transfers, inoculations, platings, etc. were performed on a normal lab-bench, taking care to work near a Bunsen burner. All transfers were done in a draft-free room. Decontamination of the work-space was accomplished with 70% spiritus. Wearing of laboratory coats may also increase the risk of contamination because accumulation of spores. I autoclaved all used cultures, contaminated glassware or media before discarding or washing.

4.1.5 Conidial suspensions-inoculum

Liquid cultures are inoculated with conidial suspensions, such that the final concentration was between 0.1 and 1 x 10^6 conidia per 1 ml of media. Suspensions for inoculation (inoculum) were made from conidia grown in 250-1000 ml Erlenmeyer flasks with 50-200 ml solid Vogel's medium for 10 to 14 days. Auxotrophs (i.e. histidine auxotrophs) may require up to twice as long to yield sufficient amounts of conidia. Inocula are prepared by adding 50-100 ml sterile distilled water into the flask cultures, reclosing the flasks, swirling and shaking for 20-40 minutes. To prevent contamination it is important that airborne conidia have settled before opening the flask. After conidia were suspended in water, they were filtered through four cheesecloth layers. Absorption of the suspension was measured at 420 nm after a 1:10 or 1:20 dilution. A conidial suspension of optical density 1.0 at 420 nm has 2.86 10^6 conidia per ml. Aliquots of conidial suspension were stored at –20°C. Conidial suspensions stored in this way have slightly lower germination capability, and are stable for at least 1 year. This guarantees repeatable and comparable experimental results if the same prep is used.

4.1.6 Liquid cultures

Liquid cultures were used to grow tissue for evaluation of molecular components. Mycelia were grown in liquid medium by inoculating conidial suspension into the modified Vogel's or Westergaard's medium. In liquid cultures in Petri dishes, *Neurospora* forms a mycelial mat on the surface of the medium, followed by subsurface growth. After incubations longer than 2 days, the mat forms aerial hyphae and conidia on

the walls of dishes and on the upper surface of the pad. Slow rotary shaking (75-100 rpm) or submersing mycelial mats with a sterile pipette tip can avoid conidia formation. The average yield per ø85mm Petri dish with 25 ml Vogels's media was around 250 mg mycelia (after drying by blotting or vacuum filtration). Agitated liquid cultures in Erlenmeyer flasks were also used. This kind of culture yields a larger amount of mycelia and minimizes problems with conidiation. Vigorous shaking (200 rpm) prevents formation of clumps and improves aeration.

4.1.7 Sexual crossing

For all crossing, synthetic medium was used (see Appendix). Crosses are made by inoculating Petri dishes with the female parent first, incubating it for three to five days at room temperature, but not higher than 25°C. Conidia of the male parent were spread over the slant. The cross was incubated in laboratory LD conditions at room temperature for two to three weeks, by which time ascospores were shot to the lid of the Petri dish. Ascospores were collected by suspending them in a drop of water. They are then plated on 2-4% agar and "picked". Picking was done with cutting out a small block of agar below the ascospore and transferring it to a slant with minimal or selective media. Ascospores were activated by heating slants at 60°C for 30 min in a water bath. The efficiency of activation is between 50 and 90%.

4.1.8 Carotenoid assay

To measure levels of mycelial carotenoids, we used cultures grown in special liquid media (see Appendix) in sterile Petri dishes (ø50 or ø85mm). 105 conidia per ml of media were inoculated into carot-media (see Appendix). 10 ml media for small (ø50mm) or 25ml media for bigger (ø85mm) Petri dishes was used. Mycelial pads were first incubated in constant light for 12-15 hours at 25 °C, then transferred to darkness (25 °C) prior to light induction. For some experiments, cultures were staggered to darkness, so that they could be light induced and harvested at approximately the same developmental stage. Prior to light induction, excess media was drained from the dishes. Sample cultures were evaluated by eye and by microscopy for the absence of conidial development.

Mycelial pads produce low levels of carotenoids even in darkness. After light exposure, samples were harvested, dried by blotting or vacuum filtration and frozen in liquid nitrogen. Samples can be stored at –20°C or –75°C for several months.

Mycelial carotenoid content was determined essentially as described earlier (Linden and Macino, 1997) with some modifications. 20-200μg of tissue was disrupted in a Ribolyzer (see Appendix) on maximal speed setting (4.5) for maximal time (1 minute). Disruption was done in 1.5-2.0 ml screw cap tubes filled with 500 μl n-hexane, 500 μl methanol (n-hexane saturated), 500μg sand and 500μg glass beads. Hexane is partially dissolvable in methanol so it has to be saturated with methanol prior to extraction. Following centrifugation (5 minutes at 10,000g) the supernatant was collected, transferred to hexane-resistent plastic or glass cuvettes and the absorption at 445nm was determined. If the absorbance of samples was too high (more then 1.0), dilutions were made.

4.1.9 Race-tube assay

A race tube is a hollow glass tube (40 or 60 cm long, 1.2 to 1.4 cm in diameter) bent at the ends and partially filled with a solid growth medium. They permit visualization of linear growth for about a week and are thus ideal for experiments aimed at describing timed developmental events. Race tube medium for these experiments is 1x Vogels salts, 2% agar, 0.5% arginine and 10 ng/ml biotin. As an additional carbon source glucose or quinic acid were used at different concentrations, as indicated. When quinic acid was used, the pH of the medium was additionally adjusted to 6.0. For some experiments additional carbon sources were not added, resulting in clearer band formation. Race tube experiments were started with inoculation, germination for 1 day in constant light and subsequent transfer to experimental conditions. Experiments ended when the growth reached the far end of the tube (>1 week). Lights source was cool white fluorescent or solarium light bulbs (L36W/67 and L80W/79, Osram, Germany). All LD experiments were strictly controlled and many were permanently recorded for temperature maintenance at 25 °C to exclude temperature effects. Race tubes were marked once per day to facilitate correlation of growth and conidial development with elapsed time.

When the mycelial front reached nearly the end of the race tubes, the tubes were scanned (AGFA Snapscan with 150 dpi resolution, grayscale). The file was saved in a PICT format and analyzed with the CHRONO program (Roenneberg and Taylor, 2000) (see also Appendix).

Fluence titration experiments were analyzed by averaging the race tube data for each strain at each fluence rate (per fluence, 2 race tubes for the wild type, and 4 to 6 race tubes for each mutant; all race tubes were used, i.e., no selection was made). The degree of light–regulated synchronization of conidiation was assessed by periodogram analysis (Sokolove and Bushell, 1978) for each averaged time series using the CHRONO program.

4.1.10 Light induction and light dark experiments with liquid cultures

After inoculation all cultures were held in constant light for the day prior transfer to constant darkness (DD) or to the dark part (D) of a light/dark (LD) cycle.

For light induction experiments, cultures were held in constant darkness and after the indicated time (in figure legend) they were exposed to continuous light until they were harvested, dried and frozen in liquid nitrogen.

For LD experiments cultures were held in LD conditions and harvested in the dark or light part of the cycle (as indicated).

In cases where the time between the first and last harvests was longer than 4 hours samples were age matched by inoculating them at different times. All experiments were done in temperature controlled rooms at 25°C. Light from cool white fluorescent bulbs was used (L36W/67, Osram, Germany). Light intensity was determined with a photometer calibrated for spectral sensitivity from 220-1000 nm.

4.2 Strains

In *N. crassa* the conidiation rhythm is obscured in wild-type strains grown in closed culture tubes, presumably owing to a high CO_2 concentration (Sargent and Kaltenborn, 1972). Strains harboring the *band* (*bd*) mutation can display circadian conidiation under the same culture conditions (Sargent and Woodward, 1969). *bd* mutation facilitates

visualization of the circadian phenotype but does not alter the circadian rhythm. All strains used in this study also contain the *bd* mutation and they are listed below:

- The *bd a* strain was used as wild-type (wt) strain in this study. This is the standard laboratory strain available from FGSC (#1859 mating type a and #1858 mating type A).
- In *bd*, frq^{9} a base pair deletion in the frq ORF results in production of a truncated protein and loss of FRQ protein function (Loros and Feldman, 1986).
- *bd,* frq^{10} was generated by deletion of the promoter and almost the entire *frq* ORF (two central Bgl II fragments, 5.3 kb) (Aronson et al., 1994a).
- *bd*, $wc\text{-}1^{RIP\#7}$ was obtained by crossing the *wc-1* RIP mutant (Talora et al., 1999) into the *bd* background. In this mutant, the *wc-1* promoter and a few hundred bps after the start codon are RIPed. For RIPed sequence, see Fig. 22.
- *bd*, $wc\text{–}1^{RIP\#21}$ is a mutant with a non-functional *wc-1* allele, generated by introducing stop codons in the entire ORF by RIP (Y. Liu, personal communication, and (He et al., 2002)).
- *bd*,$wc\text{–}1^{KO\#131}$ was made by the gene replacement method. The *wc-1* ORF-segment encoding amino acids 59-1133 and part of the 3'UTR has been replaced with the gene for hygromycin resistance (*hph, hygromycin B phosphotransferase*; (Lee et al., 2003).
- The *bd*, $wc\text{-}2^{234w}$ mutant (FGSC#3817) is a point mutant with a premature stop codon, creating a truncated WC–2 protein of 356 amino acids, lacking the zinc finger (Linden and Macino, 1997).
- The *bd*,$wc\text{-}2^{KO\#99}$ is a complete wc–2 knockout strain obtained by the gene replacement method. The ORF has been replaced by hygromycin resistance cassette (Collett et al., 2002).
- The *bd,* $wc\text{-}2^{234w}$ $wc\text{-}1^{RIP\#7}$ is triple mutant obtained by crossing the *bd*,$wc\text{-}1^{RIP\#7}$ and the *bd*,$wc\text{-}2^{234w}$ mutant. The screen for double mutants was done with western blot analysis. To determine absence of WC-1 protein and confirm presence of truncated WC-2^{234w} protein, anti-WC-1 and anti-WC-2 antibodies were used.

4.3 DNA methods

4.3.1 DNA purification

4.3.1.1 Plasmid isolation from E. coli

4.3.1.1.1 Phenol extraction –"Mini-preps"

For these preps, overnight cultures of *E.coli* were grown in 2-3 ml LB, with 100 μg/ml ampicillin added. 1.5 ml of the bacterial cultures were spun in an eppendorf tube for 1 min at 4,000-5,000 g. The media was poured off and the pellets were suspended in the residual media. 100 μl of GET buffer (see Appendix) and 150 μl of alkaline lysis buffer (see Appendix) were added to resuspended bacterial cells and incubated on ice for 5 minutes. 120 μl of 3 M sodium acetate pH 6.0 was added and mixed by inverting the tube a few times. One or two phenol extractions at pH 8.0, followed by an additional chloroform:isoamylalcohol (Ch/IAA; 24:1v/v) extraction, were done in order to remove cell debris, proteins from the aqueous phase and residual phenol. RNA was removed by digestion with RNase1. Precipitation of DNA was done with 1/10 volume sodium acetate and 1-2 volumes of ethanol.

4.3.1.1.2 Silica columns – "Midi & Maxi-preps"

For midi and maxi preps, overnight cultures of *E.coli* were grown in 150 or 300 ml LB media, with 100 μg/ml ampicillin added. For isolation of plasmid DNA. Commercial Kits (NucleoBond 500 and Jet-star 2.0) were used according to instruction manual.

4.3.1.2 DNA extraction from conidia

Conidial cultures were grown in 13 x 100 mm tubes on 1.5 ml slopes of Vogel's minimal medium with 2% glucose. 7 to 10 day old conidia were harvested by adding 2-3 ml of sterile 1x TE, pH 8.0, and vortexing. The conidial suspension was transferred into a new 2 ml Eppendorf tube (0.5 ml conidial suspension per 2 ml tube) and placed in a boiling water bath for 15 minutes. After boiling, tubes were cooled at room temperature and spun at 14,000 for 5 minutes at room temperature. DNA was precipitated with ethanol and sodium acetate as described below. The pellet was resuspended in water and stored at

–20°C or –75°C. This rapid method was used when DNA from numerous samples (e.g. mutant screening with PCR) was necessary.

4.3.1.3 DNA extraction from mycelia

We used two different methods to extract DNA from mycelial tissue, but homogenization of mycelia and DNA precipitation (see below) were always the same. Tissue was dried by vacuum filtration or blotted, placed in eppendorf tubes and frozen in liquid nitrogen. Samples were either processed immediately or stored at –75°C. Mycelial pads were disrupted with a mortar and pestle in liquid nitrogen with sand.

4.3.1.3.1 DNA extraction with phenol

For DNA preps we used phenol equilibrated to pH 8.0 (see Appendix). To prevent leakage, original Eppendorf tubes were used. For a single 1.5 ml tube, 500 μl of DNA extraction buffer (see Appendix) and 500 μl of phenol solution pH 8.0 were combined. After adding approximately 100 mg of pulverized mycelia, the tubes were tightly capped, vortexed at high speed for 15 s and placed in a horizontal tube-holder on a shaker. Samples were extracted at 300-400 rpm for 15-30 minutes at room temperature, centrifuged at 16,000 x g for 5 min at 2-4°C; tissue debris and sand pelleted to the bottom of the tube. After phenol extractions, the aqueous phase was transferred to a new tube, mixed with 500 μl of chloroform:isoamylalcohol (24:1v/v) and extracted once again. Emulsions were centrifuged at 4 °C or room temperature for 1 minute at 28,000g. The aqueous solution was transferred to a new tube and precipitated with 1/10 volume of 3M sodium acetate and 2-3 volumes of ethanol.

4.3.1.3.2 DNA extraction with CTAB

100-200 mg of ground mycelium was added to a 2.0 ml eppendorf tube with 800 μl of CTAB buffer, vortexed and incubated for 30 minutes at 60°C. An equal volume (800 μl) of Ch/IAA was added, samples were fixed horizontally, and shaken at maximal speed for 10-15 minutes. Samples were spun at 10,000 g for 5 minutes. The upper layer was removed to another tube and the chloroform extraction was repeated. RNA was removed by adding 10μl of RNase1 (1 mg/ml) per 1ml of aqueous and incubating for 15 minutes at room temperature.

4.3.2 Separation and purification of DNA on agarose gels

Agarose gel electrophoresis was performed according standard methods (Sambrook, 1989). DNA fragments used for cloning were separated by agarose electrophoresis. The gel was placed on a transilluminator and the band of interest was excised with a razor blade. DNA extraction from agarose was done by centrifugation. For gel slices under 100μl, LSKG ELO 50 filters (Millipore) were used. For slices up to 2,000 μl, Ultrafree-CL filters (Millipore) were used. The gel slice was placed in either filter and spun for 30 minutes at 5,000 g. DNA from the filtrate was precipitated with ethanol and sodium acetate to remove TAE buffer.

4.3.3 DNA quantification

DNA was quantified either spectrophotmetrically or in agarose gels. The OD for dilutions of DNA samples was determined at 260, 280 and 320 nm with a spectrophotometer. Care was taken that the OD is in the range from 0.1 to 1.0. Cuvettes made of quartz glass or disposable plastic (UV-clear) with a path-length of 1 cm were used. Quantifications were based on the assumption that an OD of 1.0 at 260 nm measured in a 1 cm cuvette indicates a concentration of 50μg/ml of DNA. A mixture of random oligomers at 20 μg/ml has an absorbance of 1.0 at 260 nm. The ratio of the absorbance at 260 to 280 was used as indication of purity. Ratios for all DNA solutions were between 1.8 and 2.0. The amount of DNA in one band (in a gel) was estimated by direct visual comparison with standardized, commercial molecular markers.

4.3.4 Sheering of DNA

For Northern analysis and gelshift assay experiments it was necessary to “sheere” high-molecular-weight DNA to a population of smaller molecules.

For Northern blots, Salmon sperm DNA is used to reduce non-specific binding of radioactive probe to DNA and RNA species on the membrane. DNA was dissolved in RNase free water at a concentration of 10 μg/μl and stirred 2-4 hours to solubilize. The DNA was sheared by passing the solution through a 17-gauge needle 20 times.

Polyguanylic acid (Poly-G) is used to block non-specific interactions in RNA gel shift assays. The length was reduced to a few hundred nucleotides by intense sonication in an ultrasound-bath (see Appendix) for 1 h. Poly-G molecules that are too long clog wells and actually bind the radioactive RNA non-specifically.

4.3.5 Digestion, ligation and transformation of DNA molecules

All restriction digestions were made with New England Biolabs (NEB) restriction enzymes and supplied buffers(see See Appendix). T4 DNA ligase (NEB) was used for ligation (see See Appendix). The overall concentration of vector + insert was always 10 ng/μl. The insert was added in 5-10 fold (molar) excess. Ligations were performed in the buffer provided with enzyme, at room temperature (20-25 °C) for 1h. For a 20 μl ligation mixture 1 μl of T4 ligase (concentration per 1 μl was 2X 10^6 NEB units) was used. The concentration of 5' termini was from 0.1 to 1 μM. Care was taken that the concentration of total DNA in the reaction mixture was not higher than 0.5 μg/μl. To avoid short-circuits and low transformation efficiency, electrolytes were removed from ligation reactions by ethanol precipitation (as described above). After precipitation, ligation products were dissolved in 10 μl of water for transformation.

4.3.6 Production of electrocompetent *E. coli* cells

XL-1 blue cells were streaked to an LB plate (no ampicillin). After overnight incubation, a single colony was inoculated to an overnight culture in 3 ml LB. On the next day, 2 ml of the overnight culture was added to 1L LB and the culture was shaken at 37°C until growth reaches mid-log phase (OD_{600} = 0.5-0.6). From this point, everything was kept ice cold and work was done in the cold room. Flasks and centrifuge bottles were chilled for at least 15 minutes on ice. The culture was split into four sterile 250 ml centrifuge bottles and spun for 15 minutes at 4000 g at 2-4°C. After decanting the supernatant the pellets were suspended in a total of 1L of ice cold HEPES and spun again under the same conditions. The supernatant was removed and the pellets were suspended in 20 ml ice cold 10% glycerol. The next centrifugation (again, 4000 g 15 min 2-4°C) was done in two sterile 15 ml falcon tubes. After centrifugation in the glycerol solution, the pellet is

loose and the supernatant should be removed by suction or by careful pipetting. In the end, the pellets were suspended in 2 ml ice cold 10% glycerol and aliquots of 50 μl per sterile eppendorf tube were made and stored at –75°C.

4.3.7 Transformation of *E. coli* cells by electroporation

Standard 0.2 cm electroporation cuvettes were cooled on ice. Electrcompetent E. coli cells were thawed on ice. The electroporation instrument was set at 2.5 kV, 200 Ω and 25 μF. 1 μl of the ligation reaction was added to 50 μl of electrocompetent cells. Cells were added to the electroporation cuvette and cuvette was immediately placed into the cuvette-holder. The electric pulse was delivered and the time constant was checked. (it should be more than 8 msec). After the pulse, 1 ml of SOC (see Appendix) was immediately added. Cells were removed to a sterile 1.5 ml tube and incubated with shaking for 30 minutes at 37°C. The cells were briefly spun, the supernatant was poured off and the cells were resuspended in the remainder of the supernatant. The cell suspension was plated on a Petri dish containing LB media supplemented with ampicillin. For 'blue-white' selection, 25 μl of X-gal (40 mg/ml in dimethyl formamide) and 25 μl of IPTG (20 mg/ml in water) were spread on the LB plate.

4.3.8 PCR

0.2 ml thin wall PCR tubes were used in a Primus MWG instrument. The template was either 500 ng to 1 μg of genomic DNA, 10-20 ng of plasmid DNA or 1 ng or less of a PCR product. The quality of genomic template significantly influenced the performance of PCR reactions. Therefore the quality of DNA was checked by agarose electrophoresis. When fragments were bigger than ~30 kb, the PCR yielded the desired products.

DyNAzyme (Taq DNA polymerase from Finnzyme company) was used at a final concentration of 0.04 U/μl (unit definition according Finnzyme company). Expand long template PCR system (Taq polymerase and Tgo DNA polymerase mix; Roche) was used at a final concentration 0.05 U/μl (unit definition according Roche). Concentration of dNTP was 350 μM for each nucleotide. All polymerases were used exclusively with supplied buffers.

List of PCR primers:

name	purpose	sequence	PCR program
wc-1 Eco (3')	5' UTR wc-1 cloning	CGG GAA TTC CAT GGT GGC TGC ATC GG	3 min 94 °C 40 cycles: ---------- 1 min 94°C 45 sec 52°C 45 sec 72°C ---------- 4 min 72°C
wc-1 Kpn (5')	5' UTR wc-1 cloning	CGG GGT ACC AAC GAC ACC CAC GGT CC	
wc1Kpn1(5')ACA-2	3' UTR wc-1 cloning	AAA GGT ACC TGC CTG CAG TGG AAG TCG G	5 min 95 °C 40 cycles: ---------- 1 min 95°C 30 sec 55°C 30 sec 72°C ---------- 4 min 72°C
wc1Sac1(3')ACA-2	3' UTR wc-1 cloning	AAA GAG CTC GTG TAA CCG TTG CCT CTG G	
wc1-orf2Kpn1(5)	ORF wc-1 cloning	AAA GGT ACC GCT CAA CAT CTT CCG CCT C	5 min 95 °C 40 cycles: ---------- 1 min 95°C 30 sec 55°C 30 sec 72°C ---------- 4 min 72°C
wc1-orf2Sac1(3)	ORF wc-1 cloning	AAA GAG CTC CTC CAT TCC GCT TCC ACG G	
Y wc1 (3')	wc-1RIP#7 cloning	CGG AGC CAC TAT CCA TG	5 min 94 °C 35 cycles: ---------- 1 min 94°C 1 min 52°C 1.5 min 72°C ---------- 4 min 72°C
Y wc1 (5')	wc-1RIP#7 cloning	TCT GCT TGA GTG ACA GC	

4.3.9 Real Time PCR analysis

For all RT PCR assays, I used a two-step SYBR green assay. In the first step samples were reverse transcribed with random hexamers and, in the second, they were quantified in a Real Time PCR reaction.

4.3.9.1 DNase digestion and reverse transcription

For Real Time PCR analysis RNA samples were prepared as described in sections 4.4.1 to 4.4.3. To remove residual DNA, RNA samples were treated with RNase-free Dnase 1 (Roche) at a final concentration 3U/μl (Unit definition according Roche) in 1X Dnase1 buffer (see Appendix). In the DNase1 mixture, the final RNA concentration was 0.1 μg/μl. The incubation was 10 min at 25°C followed by 10 min at 65°C. RNA was reverse transcribed to cDNA in a three-step incubation: 10 min at 25 °C, 30 min at 42°C and 5 min at 95 °C. For reverse transcription I used chemicals from an AB Kit for reverse transcription (Reverse transcription reagents N8080234). Final concentrations were as follows:

RNA (final concentration)	0.02 μg/μl
Reverse Transcriptase buffer	1X
MgCl2	5.5 mM
dNTPs	500 μM each
Random hexamers	2.5 μM
RNase inhibitor	1 U/μl
Reverse transcriptase	3.125 U/μl
water	Up to desired volume
Volume of reaction:	min 25 max 100 μl

After reverse transcription samples were diluted 1:1 with RNase free water.

4.3.9.2 Primer design

Primers for RT PCR reaction were designed with Primer Express software version 2.0 (Applied Biosystems). The desired DNA sequence was copied into a blank 'DNA PCR Document'. All primers were chosen based on following parameters (Params Tab):

Minimal melting temperature 58°C

Maximal melting temperature 60°C

Optimal melting temperature 59°C

Minimal GC % 20

Maximal GC % 80

3' GC clamp of 0 residues

Minimal primer length 9

Maximal primer length 40

Optimal primer length 20

Minimal amplicon melting temperature 0°C

Maximal amplicon melting temperature 85°C

Minimal amplicon length 50 bp

Maximal amplicon length 150 bp

Care was taken that primer pairs have a 'penalty score' lower than 10 points. All primers were ordered (from SigmaARK, http://www.sigma-ark.com/ or Metabion, http://www.metabion.com/) as HPLC purified. The final concentration of primers in the RealTime PCR reaction was 200 nM.

4.3.9.3 Real Time PCR analysis

An ABI Prism 7000 Sequence Detection System was used.
The thermal cycler was set for three stages:

- Stage 1: 50°C for 2 minutes
- Stage 2: 95°C for 10 minutes
- Stage 3: 40 cycles of: 95°C for 15 seconds followed by 60°C for 1 minute.
- Volume of the samples: 25μl
- "Emulation" of the 9600 ABI instrument was disabled.

All detectors were set for the fluorescent dye SYBR Green, which does not require a quencher. ROX was used as a passive reference.

Dissociation analysis was used to check the quality of PCR products by determining the dissociation temperature of the amplicon. This analysis is available when the SYBR Green based chemistry is used. It was used when a new set of primers was characterized.

Once the run was finished, the raw data were saved and the instrument was disconnected. To analyze the data, seven sub-tabs in the "Results" tab of the ABI 7000 software were checked and set according to the instruction manual. Once all of the

criteria were satisfied and the analysis finished, the plate document was saved. The results from the Report tab were printed or exported as a comma-separated *.csv* file.

List of primers for Real Time PCR analysis:

Name	sequence
26s FO	AGC GGA GGA AAA GAA ACC AAC
26s RE	CGC TTC ACT CGC CGT TAC TAG
con-6 FO	GAC GGC CTC GAG TAA GCT CA
con-6 RO	TCC CCT CGT CGA ATG GTT C
cry N.c. FO	AGT GAA AAC CCC CAT CCT GC
cry N.c. RE	TCT TGC ATA CCC TCC AAC GG
frq-FO sy1	CGC CTT GCG CGA GAT ACT AG
frq-RE sy1	TCC CAG TGC GGA AGA TGA AG
phy 04834.1 FO	AAC GCT CCC AAT CTG GAA AA
phy 04834.1 RE	CTT GAC AAT GCC GAC CAA GA
phy 05790.1 FO	GGC GTA TAA TTG GCG GAG AC
phy 05790.1 RE	GTA CGT TTG GGA CCT CGA GG
wc-1 sy2 FO	CCG ACT GGC ACA AAC AAT CC
wc-1 sy2 RE	CGT CTG CGT TCT CAA AAA GC
SM1C8 5'-FO (primer system 1)	ATT CCA CGC CAC CAC TTG TC
SM1C8 5'-RE (primer system 1)	GTG GTG AAG CAA ACA CCG C
SM1C8 3'-FO (primer system 2)	CCA AGC AAA CGT TAC CCC AT
SM1C8 3'-RE (primer system 2)	GCA CCG GCC TTT GTC CTA G
NM2B8 –1FO (primer system 1)	ATC CAA TGT TCT GCC CCT TG
NM2B8 –1RE (primer system 1)	ACC GAA GAC CGG ACC TGA TA
NM2B8 –2FO (primer system 2)	CAC CTC TCG CCG AGT ACC TT
NM2B8 –2RE (primer system 2)	TGG GTT CTG CTA TGG ACC GT
NC1A11-FO (primer system 1)	TTC GGT TCT GGC TCT GAT ATG G
NC1A11-RE (primer system 1)	TGA TCA TGC GGC TGT TGC T
NC1A11-FO (primer system 2)	CCT TCC CTC TTT GCT TGC AG
NC1A11-RE (primer system 2)	TCA CCA TCG GAT TCT CTC GTG
C5E3-FO	ACC TTC ATC CCC CAA AAC CA

C5E3-RE	GGA CGC AAC AGA AGC CGA TA
NM1C3-FO	GCT GAA GGG TTA CTC ACC GC
NM1C3-RE	TGT TTC AGG CTG GAA GTC CG
bli-3 FO;sy1	CTC CTC TTC CAC ACC AAC ACC
bli-3 RE;sy1	CGA CTT GAG GTC GTC CGT CT
vvd FO;sy1	GAC ACG TCA TGC GCT CTG AT
vvd RE;sy1	TGG CGT GTC TTT TTG CTT CA
bli-4 FO;sy1	GTG AGA AGA CGT GGC CCA AG
bli-4 RE;sy1	CAT CAT CCA TCG GAC ATC CC
con-8 FO;sy1	CTC TTT CCT AAT GTC GCG GG
con-8 RE;sy1	CCG CTC ACT CCT GAA TGC TT
con-10 FO;sy1	CTG GTA ACG ACA ACC CCG G
con-10 RE;sy1	GCC TGA ACC TCT TCC TTG GG
Wor.Bod.sy1;FO	CTC CCC GTC ATT GAC CAG AG
Wor.Bod.sy1;RE	GAA AGC CTT CTG GAG ACG GTT
ccg-6.sy1;FO	ACC TAC TGG CCT GGT CCC AC
ccg-6..sy1;RE	GGT GTA AGT GTT GCC GCC AT
CaCam1.sy1;FO	TTC GCC AAC ATG CTT AAT CG
CaCam1.sy1;RE	CTT GTC GTA GCT TTC GGG CT
NM1B8-sy1-FO	CGG CAT CAA CTC CTC GCT AA
NM1B8-sy1-RE	GAA GAC GGA AAG GCC GAC A
W17G3-sy1-FO	CCT CGA CCG GTG CAT TTC TA
W17G3-sy1-RE	CTA ACC CCA AAA GGG CGT
phr-FO	GCA CTA GCT GAG ACT GCG GC
phr-RE	CGC TTG GCG AAC TGG TAA AG
mus-11 FO	AAA CTC ATC GCC AAC CCG T
mus-11 RE	GTA TTC GCT GAT TCG CCG TT
mus-25 FO	TCA GTG CCT TGA ACA GCC TG
mus-25 RE	TAC CCG ACA AGA TGA CCC TCC
nop-1 FO	TCA AAC CCT TGG CGA AAC AG
nop-1 RE	AGG GCG AAG GTC ACC CAT AG
al-1 FO	AGT TGG CCG AGG GTA TCT GG
al-1 RE	CCA ACA CCT TGT GGA AGC CT
NRC1-FO	CCA ATT GAG CCC AGC GAT AA
NRC1-RE	CAG CAC CTT TTG CAG CTT CAG
NRC2-FO	ATC CGC TCG ACG AAT CCA T
NRC2-RE	CAA AAT ACG GGT TCG CGT GT

4.4 RNA methods

4.4.1 RNA extraction

Frozen *Neurospora* tissue was ground with a mortar and pestle, with liquid nitrogen and sand. The addition of sand was necessary to obtain good homogenization. Powdered, frozen mycelial tissue was added to 600 μl of RNA extraction buffer (see Appendix) and 500 μl "phenol for RNA extraction", pH 4.5-5.0 (see Appendix). The tube was vigorously vortexed (and again in 10 minutes intervals) and shaken at maximal speed (300 rpm or more). After 30 min of extraction, the samples were spun at 28,000g at 4 °C for 30 minutes. The supernatant was removed to 500 μl of chloroform:isoamylalchocol (24:1), vortexed, briefly extracted and spun. After this second extraction, the supernatant (300-400 μl) was precipitated with 40 μl of 3 M NaOAC and 1 ml ice cold 100% ethanol for 1-2 hours at –20°C. The sample was centrifuged at 28,000g at 4 °C for 30 minutes. The supernatant was removed and the pellet was washed with 70 % ethanol. After removing all ethanol, the pellet was air-dried for 20 minutes with a vacuum centrifuge. The dry pellet was suspended in 100 μl RNase free water (for Northern analysis) and stored at –75 °C. For Real Time PCR analysis samples were dissolved in 1X RNAsecure reagent (see Appendix) and treated according to the instruction manual.

4.4.2 RNA quantification

The concentration of RNA was determined spectrometrically. Absorbances at 260, 280 and 320 nm were determined. A ratio of OD_{260}:OD_{280} between 1.8-2.0 indicates an absence of phenol. OD_{320} was always lower than 0.01, indicating a low level of protein contaminants. Calculations assumed that at 260 nm, an absorbance of 1.0 in a cuvette with a 1 cm path length indicates RNA 40 mg/ml RNA.

4.4.3 Northern blot analysis

Formaldehyde-agarose gels were used for fractionation of RNA prior to transfer to membranes.

30 μg of RNA were loaded per well. Samples were diluted to 2 μg/μl and 15 μl of this dilution was mixed with 15 μl "RNA running dye" (see Appendix). RNA probes were denatured at 70°C for 10 min and then cooled to room temperature. Prior to loading, probes were briefly spun to consolidate. The electrophoresis was usually run at room temperature overnight (16 -18h) at 1 V/cm of gel length.

After electrophoresis, the gel was incubated 2 X 15 min in 10 X SSC buffer with slow shaking. During that time a glass plate was placed across two reservoirs (like a bridge) filled with 10 X SSC. A long piece of 3M paper was soaked with 10 X SSC and placed on the glass 'bridge' with two ends dipping in buffer to serve as a wick. The gel was placed upside down on the 3M paper, and a pre-wetted sheet of nylon membrane (Hybond-N Amersham) was placed on it. Bubbles were removed by rolling a glass pipette over the membrane. Four stripes of parafilm (3 cm x 20 cm) were placed on the edges of the membrane, forming a "gasket". Two sheets of filter paper and around 20 paper towels (10 cm) were placed on them. 2 X 0.5 kg weights were placed on top, evenly pressing the blot setup. The gel was blotted 24 h at room temperature. After blotting, the membrane was crosslinked with UV light. The automatic crosslink setting on Stratagenes UV Stratalinker was used (120 mJoules, 1 min). After blotting, the RNA on the membrane was visualized with UV light and photos were taken.

4.4.4 Synthesis of radioactive RNA probes

Single–stranded RNA was internally labeled during *in vitro* transcription and used as a substrate for RNA gel-shift assays or as a riboprobe for Northern blots. RNA probes were synthesized using commercially available T3 and T7 bacteriophage RNA polymerases.

The DNAs to be transcribed are cloned into a plasmid vector downstream of the bacteriophage (T7 or T3) promoter element. After linearization the plasmid was used as a template for transcription. For the RNA shift assays, it is preferable to use two enzymes, so that the insert is removed from the vector.

For gel shift assays the template DNA, after digestion, was gel purified and phenol extracted. Template DNA was dissolved in RNase-free water and stored at –20°C.

4.4.4.1 *In vitro* transcription

The transcription reaction should be set up at room temperature, as the reaction buffer usually contains spermidine which will precipitate the template DNA at low temperature. All work was done under "RNase free" conditions. The reaction buffer was warmed at room temperature to avoid precipitation of spermindine .

Reagents were added into a microfuge tube, mixed and made up to a final volume of 20 μl: Template DNA (0.5 μg); Nucleotides (ATP, GTP, CTP each 500 μM final); unlabeled UTP 125 μM final; labeled UTP 1 μM final (α 32P, 3000 Ci/mmol); supplied T7 or T3 buffer (1x final); polymerase (20 Units according Roche, 1 U/ μl final); Rnase inhibitor (1 U/μl final) and Rnase-free water up to 20 μl. The reaction was spun for 30 sec at max. speed and incubated for 1 h at 37 °C.

Ethanol precipitation is the simplest method for purification of labeled RNA probes but it is suitable only for RNAs larger than 100 bp. 1/10 volume of 3M NaOAc and 2-3 volumes of ethanol were added, followed immediately by centrifugation for 30 min at 28,000 g. This leaves most of the unincorporated radioactive nucleotides in the supernatant. After centrifugation, the supernatant was entirely removed, the pellet was dissolved in Rnase-free water and stored at –20°C. Also Stratagene's NucTrap push-columns and Beta-shield device were used for rapid (~5 min) separation of unincorporated nucleotides. Columns and the shielding device were done according to the instruction manual.

4.4.4.2 Polyacrylamide gel purification of labeled RNA

For gelshift assays, RNA probes were purified on polyacrylamide gels. For gel purification of the transcript, Biorad's "xi" commercial vertical electrophoresis system was usedwith 160 x180 x 0.75mm gels. The glass plates were treated with 5% dichlordimethylsilane and dried in a fume hood (silane is toxic!) and wiped with ethanol. This process was repeated only when plates lost the silane "cover" and became too adhesive. Scrupulous cleaning with SDS and deionized water was done before assembling.

A UREA gel (see Appendix) was mixed in 50 ml sterile falcon tubes, and poured between the plates. The gel comb was inserted immediately. 1 h was sufficient for complete polymerization. After removing the comb, unpolymerized acrylamide mix was removed from wells with a sterile syringe and needle using running buffer. The transcription reaction was mixed with gel loading buffer (see Appendix) in a 1:1 ratio, incubated 5 min at 65-70 °C and then loaded on to the gel. Electrophoresis was run at 150 V (constant voltage) until the bromphenol blue dye migrated approximately 2/3 of the distance down the gel. On a 5-6% gel, RNAs of approximately 150 nucleotides migrate with the xylene-cyanol dye front.

After disassembling the apparatus, care was taken with the bottom tank buffer, which contains unincorporated radioactive nucleotides. Gel plates were separated with a spatula and the 'gel+plate' was covered with saran wrap. When RNA was radioactively labeled, the position of the main transcript was detected by direct autoradiography, whereas for unlabeled RNA, the gel was stained with ethidiumbromide and the position was detected with UV light.

Brief (1-5 minutes) autoradiography gave a signal strong enough to locate the main RNA transcript. After developing, the film was placed under the glass plate and aligned with the gel. The position of the transcript was marked directly on saran wrap and the region was cut out with sterile scalpel. The saran wrap was removed, and the gel slice was transferred to a 1.5 ml Eppendorf tube. The gel was reautoradiographed to confirm that the correct band was cut.

Elution of the RNA transcript was done in 400-500 μl TE/SDS elution buffer (see Appendix) for 2h on a shaker or rotator at room temperature. After elution, the transcript was removed to a new tube, precipitated by the addition of a 1/10 of volume 3M sodium acetate and 2 volumes of ethanol and immediately spun for 5 min at room temperature. After complete removal of the supernatant, the pellet was resuspended in 50-150 μl RNase-free water. The specific activity of labeled RNA was estimated in a scintillation counter. After this procedure, careful decontamination was necessary. This was done with 2% Deconex.

4.4.5 Radioactive labeling of Northerns

Nylon membranes were first blocked (prehybridized) with hybridization solution (see Appendix) for 30 minutes at 65 °C in a hybridization oven. 15-20 ml of hybridization solution was used per 25 cm long, 3 cm in diameter, glass bottle. After blocking, the prehybridization solution was drained and 15 ml new hybridization solution was added with the probe. Radioactive probe was added to a final specific activity of 2.5 X 10^6 cpm/ml hyb. solution. For high abundance (mRNA), 10 fold less radioactive probe was used. The membranes were hybridized overnight at 65 °C. The next day, the probe was poured off and membranes were rinsed 3 times briefly with 2 X SSC with 0.1 %SDS. After rinsing, membranes were washed in the hybridization oven (see See Appendix) at 70°C 2X 15 minutes with 2 X SSC, 0.1 %SDS and 2X 15 minutes with 0.2 X SSC, 0.1 %SDS. After washing, membranes were wrapped with saran wrap, placed in a cassette and exposed to X-ray films. Exposures of different lengths were taken. Quantifications were done as for western blots (section 4.6).

4.4.6 Gel mobility shift assay

This technique makes use of native polyacrylamide gels to resolve the free RNA from the RNA-protein complexes, which have lower mobility and are therefore “shifted” in the gel.

4.4.6.1 Preparation of RNA and protein

The protocol requires that the radiolebeled RNA is homogenous in size and structure because it is important that the RNA migrate as a discrete, unique species on the native gel used to separate free RNA from RNA-protein complexes. This is facilitated by gel purification of the transcript (section 4.4.7.3) As a source of the RNA-binding proteins we used total protein extracts from mycelial tissue. These extracts were prepared as described in section 4.5.1.

4.4.6.2 RNA-protein binding reaction

30 μg of total protein extract was mixed with 30 μg of polyguanylic acid (prepped as in section 4.3.5) and incubated for 20 min at RT. During this incubation, the majority of non-specific RNA binding proteins bind to polyG. After this first incubation, 200 counts of labeled RNA probe was added to the reaction and incubated for an additional 20 minutes. The binding reaction was performed in 1 X PEB buffer (see Appendix) supplemented with placental RNase inhibitor at final concentration of 1 U/μl (Unit definition according Roche). The total reaction volume was 15 μl. Prior to loading, 1μl of RNase free loading dye (see Apendix) was added per reaction.

4.4.6.3 Preparation, loading and running of native polyacrylamide gels

For gel shift assays, Biorad xi commercial vertical electrophoresis system with 160 x180 x 2 mm gels was used. A Native gel was mixed in a sterile falcon-tube (see Appendix) and poured in a "glass sandwich". Clamping the comb in place resulted in wells free of thin polyacrilamide films on the walls. After polymerization the comb was removed and the gel was attached to the electrophoresis apparatus. The wells were rinsed a few times with the running buffer (TBE, see Appendix). The loading technique is critical for the quality of results. A automatic pipettor with a capillary-loading-tip avoids mixing of sample with the running buffer. Native polyacrylamide gels were run at room temperature without cooling at 8 V/cm of gel length. After the electrophoresis is completed, the gel holder was removed from the chamber and the upper plate was gently pried off from one corner leaving the gel on the lower plate. One sheet of Whatman N°1 or similar paper was pressed onto the gel. Peeling paper back adheres the gel to it. The opposite side of the gel was covered with plastic wrap (household cling-film wrap).

4.4.6.4 Drying and autoradiography of gels

A paper-gel sandwich was placed in commercial gel dryer and dried for 1.5 hours at 80°C under vacuum. After drying, gels were placed in an autoradiography cassette and exposed to X-ray film.

4.4.7 Microarray experiments

mRNA isolation, cDNA labeling, hybridization and data analysis were done as described in Lewis et al. 2002. For microarray analysis *wc-2*^{234w} strain was used (strain description in subchapter 4.2). Conidia were inoculated into 25 ml of Vogels liquid media (1X Vogels, 0.5% Arginin, 0.3% glucose) and grown for 3 days in LD 12:12 cycle at 25°C. During the last 12 hours of light, mycelial disks (8 mm big) were cut from the mycelial pads and transferred into 50 ml flasks containing 25 ml Quinic acid media (0.3% QA, 1X Vogel's salts and 0.5% Arginin). The cultures were grown in the 12:12 LD cycles at 25°C for two days. Dark controls (D) were harvested at the end of second dark period (5 min. before lights on). Light induced probes were collected after additional 2 h in constant light. White fluorescent light source (5 μEm^{-2}sec^{-1}) was used.

4.5 Protein methods

4.5.1 Protein extraction

Tissue was harvested with blotting or vacuum filtration and frozen in liquid nitrogen. Frozen tissue was homogenized with a mortar and pestle with liquid nitrogen and 200-300 μg of sand. The ground tissue added to 1.5 ml tubes with 300-500 μl of protein extraction buffer (see Appendix). The volume of protein extraction buffer and pulverized mycelia should be approximately the same. The ground tissue was mixed vigorously by vortexing and incubated on ice for 20 minutes. Additional vortexing during the incubation increased the yield. Samples were centrifuged at 2-4 °C for 20-40 minutes and the clear supernatant was removed and stored at –20 or –75 °C.

4.5.2 Protein quantitation- Bradford Assay

1 ml of 1x Bradford reagent (see Appendix) was pipeted into 1.5 ml disposable test tubes. 10 μl of protein solution was added and mixed by inverting the tube a few times (not vortexing). Development time for this reaction is 5 min. OD595 was measured within the next 15 minutes to prevent error due to protein precipitation and subsequent color loss.

Each assay was accompanied by the generation of a new standard curve. As a protein standard, we used bovine IgG or BSA, (see Appendix). A standard curve was determined as a best linear fit for 4-5 dilutions of the standard protein solution. This formula was then applied to samples with unknown concentrations. For these calculations, the Kaleidagraph program was used (www.synergy.com). The Bradford assay remained linear only in the range of 0.1-0.7 (A595). Care was taken to ensure that the absorbance of unknown protein samples did not fall outside of this range. If the protein concentration of the sample was too high, dilutions were made. Disposable plastic cuvettes were used to prevent error arising from dye carryover in the cuvette and on cuvette walls.

4.5.3 TCA precipitation

If the protein concentration was too low, precipitation with 12% (w/v) TCA (trichloracetic acid) was performed. After 30 min incubation on ice, denatured proteins were centrifuged 20 min at 20,000g. The pellet was washed two times with cold (-20°C) acetone and dried approximately 5 minutes at room temperature. Dry pellets were resuspended in 1x Laemli buffer and loaded on gel.

4.5.4 Protein electrophoresis SDS-PAGE

For SDS polyacrylamide gel electrophoresis, two different gel apparati were used:

- BioRad Mini-Protean II cell
- Custom made gel apparatus (see Appendix for specifications)

The gel sandwich was assembled according to the manufacturer's instructions for the Biorad setup. For the custom-made gel apparatus, a gel-sandwich was assembled with heavy-duty paper-clips. Plates and spacers should always be perfectly flush before tightening the sandwich assembly. A mark 2.5 cm below the top of the front plate (with section cut out) was made to indicate where the “separating” or “running” gel should stop. Liquid 1% agar or agarose was added to bottom of the base to prevent leakage and the plate sandwich was inserted. A toothpick was stuck between the base and the glass plate to insure a tight seal. The agar solidified in 10-15 min, the running gel (see Appendix) was added and covered with isopropanol to prevent contact with air and allow

polymerization. After polymerization (45 min to 1 h) isopropanol was entirely washed out with water and the gel was briefly dried. A stacking gel (see Appendix) was poured on the solidified running gel and a comb was inserted and fixed with paper-clip for next 30 min. Prior to running, the gel-sandwich was placed in an electrophoresis chamber. Protein extracts were denatured in 1X Laemmli buffer (see Appendix) at 95°C for 5 minutes, cooled at room temperature and briefly spun. Prior to loading, the wells were washed with running buffer (important). Electrophoresis was run at 80 V for 1.5 hours and then changed to 125 V. The electrophoresis was run until the dye reached the end of the gel.

4.5.5 Western blotting

For all applications, nitrocellulose was used because it has a high protein binding and is compatible with different kinds of stains. Blocking for nonspecific antibody binding is simple, and it is relatively inexpensive.

4.5.5.1 Wet blotting

For wet bloting I used two apparati: Biorad trans blot cell and Biorad mini protean II cell. For the transfer buffer, 2X Towbins transfer buffer (see Appendix) without SDS and with 20%(v/v) methanol was used. This buffer was kept at 4°C. The bloting chamber was filled with transfer buffer to 3/4 full. The opened transfer cassette was submerged in a shallow tray, half full with the transfer buffer. On each side of the transfer cassette a well-soaked fiber pad was placed. The gel was wetted by pouring 10-20 ml of buffer on to it. A wetted sheet of nitrocellulose (see Appendix) was placed on the gel and wetted Whatman paper over the nitrocellulose. A small glass test tube was rolled over the sandwich to remove any air bubbles. This sandwich was carefully removed from the other glass plate, turned upside-down and placed on the same glass plate. Another Whatman paper was placed on gel, bubbles were removed and the sandwich was placed in the opened transfer cassette. The sandwich was covered with the second fiber-pad, the cassette was closed and slid into the buffer tank (when the Biorad protean II cell was used, a frozen cooling unit was also inserted). The tank was topped off with transfer

buffer. A stir bar was inserted into the chamber and the entire apparatus was placed on a magnetic stir plate. The electrode-lid was attached and the power supply was switched on. For the Biorad trans blot cell, 800 mA (constant current) for 2 h wass used. The electrode distance was always 8 cm. For the small BioRad cell, 100 V (constant voltage) for 1 h was used.

4.5.5.2 Semi-dry blotting

For proteins smaller than 80-90 kD, it was also possible to use semi-dry blotting. A custom-made transfer cells with two graphite electrodes (see Appendix) were used. For semi dry transfers, constant current of 2 mA per 1cm^2 of sandwich area was used. Transfer time was usually 1.5 h.

4.5.6 Staining of SDS-polyacrilamide gels with coomasssie blue (CB)

After electrophoresis, the stacking gel was removed from the running gel. The running gel was submerged in CB staining solution (see Appendix). The CB solution and gel were briefly boiled (only a few seconds) in the microwave oven and incubated an additional 10 min at RT. After staining, the CB solution was poured off and the gel was rinsed with the destaining solution (see Appendix). To get sufficient destaining, 3 incubations of 15 min in new destaining solution was necessary. For permanent storage gels were dried on 3MM filter paper for 2 h with vacuum and heat (80°C).

4.5.7 Staining of nitrocellulose membranes with ponceau-S

To verify the efficiency of Western blotting, proteins transferred to nitrocellulose were reversibly stained with Ponceau-S staining solution (see Appendix). The membrane was rinsed with distilled water and submerged in staining solution for 1-2 minutes. The membrane was destained with water and dried by air at room temperature. To remove Ponceau-S stain, the membrane was soaked in TBS (see Appendix) and placed on a shaker for 10 to 20 minutes.

4.5.8 Immunodetection of proteins

The membrane was blocked in 5% low-fat milk in TBS. The membrane was shaken gently for 1 h at RT, taking care that the entire sheet is in contact with the blocking solution. Primary antibodies were added to the blocking solution and incubated for an additional hour. After incubation, the primary antibody was poured off, the membrane was rinsed three times and washed on a shaker 2X for 15 minutes with TBS. Secondary, HRP labeled, antibody (see Appendix) was added at a 1:5,000 dilution (for primary monoclonal antibodies) or 1:10,000 (for primary polyclonal antibodies). Membranes were usually incubated with secondary antibodies on a shaker, overnight at +4°C. After this incubation, the membrane was vigorously rinsed a few times and washed in TBS with at least 3 changes. To develop the membrane, a commercial ECL substrate was used (see Appendix). In this part of the procedure, care was taken that the membrane did not dry out. The nitrocellulose was carefully placed in a clear plastic bag and excess TBS was removed. 1ml of ECL solution was spread over the membrane. After 1 minute, excess liquid was removed, the membrane was placed in a cassette and exposed to X-ray film. Multiple exposures of different length were made for each membrane.

List of antibodies used in this study:

Antibody	Antigen	Origin
a FRQ (3G11)	MPB-FRQ(65-989 aa) (Merrow et al., 2001)	monoclonal, mouse
a WC-1	GST-WC-1 (354-838 aa) (Talora et al., 1999)	polyclonal, rabbit
a WC-1 (4H4)	GST-WC-1 (972-1168 aa)	monoclonal, mouse
a WC-2	GST-WC-2-PAS (Goerl M, 2002, PhD Thesis)	polyclonal, rabbit

4.6 Densitometric analysis of the Western and Northern blots

X-ray films exposed for different amount of time were scanned at a resolution of 72 dpi or more and saved as PICT files. For densitometric analysis, the program VideoAnalysis 1.8 was used (see Appendix). Densitometric values for different exposures (expressed as pixel densities, 0=all pixels white; 100=all pixels black, were transferred to Kaleidagraph

(www.synergy.com) program. Then the different values for the different exposure times were fitted to the sigmoidal curve: *y=a*(((x+b)/c)/(1+((x+b)/c)^ 2)^ 0.5)+d.*
The *y* axis is pixel density and the *x* axis is the duration of exposure. The relative amounts of protein per lane were determined at exposure time, which falls in the linear part of the sigmoidal curve. In effect this was done to ensure, that we did not use a "staining" signal when it was either overmaximally exposed or underminimally exposed.

4.7 Mathematical fits

All mathematical fits were carried out by an iterative, least square method. Adaptation profiles were fitted with an equation combining a Gauss distribution (G), a saturated curve (S), and an exponential decay (D):

$$y = G + S + D;$$

$$\text{with } G = a^{\frac{-(X-b)^2}{2c^2}};\ S = d\frac{\frac{X}{e}}{\sqrt{1+\left(\frac{X}{e}\right)^2}};\ \text{and } D = \frac{f}{(x+1)};$$

All rhythmic time courses were fitted with a cosine function with one exception: due to the non-sinusoidal shape of the time series, WC–1 (Fig. 2B) was fitted by eye. The S-curves in figure 6B were fitted with the following equation:

$$y = a\frac{\frac{(x+b)}{c}}{\sqrt{1+\left(\frac{x+b}{c}\right)^2}}$$

Data from dose-response experiments were fitted with a three parameter sigmoidal curve:

$$y=a\frac{\frac{(x+b)}{c}}{1+\sqrt{\frac{(x+b)^2}{c}}}$$

The half saturation constants were derived from the 11 dose-response curves shown in figure 28, by designating y as 0.5 and calculating the x value. The relative quantum efficiency for each wavelength is plotted in figure 29 to illustrate the resulting action spectrum of FRQ protein induction.

4.8 Time measurement in chronobiology

Definitions:

Subjective Circadian Time (SCT) 00 is the point in the cycle which occurs when dawn would have fallen on the first day of a DD freerun following a light-dark cycle of 12:12. SCT 24 occurs one full cycle later (Pittendrigh and Minis, 1964).

Arbitrary Zeitgeber Time (AZT) is the onset of the light in the main (or only) photoperiod in that cycle (Pittendrigh and Minis, 1964).

External time (ET) is the number of hours x 24/T elapsed since the middle of the dark period, where T is the duration of the LD cycle in hours. In natural conditions T equals 24h and ET always correspond with sidereal time (Daan et al., 2002).

Internal time (IT) is the number of hours x 24/t elapsed since the middle of the subjective night, where t is the free-running period length. IT=(CT-18)mod24 (Daan et al., 2002).

5 SUMMARRY

Circadian clocks are endogenous cellular mechanisms that control daily rhythms of physiology and behavior. The adjustment of the circadian clock to the 24 h period of a day is most commonly accomplished by light. Therefore it is important to understand how light is "seen" by the circadian clock. In this study, the filamentous fungus *Neurospora crassa* is used as a model system to elucidate the circadian light input pathway. Key players of the circadian mechanism in *Neurospora* are three proteins: FRQ, WC-1 and WC-2. FRQ is a critical element of the circadian clock. WC-1 and WC-2 were discovered because of their involvement in light signaling.

The recently described lack of light-regulated conidiation in FRQ-deficient mutants indicated an additional role for FRQ in the light input pathway. In this thesis some mechanisms for regulation of light signaling by FRQ are described. Investigation of a light regulated physiological response (carotenogenesis) revealed that light responses in *Neurospora* are modulated by the circadian clock. Interdependent regulation of *frq* and *wc-1* gene expression indicated that clock and light input are functionally inseparable in this model system.

The unexpected observation that non-circadianly regulated *wc-1* transcription gave rise to circadianly rhythmic WC-1 protein revealed the involvement of posttranscriptional regulation in the light input pathway. Investigations of *wc-1* regulation indicated the existence of protein complexes that bind specifically to the 5' and 3' ends of *wc-1* mRNA untranslated regions. Identification of these specific protein complexes can now be used to further investigate posttranscriptional regulation of the light input pathway in *Neurospora*.

The discovery of a light regulated physiology in blind *wc* mutants was an important step towards understanding the molecular aspects of light input to the clock. *wc* mutants with the same phenotypic characteristics had different gene expression profiles. These data suggest the existence of a novel, as yet unidentified, photoreceptor in *Neurospora*. An action spectrum for light induction of FRQ protein indicated that a chromophore closely related to flavin is involved in circadian photoreception in this model system. The recently annotated *Neurospora* genome revealed the existence of one cryptochrome and two phytochromes orthologues. Homology of the protein sequences to

other, already known, photoreceptors and profiles of the light induction of their mRNA suggests their involvement in light transduction in *Neurospora*.

6 Appendix

6.1 List of Instruments

Autoclave, type 300, Varioklav

Blotting apparatus, Trans-Blot cell (with plate electrodes), BioRad

Blotting apparatus, custom made; Specification: Helmut Klausner, workshop of Inst. für Med Psych. Goethestr. 31/U1, 80336 Munich, Germany

Centrifuge, 5415C, Eppendorf

Centrifuge, 5417R, Eppendorf

Centrifuge, Biofuge Primo-R, Heraeus

Cooling unit, FBC 620, Fisher

Cooling unit, RM6, Lauda

Dark-room light bulb, E27 PF 712E, Philips

Developer for X-films, Curix 60&35 compact, AGFA

Dispenser, Multipette-plus, Eppendorf

Dispenser, Seripettor, Brand

Electrophoresis apparati, vertical (gel size 120x140x0.75, 1.00 or 1.50mm) and horizontal (for DNA and RNA, gel size 5x7.5, 9x7.5, 11x14 and 14x23 cm) all custom made; Specification: Helmut Klausner, workshop of Inst.für Med Psychologie. Goethestr. 31/U1, 80336 Munich, Germany

Electrophoresis apparatus, Mini Protean II cell, BioRad

Electrophoresis apparatus, Protean II xi cell, BioRad

Freezer,-20°C, different models for household

Freezer,-80°C, Heraeus

Gene-Pulser, Pulse controller and Capacitance extender, BioRad

Homogenizer&cell-disruptor, Ribolyzer, FP120, Savant, Hybaid

Hybridization oven Bachofer, Germany

Incubator, 50L&100°C, Memmert (Germany)

Incubator, BD 240/E2, Binder

Incubator, KB 240/E2, Binder

Magnetic mixer, Ikamag, Junke&Kunkel-Ikawerk

Monochromator, T.I.L.L Photonics (Germany)

Picoammeter, Autoranging 485, Keithley

pipet, with positive displacement, Biomaster, Eppendorf

Pipets, Pipetman (10,20,100,200,1000μl), Gilson

Pipets, Reference (10,20,100,1000,2500μl), Eppendorf

Power Supply, EC 105, EC

Power Supply, EPS 2A200, Amersham

Power Supply, EPS 301, Amersham

Power Supply, EPS 601, Amersham

Power Supply, Model 1000/500, Biorad

Power supply, SP340, Tectron

Pulse-giving Unit (0.01-9.99 Period & 0.001-9.999 seconds Time)

Pump (with diaphragm), ME2, Vacuubrand

Radioactivity-counter, 900 Mini Monitor, Mini Instrments (England)

Radioactivity-counter,LB122, Berthold

Real Time PCR system, ABI PRISM 7000, Applied Biosystems

Scale, Handy H 110, Sartorius

Scale, L2200S Sartorius

Scale, Mettler, AE 50, Mettler,

Scintillation counter, LS 1801, Beckman

Shaker, KL2, Bachofer

Shaker, LS10, Gerhard

Shutter (photo), WILD MPS 51, Heerburg, Swiss

Spectrophotometer, DU64, Beckman

Spectrophotometer, Ultrospec 3000, Pharmacia

Speed-Vac, Bachofer

Thermal cycler, Primus, MWG Biotech

Thermomixer, 5436, Eppendorf

Thermomixer, comfort, Eppendorf

Timer, mechanical, Junghans

Timers,WB-388 and TR-118, Oregon Scientific;

Ultrasonic bath, Ultrason E, Greiner, Germany

Vortex, k-550-GE, Bender&Hobein AG

Writer (analog), ABB SE 120, Bachofer (Germany)

6.2 List of chemicals

Substance	Company	Order Nº.
Acetic Acid	SIGMA	A-6283
Acetone	ALDRICH	17,997-3
Acrylamide	APPLICHEM	A3705,0500
Acrylamide	GERBU	1002
Agarose LOW EEO	APPLICHEM	A2114,0500
Agarose QA TM	Q-BIOGEN	AGR0050
Albumin Bovine	SIGMA	A-3350
Ammonium acetate	SIGMA	A-1542
Ammonium chloride	SIGMA	A-4514
Ammonium nitrate	SIGMA	A-1308
Ammonium peroxodisulfate (APS)	ROTH	9592.3
Ammonium sulfate	ALDRICH	22.125-2
Ampicillin, sodium salt	SIGMA	A-9518
Arginine hydrochlorid (L+)	USB	US 11500
Bacto Agar	DIFCO	214010
Biopterin	SIGMA	B-2517
Bis acrylamide	SIGMA	M-7279
Boric acid	APPLICHEM	A2940,1000
Boric acid	APPLICHEM	A3581,0500
Bromphenol blue sodium salt	USB	US12370
Calcium chloride x 2H2O	ROTH	5239.1

Casein Enzymatic Hydrolysate	SIGMA	C-0626
Celite	ROTH	535
Chloramphenicol	SIGMA	C-0378
Chloroform	SIGMA	C-5312
Chloroform:Isoamylalcohol	SIGMA	C-0549
Citric acid	ALDRICH	24,062-1
Comassie brilliant blue	SIGMA	B-0149
Diethyl pyrocarbonate	USB	14710
DMSO / Dimethylsulfoxide Lsg.	MERCK	109678.01
EDTA 0.5M solution	AMBION	9261
EDTA Ehtylenediaminetetraacetic acid	SIGMA	EDS
Ethanol	ROTH	9065.2
Formaldehyde	SIGMA	F-8775
Formamide	SIGMA	F-7508
Glass beads	ROTH	A553.1
Glucose monohydrate	MERCK	1.04074
Glycerol	APPLICHEM	A2926,1000
Heparin	SIGMA	H-9768
Hepes	SIGMA	H-3375
Hexane	ALDRICH	29,325.30
Hygromycin B	ROCHE	843555
IPTG	APPLICHEM	A-1008,0005
Isoamyalcohol	ROTH	8930.1
Leupeptin	USB	18413
Magnesiumchlorid x 6H2O	MERCK	1.05835.0500
Methanol	ROTH	4627.1
MOPS	APPLICHEM	A1076,0250
Orange-G	MERCK	1.15925.0025
Pepstatin A	USB	US20037
Phenol	APPLICHEM	A1153,0100

Phenol (DNA/RNA)	ROTH	A.156.1
Phenol (RNA)	ROTH	A.980.1
Phenylmethanesulfonyl fluoride (PMSF)	FLUKA	78830
Polyethyleneglycol PEG 4000	ROTH	156.1
Ponceau S	FLUKA	81460
Potassium chloride	SIGMA	P-3911
Quinic acid (-)	SIGMA	Q-0500
Sand	SIGMA	S-9887
SDS / Sodium Dodecyl Sulfate	ROTH	2326.2
Sodium azide	SIGMA	S-2002
Sodium chloride	MERCK	1.06404
Sodium chloride	APPLICHEM	A2942,1000
Sodium citrate	ROTH	3580.1
Sodium dihydrogenphosphate	MERCK	6346
Sodium hydroxid	ROTH	6771.1
Sodium nitrate	FLUKA	71755
Sodium nitrit	ALDRICH	20,783-7
Sorbitol	USB	21710
Sorbose	SIGMA	S-2001
Sucrose	FLUKA	84100
Temed	SIGMA	T-8133
Tergitol NP 40	SIGMA	NP-40
Trichloracetic acid	SIGMA	T-4885
Tris	USB	US 75825
Tris	APPLICHEM	A1086,100
Triton X-100	SIGMA	X-100
Tween 20	USB	20605
Urea	SIGMA	U-0631
Urea	USB	US 75826
Vitamin B12	SIGMA	V-2876

X-Gal	APPLICHEM	A1007,0001
Xylencyanole	ROTH	A513.1
Yeast Extract	SIGMA	Y-1625

6.3 List of Biochemicals

Name	Company	Cat No
Anti.Mouse Polyvalent immunoglobulins	SIGMA	A-0412
Deoxyribonucleic acid; (salmon testes)	SIGMA	D-1626
DNA ladder 100 bp	NEB	N3231
DNA ladder 1Kbp	INVITROGEN	15615-016
DNA Ligase T4	NEB	M0202M
DNase1 (RNase free)	ROCH	776785
dNTPmix	AB	N8080260
Lambda BstEII digest (DNA ladder)	NEB	N3014
Lysing enzyme (for *N.crassa* cell wall)	SIGMA	L-2265
PCR system, Exp. Long Template	ROCHE	1-681-842
Protein Assay (Bradford)	BIORAD	500-0006
Protein Assay (gamma glob. standard)	BIORAD	500-005
Protein Markers (pre-stained ladder)	BIORAD	161-0373
Restriction enzymes	NEB	misc.
Reverse Transcription reagents	AB	N8080234
Reverse Transcriptase	AB	4311235
Ribonuclease A	ROTH	7156.1
Ribonucleosides	ROCHE	1277057
RNA polymerase	PROMEGA	P2075
RNA Secure	AMBION	7005
RNAguard Rnase inhubitor	AMERSHAM	27-0815-01
SYBR Green PCR master mix	AB	4309155
Western. blotting sub. ECL	ROCHE	2015196

6.4 Abbreviations

µ	micro (10^{-6})
A	Ampere
aa	amino-acid
al-1	*albino-1*
Amp	Amplicillin
APS	Amoniumperoxosulfate
bp	base pairs
BSA	Bovine serum albumin
C-	carboxy-
cDNA	Complementary DNA
DD	Constant darkness
DMSO	Dimethylsulfoxide
DNA	Deoxyribonucleic acid
dNTP	Deoxynucleoside triphosphate
E	Einstein, 1 mol photons per second and m^2
E. coli	Escherichia coli
FGSC	Fungal Genetic Stock Centre
FRP	Free running period
frq	*frequency* gene
FRQ	*frequency* gene product (FRQ protein)
g	gram
h	hour
HEPES	4-(2-Hydroxyethil)-1-piperazineethanesulfonic acid (buffer)
IgG	Immunoglobulin G
IPTG	Isopropyl-b-D-thiogalactopyranoside
k	kilo (10^3)
L	liter
LB	Luria-Bertani (medium)
LD	Light-Dark

LL	Constant light
M	molar
m	milli (10^{-3})
min	minute
mRNA	Messenger ribonucleic acid
n	nano (10^{-9})
N-	Amino-
NTP	Nucleoside triphosphate
OD	Optical density
PAGE	Polyacrilamide gel electrophoresis
PCR	Polymerase Chain Reaction
PMSF	Phenyl-methyl-sulfonyl-fluoride
RNA	Ribonucleic acid
rpm	Rotation per minute
RTPCR	Real Time Polymerase Chain Reaction
Taq	*Thermus aquaticus*
UTP	Uridine-triphosphate
UV	Ultraviolet
V	Volt
v/v	Volume in volume
w/v	Weight in volume
wc-1	*white collar-1*gene
WC-1	*white collar-1* gene product (WC-1 protein)
wc-2	*white collar-2*gene
WC-2	*white collar-2* gene product (WC-2 protein)
wl	wavelength
wt	wild type
X-Gal	5-Bromo-4-chloro-3-indolyl-b-D-galactopyranoside

6.5 Recipes

Acrylamide solution

29.2 g	Acrylamide
0.8 g	N, N'-Methylene-bis-acrylamide
Up to 100 ml	Water

Lysis buffer

0.2 M	NaOH
1%	SDS

Ampicilline stock 1000X

1 g	Ampicillin
Up to 10 ml	Water

Filter sterilize and keep at –20°C

Biotine stock 10,000X

10 mg	Biotine
100 ml	Ethanol

Keep at –20°C

Blotting Buffer for semi-dry blot

14.4 g	Glycin
3 g	Tris
200 ml	Methanol
Up to 1 liter	Water

First dissolve salts in aprox. 0.5 liter water then add Methanol

Blotting Buffer for wet-blot

288 g	Glycin
60 g	Tris
2 L	Methanol
Up to 1 L	Water

First dissolve salts in aprox. 5 liter water then add Methanol

Bottom Agar

10ml	Vogel's salts
440ml	Water
7.5g	Agar
91g	Sorbitol

Add 50 ml 10X Figs after autoclaving

Carot-media

20 g	Glucose
1X	Vogel's salts
Up to 1L	Water

CBB staining solution

0.1 % w/v	Coomassie-Blue G250
10 % v/v	Acetic acid
40 % v/v	Methanol

CTAB buffer 2X

10ml	1 M Tris pH 7.5
2g	CTAB (First dissolve this substance in water!)
28ml	5M NaCl
4ml	0.5 M EDTA pH 8.0
1g	Sodium bisulfite
To 100 ml	Water

Denhards 50X

5g	Ficoll
5g	Polyvinylpyrrolidine
5g	BSA
Up to 500 ml	Water, Rnase free

RNase free chemicals, filtrate and freeze at –20°C. Denhards 50X is very hard to thaw. Make aliquots before freezing.

DNA/RNA loading dye

0.5 ml	Glycerol
40 mg	EDTA
40mg	Bromphenol Blue
40mg	Xylene Cyanol
0.5 ml	Water

DNA agarose gel

0.8-2.0% w/v	Agarose
1X	TAE
0.02-0.05 μg/ml	Ethidium bromide

Work in hood if possible!

Destaining solution (for CBB stained gels)

10 % v/v	Acetic acid
40 % v/v	Methanol

DNase1 buffer 10X

200 mM	TRIS pH 8.3
500 mM	KCl
20 mM	$MgCl_2$

RNase free chemicals!

Electrophoresis buffer (SDS-PAGE) 10 X

144.13 g	Glycin
30.28 g	TRIS
10 g	SDS
To 1 L	Water

Electrocompetent cells, media and buffers

- 1 liter LB media with pH adjusted to 7.5 and sterilized by autoclaving
- 2 liters of autoclaved 1 mM HEPES pH 7.0
- 3 liters of sterile water stored in the cold room
- LB plates with no additional supplements (i.e. ampicillin)

Elution buffer for gel purification of transcript

260 μl	Ammonium acetate
100 μl	10 % SDS
20 μl	0.5 M EDTA pH 8.0
Up to 10 ml	Water

RNase free chemicals have to be used!

FIGS 10X

100 g	L-sorbose
2.5 g	D-fructose
2.5 g	Glucose
To 500 ml	Water

Autoclave!

GET

25 ml	40% Glucose stock
2.5 ml	1M TRIS pH 7.5
2.0 ml	0.5 m EDTA pH 8.0
70.5 ml	Water

Add 3 mg/ml (final) lysozyme before use!

Gel, Native for RNA gel shifts

3.9% w/v	Acryamide
0.1% w/v	Bis-Acrylamide
1X	TBE buffer
10% v/v	Glycerin

RNase free water and chemicals should be used

Gel, UREA for transcript purification

4.85% w/v	Acryamide
0.15% w/v	Bis-Acrylamide
1X	TBE buffer
40% w/v	UREA

RNase free water and chemicals should be used

Laemmli buffer 4X (Reductive)

4 mg or 100μl	Solid or 100X stock Bromphenol Blue
800 mg	SDS
5 ml	1M TRIS pH 6.8
350 μl	2-mercapto ethanol
To 10 ml	Glycerol

Follow the order! After adding 1M TRIS warm solution up (≈50°C)!

Luria-Bertani medium

5 g	Tryptone
2.5 g	Yeast extract
5 g	NaCl
7.5 g	Agar

For liquid LB omit Agar!

Mg solution

12 g	$MgSO_4$
9.5 g	$MgCL_2$
To 100 ml	Water

MOPS 20X

92.4 g	MOPS
33.3 g	3M Sodium Acetate
40 ml	0.5 M EDTA
Up to 1L	Water

First adjust pH to 7.0 with 10 M NaOH then add water to 1L

TBE buffer 10X

54.5 g	TRIS
27.8 g	Boric acid
4.47 g	EDTA
Up to 1 L	Water

PBS 10X

80 g	NaCl
2 g	KCl
11.5 g	$Na_2HPO_4x7H_2O$
2 g	K_2HPO_4
Up to 1 L	Water

PTC and PMC

40 % w/v	PEG 4000
50 mM	$CaCl_2$
For PTC 50mM	TRIS pH 8.0
For PMC 10 mM	MOPS pH 6.3

Ponceau-S solution (water based)

0.2 % w/v	Ponceau S
3% w/v	TCA

Hybridization solution

100 ml	50 X Denhards
250 ml	Formamide, quality for Northerrns only!
25 ml	1M TRIS pH 7.5
29.2 g	NaCl
0.5 g	Sodium pyrophosphate
5 ml	10 mg/ml denatured salmon sperm DNA
90 ml	Water

Protein extraction buffer

1.2 g	HEPES
10 ml	Glycerol
2.7 ml	5M NaCl
1 ml	0.5 M EDTA pH 8.0

To prevent proteolysis PMSF (5mM final concentration), leupeptin (10μg/ml final) and pepstatine-A (10 μg/ml final were added). PMSF is poorly dissolvable in water and usually partially precipitates after adding. This does not influence protein quality.

rG buffer

0.8 ml	5M NaCl
0.5 ml	1M TRIS pH 7.5
0.1 ml	0.5 M EDTA pH 8.0
5 ml	50% v/v Glycerol
200 μM final	DTT
Up to 50 ml	Water

RNA agarose gel

0.8-2.0% w/v	Agarose
1X	MOPS
5% v/v	Formaldehyde, RNA quality only
0.05 μg/ml	Ethidium bromide
Work in hood!	

RNA extraction buffer

2 ml	0.5 M EDTA pH 8.0
10 ml	1 M Tris pH 8.0
40 ml	10 % SDS
12 ml	5 M NaCl
36 ml	Water

RNA running dye (for RNA denaturation)

1X	MOPS
50 % v/v	Formamide
1X final	Loading dye

SOC

2.5 g	Yeast extract
10 g	Tryptone
0.25 g	NaCl

Fill water to 500 ml and autoclave, then add 2.5 ml sterile Mg solution and 5 ml 2M glucose. Make aliquots and keep sterile.

SSC 20X

526 g	NaCl
265 g	Sodium citrate
To 3 L	Water

RNase free solution!

STC

1M	Sorbitol
50 mM	$CaCl_2$
50 mM	Tris pH 8.0

STE

2 ml	5 M NaCl
2 ml	Tris pH 7.5
2 ml	0.5 M EDTA pH 8.0
94 ml	Water

TBS 10X

90 g	NaCl
200 ml	1 M Tris pH 7.5
To 1 L	Water

Top agar

10 ml	50 X Vogel's salts
91 g	Sorbitol
14 g	Agar
450 ml	Water

Add 50 ml 10X FIGS after autoclaving

Trace elements-standard

In 95 ml distilled water, dissolve successively with stirring at room temperature:

5 g	Citric acid x 1 H_20
5 g	$ZnSO_4$ x 7 H_20
1 g	$Fe(NH_4)2(SO_4)2$ x 6 H_20
0.25 g	$CuSO_4$, x 5 H_20
0.05 g	$MnSO_4$, x 1 H_20
0.05 g	H_3BO_3, anhydrous
0.05 g	Na_2MoO_4 x 2 H_20

The resulting total volume is about 100 ml. Chloroform (1 ml) is added as a preservative, and the trace element solution is stored at room temperature.

Trace elements-modified

5.25 g	$Na_2B_4O_7$ x 10 H_20
0.1 g	$CuCl_2$ x 2 H_20
0.2	$FeCl_3$ x 6 H_20
0.02	$MnCl_2$ x 4 H_20
0.02	$(NH_4)_6Mo_70_{24}$ x 4 H_20
0.002	$CoCl_2$
To 1 L	Water

Westergaard's salts (5X), standard

2.5 g	KNO_3
2.5 g	KH_2PO_4
1.25 g	$MgSO_4$
0.25 g	$CaCl_2$
0.25 g	NaCl
0.5 μl/ml	Trace elements
To 500 ml	Water

Westergaard's salts (5X), modified

1.25 g	KNO_3
1.25	KH_2PO_4
0.625	$MgSO_4$
0.125	$CaCl_2$
0.125	NaCl
6.25 μg	Biotin
1 μl/ml	Trace elements
To 250 ml	Water

Westergaard's media with 2% sucrose

2 %	Sucrose
5 μg/ml	Biotin
1X	Westergaard's salts

For solid Westergaard's media add agar (2%).

Vogel's salts 50X

750 ml	Water
150g	Na3Citrate
250g	KH2PO4 (anhydride)
100g	NH4NO3
10g	MgSO4x7H2O
5g	CaCl2x2H2O
5ml	Biotin stock
5ml	Trace elements stock
To 1L	Water

Additions were made in the following order always with continuous stirring. Each ingredient was completely dissolved before adding next. With 5 ml Chloroform added, solution can be stored at room temperature for few months.

Vogel's minimal media with 2% glucose

20 g	Glucose
5g	Arginine
1X	Vogel's salts
Up to 1L	Water

How to prepare 'slants': Test tubes were filled with molten agar (10-15% of total tube volume), plugged with cotton and autoclaved. After autocalaving (120°C for 20 minutes) tubes were slanted so that media does not reach beyond the first third of the tube. After media solidified, tubes (so called "slants") were stored at 4°C for up to a few months. The quality of agar can have a large influence on the amount of conidia produced; we have best experience with Difco's agar. We usually used 13x100mm test tubes but for processing large number of isolates smaller test tubes turned to be more convenient. Transfers were done with long sterile inoculation loop (7cm long, loop diameter 2-3 mm, platinum /iridium alloy).

Vogel's minimal solid media with 2% glucose

20 g	Glucose
20 g	Agar
5g	Arginine
Up to 1L	Water

6.6 List of software

Mac OSX 10.2.5

Microsoft Office X for Mac

End Note 6.0.1 for Mac OSX

AppleWorks 6.2.4

Adobe Photoshop 7.0.1

Gene Construction Kit 2

KaleidaGraph 3.6

Chrono II; Till Roennenberg&Walter Taylor

VideoAnalysis 1.8; Till Roenneberg

7 REFERENCES

Ahmad, M. and Cashmore, A.R. (1998) The *CRY1* blue light photoreceptor of *Arabidopsis* interacts with phytochrome A in vitro. *Mol. Cell*, **1**, 939-948.

Alabadi, D., Oyama, T., Yanovsky, M.J., Harmon, F.G., Mas, P. and Kay, S.A. (2001) Reciprocal regulation between TOC1 and LHY/CCA1 within the *Arabidopsis* circadian clock. *Science*, **293**, 880-883.

Aronson, B.D., Johnson, K.A. and Dunlap, J.C. (1994a) The circadian clock locus *frequency*: a single ORF defines period length and temperature compensation. *Proc. Natl. Acad. Sci., USA*, **91**, 7683-7687.

Aronson, B.D., Johnson, K.A., Loros, J.J. and Dunlap, J.C. (1994b) Negative feedback defining a circadian clock: autoregulation of the clock gene *frequency*. *Science*, **263**, 1578-1584.

Arpaia, G., Cerri, F., Baima, S. and Macino, G. (1999) Protein kinase C may be a novel component of the blue light transduction pathway in *Neurospora crassa*. *Mol. Gen. Genet.*.

Arpaia, G., Loros, J.J., Dunlap, J.C., Morelli, G. and Macino, G. (1993) The interplay of light and the circadian clock. *Plant Physiol.*, **102**, 1299-1305.

Bae, K., Lee, C., Sidote, D., Chuang, K.Y. and Edery, I. (1998) Circadian regulation of a *Drosophila* homolog of the mammalian *Clock* gene: PER and TIM function as positive regulators. *Mol. Cell Biol.*, **18**, 6142-6151.

Ballario, P. and Macino, G. (1997) White collar proteins, PASsing the light signal in *Neurospora crassa*. *Trends Microbiol.*, **5**, 458-462.

Ballario, P., Vittorioso, P., Magrelli, A., Talora, C., Cabibbo, A. and Macino, G. (1996) *White collar-1*, a central regulator of blue light responses in *Neurospora*, is a zinc finger protein. *EMBO J.*, **15**, 1650-1657.

Bell-Pedersen, D., Shinohara, M.L., Loros, J. and Dunlap, J.C. (1996) Circadian clock-controlled genes isolated form *Neurospora crassa* are late night- to early morning-specific. *Proc. Natl. Acad. Sci.*, **93**, 13096-13101.

Berson, D.M., Dunn, F.A. and Takao, M. (2002) Phototransduction by retinal ganglion cells that set the circadian clock. *Science*, **295**, 1070-1073.

Bhoo, S.H., Davis, S.J., Walker, J., Karniol, B. and Vierstra, R.D. (2001) Bacteriophytochromes are photochromic histidine kinases using a biliverdin chromophore. *Nature*, **414**, 776-779.

Bieszke, J.A., Braun, E.L., Bean, L.E., Kang, S., Natvig, D.O. and Borkovich, K.A. (1999a) The nop-1 gene of Neurospora crassa encodes a seven transmembrane helix retinal-binding protein homologous to archaeal rhodopsins. *Proc Natl Acad Sci U S A*, **96**, 8034-8039.

Bieszke, J.A., Spudich, E.N., Scott, K.L., Borkovich, K.A. and Spudich, J.L. (1999b) A eukaryotic protein, NOP-1, binds retinal to form an archaeal rhodopsin-like photochemically reactive pigment. *Biochemistry*, **38**, 14138-14145.

Bognar, L.K., Adam, A.H., Thain, S.C., Nagy, F. and Millar, A.J. (1999) The circadian clock controls the expression pattern of the circadian input photoreceptor, *phytochrome B*. *Proc. Natl. Acad. Sci. USA*, **96**, 14652-14657.

Bowler, C., Yamagata, H., Neuhaus, G. and Chua, N.H. (1994) Phytochrome signal transduction pathways are regulated by reciprocal control mechanisms. *Genes Dev*, **8**, 2188-2202.

Briggs, W.R. and Olney, M.A. (2001) Photoreceptors in plant photomorphogenesis to date. five phytochromes, two cryptochromes, one phototropin, and one superchrome. *Plant Physiol*, **125**, 85-88.

Brown, L.S., Dioumaev, A.K., Lanyi, J.K., Spudich, E.N. and Spudich, J.L. (2001) Photochemical reaction cycle and proton transfers in Neurospora rhodopsin. *J Biol Chem*, **276**, 32495-32505.

Brudler, R., Hitomi, K., Daiyasu, H., Toh, H., Kucho, K., Ishiura, M., Kanehisa, M., Roberts, V.A., Todo, T., Tainer, J.A. and Getzoff, E.D. (2003) Identification of a new cryptochrome class. Structure, function, and evolution. *Mol Cell*, **11**, 59-67.

Casey, J.L., Di Jeso, B., Rao, K.K., Rouault, T.A., Klausner, R.D. and Harford, J.B. (1988) Deletional analysis of the promoter region of the human transferrin receptor gene. *Nucleic Acids Res*, **16**, 629-646.

Ceriani, M.F., Darlington, T.K., Staknis, D., Mas, P., Petti, A.A., Weitz, C.J. and Kay, S.A. (1999) Light-dependent sequestration of TIMELESS by CRYPTOCHROME. *Science*, **285**, 553-556.

Chang, B. and Nakashima, H. (1997) Effects of light-dark cycles on the circadian conidiation rhythm in *Neurospora crassa*. *J. Plant Res.*, **110**, 449-453.

Chattopadhyay, S., Ang, L.H., Puente, P., Deng, X.W. and Wei, N. (1998) Arabidopsis bZIP protein HY5 directly interacts with light-responsive promoters in mediating light control of gene expression. *Plant Cell*, **10**, 673-683.

Cheng, P., Yang, Y., Heintzen, C. and Liu, Y. (2001a) Coiled-coil domain medaited FRQ-FRQ interaction is essential for its circadian clock function in Neurospora. *EMBO J.*, **20**, 101-108.

Cheng, P., Yang, Y. and Liu, Y. (2001b) Interlocked feedback loops contribute to the robustness of the *Neurospora* circadian clock. *Proc. Natl. Acad. Sci. USA*, **98**, 7408-7413.

Cheng, P., Yang, Y., Wang, L., He, Q. and Liu, Y. (2003) WHITE COLLAR-1, a multifunctional neurospora protein involved in the circadian feedback loops, light sensing, and transcription repression of wc-2. *J Biol Chem*, **278**, 3801-3808.

Christie, J.M., Reymond, P., Powell, G.K., Bernasconi, P., Raibekas, A.A., Liscum, E. and Briggs, R. (1998) *Arabidopsis* NPH1: a flavoprotein with properties of blue light photoreceptor for phototrophism. *Science*, **282**, 1698-1701.

Christie, J.M., Salomon, M., Nozue, K., Wada, M. and Briggs, W.R. (1999) LOV (light, oxygen, or voltage) domains of the blue-light photoreceptor phototropin (nph1): binding sites for the chromophore flavin mononucleotide. *Proc. Natl. Acad. Sci. USA*, **96**, 8779-8783.

Collett, M.A., Garceau, N., Dunlap, J.C. and Loros, J.J. (2002) Light and clock expression of the *Neurospora* clock gene frequency is differentially driven by but dependent on WHITE COLLAR-2. *Genetics*, **160**, 149–158.

Corrochano, L.M., Lauter, F.R., Ebbole, D.J. and Yanofsky, C. (1995) Light and developmental regulation of the gene con-10 of Neurospora crassa. *Dev Biol*, **167**, 190-200.

Crosthwaite, S.K., Dunlap, J.C. and Loros, J.J. (1997) *Neurospora wc-1* and *wc-2*: Transcription, photoresponses, and the origin of circadian rhythmicity. *Science*, **276**, 763-769.

Crosthwaite, S.K., Loros, J.J. and Dunlap, J.C. (1995) Light-induced resetting of a circadian clock is mediated by a rapid increase in *frequency* transcript. *Cell*, **81**, 1003-1012.

Daan, S., Merrow, M. and Roenneberg, T. (2002) External Time - Internal Time. *J. Biol. Rhythms*, **17**, 107-109.

Dandekar, T. and Hentze, M.W. (1995) Finding the hairpin in the haystack: searching for RNA motifs. *Trends Genet*, **11**, 45-50.

De Fabo, E.C., Harding, R.W. and Shropshire jr., W. (1976) Action spectrum between 260 and 800 nanometers for the photoinduction of carotenoid biosynthesis in *Neurospora crassa*. *Plant Physiol.*, **57**, 440-445.

DeCoursey, P.J. and Krulas, J.R. (1998) Behavior of SCN-lesioned chipmunks in natural habitat: a pilot study. *J. Biol. Rhythms*, **13**, 229-244.

Degli-Innocenti, F. and Russo, V.E. (1984) Isolation of new *white collar* mutants of *Neurospora crassa* and studies on their behavior in the blue light-induced formation of protoperithecia. *J-Bacteriol.*, **159**, 757-761.

Denault, D.L., Loros, J.J. and Dunlap, J.C. (2001) WC-2 mediated WC-1-FRQ interaction within the PAS protein-linked circadian feedback loop of *Neurospora*. *EMBO J.*, **20**, 109-117.

Deng, T.-S. and Roenneberg, T. (1997) Photobiology of the *Gonyaulax* circadian system: II Allopurinol inhibits blue light effects. *Planta*, **202**, 502-509.

Dharmananda, S. (1980) Studies of the circadian clock of *Neurospora crassa*: light-induced phase shifting. University of California, Santa Cruz, Santa Cruz, CA.

Ding, J.M., Buchanan, G.F., Tischkau, S.A., Chen, D., Kuriashkina, L., Faiman, L.E., Alster, J.M., McPherson, P.S., Campbell, K.P. and Gillette, M.U. (1998) A neuronal ryanodine receptor mediates light-induced phase delays of the circadian clock. *Nature*, **394**, 381-384.

Ding, J.M., Faiman, L.E., Hurst, W.J., Kuriashkina, L.R. and Gillette, M.U. (1997) Resetting the biological clock: mediation of nocturnal CREB phosphorylation via light, glutamate, and nitric oxide. *J Neurosci*, **17**, 667-675.

Dragovic, Z., Tan, Y., Görl, M., Roenneberg, T. and Merrow, M. (2002) Light reception and circadian behavior in 'blind' and 'clock-less' mutants of *Neurospora crassa*. *EMBO J.*, **21**, 3643-3651.

Dreyfuss, G., Hentze, M. and Lamond, A.I. (1996) From transcript to protein. *Cell*, **85**, 963-972.

Dunlap, J.C. (1999) Molecular bases for circadian clocks. *Cell*, **96**, 271-290.

Edery, I. (1999) Role of posttranscriptional regulation in circadian clocks: lessons from Drosophila. *Chronobiol Int*, **16**, 377-414.

Emery, P., So, W.V., Kaneko, M., Hall, J.C. and Rosbash, M. (1998) CRY, a *Drosophila* clock and light-regulated cryptochrome, is a major contributor to circadian rhythm resetting and photosensitivity. *Cell*, **95**, 669-679.

Eskin, A. (1979) Identification and physiology of circadian pacemaker. *Federation Proceedings*, **38**, 2570-2572.

Faeder, E.J. and Siegel, L.M. (1973) A rapid micromethod for determination of FMN and FAD in mixtures. *Anal Biochem*, **53**, 332-336.

Feldman, J.F. and Dunlap, J.C. (1983) *Neurospora grassa*: a unique system for studying circadian rhythms. *Photochem. Photobiol.*, **7**, 319-368.

Feldman, J.F. and Hoyle, M.N. (1973) Isolation of circadian clock mutants of *Neurospora crassa*. *Genetics*, **75**, 605-613.

Fleissner, G. and Fleissner, G. (1996) The scorpion's clock as a model for feedback mechanisms in circadian systems. In Brownell, P. and Polis, G. (eds.), *Scorpion Biology and Research*. Oxford University Press, Oxford, pp. 11-17.

Freedman, M.S., Lucas, R.J., Soni, B., von Schantz, M., Munoz, M., David-Gray, Z.K. and Foster, R.G. (1999) Non-rod, non-cone ocular photoreceptors regulate the mammalian circadian behaviour. *Science*, **284**, 502-504.

Froehlich, A.C., Liu, Y., Loros, J.J. and Dunlap, J.C. (2002) White Collar-1, a circadian blue light photoreceptor, binding to the *frequency* promoter. *Science*, **297**, 815-819.

Garceau, N.Y., Liu, Y., Loros, J.J. and Dunlap, J. (1997) Alternative initiation of translation and time specific phosphorylation yield multiple forms of essential clock protein FREQUENCY. *Cell*, **89**, 469-476.

Gelder, R.N.V., Wee, R., Lee, J.A. and Tu, D.C. (2003) Reduced pupillary light responses in mice lacking cryptochromes. *Science*, **299**, 222.

Ginty, D.D., Kronhauser, J.M., Thompson, M.A., Bading, H., Mayo, K.E., Takahashi, J.S. and Greenberg, M.E. (1993) Regulation of CREB phosphorylation in the suprachiasmatic nucleus by light and a circadian clock. *Science*, **260**, 238-241.

Glossop, N.R.G., Lyons, L.C. and Hardin, P.E. (1999) Interlocked feedback loops within the *Drosophila* circadian oscillator. *Science*, **286**, 766-778.

Gooley, J.J., Lu, J., Chou, T.C., Scammell, T.E. and Saper, C.B. (2001) Melanopsin in cells of origin of the retinohypothalamic tract. *Nat Neurosci*, **4**, 1165.

Goossen, B., Caughman, S.W., Harford, J.B., Klausner, R.D. and Hentze, M.W. (1990) Translational repression by a complex between the iron-responsive element of ferritin mRNA and its specific cytoplasmic binding protein is position-dependent in vivo. *Embo J*, **9**, 4127-4133.

Görl, M., Merrow, M., Huttner, B., Johnson, J., Roenneberg, T. and Brunner, M. (2001) A PEST-like element in FREQUENCY determines the length of the circadian period in *Neurospora crassa*. *EMBO J.*, **20**, 7074-7084,.

Green, R.M. and Tobin, E.M. (1999) Loss of the circadian clock-associated protein 1 in Arabidopsis results in altered clock-regulated gene expression. *Proc Natl Acad Sci U S A*, **96**, 4176-4179.

Guo, H., Duong, H., Ma, N. and Lin, C. (1999) The Arabidopsis blue light receptor cryptochrome 2 is a nuclear protein regulated by a blue light-dependent post-transcriptional mechanism. *Plant J*, **19**, 279-287.

Hannibal, J., Hindersson, P., Knudsen, S.M., Georg, B. and Fahrenkrug, J. (2002) The photopigment melanopsin is exclusively present in pituitary adenylate cyclase-activating polypeptide-containing retinal ganglion cells of the retinohypothalamic tract. *J. Neurosci.*, **22**, RC191.

Harding, R.W. and Melles, S. (1984) Genetic analysis of the phototrophism of *Neurospora crassa* parethecial beaks using*white collar* and *albino* mutants. *Plant Physiol.*, **72**, 996-1000.
Harding, R.W. and Shropshire, W. (1980) Photocontrol of carotenoid biosynthesis. *Annu. Rev. Plant Physiol.*, **31**, 217-238.
Harding, R.W. and Turner, R.V. (1981) Photoregulation of the carotenoid biosynthetic pathway in *albino* and *white collar* mutants of *Neurospora crassa*. *Plant Physiol.*, **68**, 745-749.
Hattar, S., Liao, H.W., Takao, M., Berson, D.M. and Yau, K.W. (2002) Melanopsin-containing retinal ganglion cells: architecture, projections, and intrinsic photosensitivity. *Science*, **295**, 1065-1070.
He, Q., Cheng, P., Yang, Y., Wang, L., Gardner, K.H. and Liu, Y. (2002) White Collar-1, a DNA binding transcription factor and light sensor. *Science*, **297**, 840-843.
Heintzen, C., Loros, J.J. and Dunlap, J.C. (2001) The PAS Protein VIVID Defines a Clock-Associated Feedback Loop that Represses Light Input, Modulates Gating, and Regulates Clock Resetting. *Cell*, **104**, 453-464.
Hentze, M.W., Goossen, B. and Caughman, S.W. (1990) Complex formation between a cytoplasmic protein and the ferritin mRNA regulates translation initiation. *Mol Biol Rep*, **14**, 61.
Hentze, M.W. and Kulozik, A.E. (1999) A perfect message: RNA surveillance and nonsense-mediated decay. *Cell*, **96**, 307-310.
Huang, Z.J., Edery, I. and Rosbash, M. (1993) PAS is a dimerization domain common to Drosophila period and several transcription factors. *Nature*, **364**, 259-262.
Karniol, B. and Vierstra, R.D. (2003) The pair of bacteriophytochromes from Agrobacterium tumefaciens are histidine kinases with opposing photobiological properties. *Proc Natl Acad Sci U S A*, **100**, 2807-2812.
Kim, E.Y., Bae, K., Ng, F.S., Glossop, N.R., Hardin, P.E. and Edery, I. (2002) Drosophila CLOCK protein is under posttranscriptional control and influences light-induced activity. *Neuron*, **34**, 69-81.
Kleiner, O., Kircher, S., Harter, K. and Batschauer, A. (1999) Nuclear localization of the Arabidopsis blue light receptor cryptochrome 2. *Plant J*, **19**, 289-296.
Kramer, C., Loros, J.J., Dunlap, J.C. and Crosthwaite, S.K. (2003) Role for antisense RNA in regulating circadian clock function in Neurospora crassa. *Nature*, **421**, 948-952.
Lakin-Thomas, P.L. and Brody, S. (2000) Circadian rhythms in *Neurospora crassa* : Lipid deficiencies restore robust rhythmicity to null *frequency* and *white-collar* mutants. *Proc. Natl. Acad. Sci. USA*, **97**, 256-261.
Lakin-Thomas, P.L., Coté, G.G. and Brody, S. (1990) Circadian rhythms in *Neurospora crassa*: Biochemistry and Genetics. *Crit. Rev. Microbiol.*, **17**, 365-416.
Lauter, F.-R. and Yanofsky, C. (1993) Day/night and circadian rhythm control of con gene expression in *Neurospora*. *Proc. Natl. Acad. Sci. USA*, **90**, 8249-8253.
Lee, K., Dunlap, J.C. and Loros, J.J. (2003) Roles for WHITE COLLAR-1 in circadian and general photoreception in *Neurospora crassa*. *Genetics*, **168**, 103-114.
Lee, K., Loros, J.J. and Dunlap, J.C. (2000) Interconnected feedback loops in the *Neurospora* circadian system. *Science*, **289**, 107-110.

Lewis, Z., Correa A, Schwerdtfeger C, Link KL, Xie X, Gomer RH, Thomas T, Ebbole DJ, Bell-Pedersen D. (2002) Overexpression of White Collar-1 (WC-1) activates circadian clock-associated genes, but is not sufficient to induce most light-regulated gene expression in Neurospora crassa. *Mol Microbiol.*, **Aug;45(4)**, 917-931.

Li, C. and Schmidhauser, T.J. (1995) Developmental and photoregulation of al-1 and al-2, structural genes for two enzymes essential for carotenoid biosynthesis in Neurospora. *Dev Biol*, **169**, 90-95.

Linden, H., Ballario, P., Arpaia, G. and Macino, G. (1999) Seeing the light: news in *Neurospora* blue light signal transduction. *Adv. Genet.*, **41**, 35-54.

Linden, H. and Macino, G. (1997) *White collar 2*, a partner in blue-light signal transduction controlling expression of light-regulated genes in *Neurospora crassa*. *EMBO J.*, **16**, 98-109.

Linden, H., Rodriguez-Franco, M. and Macino, G. (1997) Mutants of *Neurospora crassa* defective in regulation of blue light perception. *Mol. Gen. Genet.*, **254**, 111-118.

Liu, Y., Loros, J. and Dunlap, J.C. (2000) Phosphorylation of the *Neurospora* clock protein FREQUENCY determines its degradation rate and strongly influences the period length of the circadian clock. *Proc. Natl. Acad. Sci. USA*, **97**, 234-239.

Loros, J.J. and Dunlap, J.C. (2001) Genetic and molecular analysis of circadian rhythms in *Neurospora*. *Annu. Rev. Physiol.*, **63**, 757-794.

Loros, J.J. and Feldman, J.F. (1986) Loss of temperature compensation of circadian period length in the *frq*-9 mutant of *Neurospora crassa*. *J. Biol. Rhythms*, **1**, 187-198.

Loros, J.J., Richman, A. and Feldman, J.F. (1986) A recessive circadian clock mutation at the *frq* locus of *Neurospora crassa*. *Genetics*, **114**, 1095-1110.

Lucas, R.J., Freedman, M.S., Munoz, M., Garcia-Fernandez, J. and Foster, R.G. (1999) Non-rod, non-cone ocular photoreceptors regulate the mammalian pineal. *Science*, **284**, 505-507.

Lucas, R.J., Hattar, S., Takao, M., Berson, D.M., Foster, R.G. and Yau, K.-W. (2003) Diminished pupillary light reflex at high irradiances in melanopsin-knockout mice. *Science*, **299**, 245-247.

Luo, C., Loros, J.J. and Dunlap, J.C. (1998) Nuclear localization is required for function of the essential clock protein FRQ. *EMBO J.*, **17**, 1228-1235.

Martinez-Garcia, J.F., Huq, E. and Quail, P.H. (2000) Direct targeting of light signals to a promoter element-bound transcription factor. *Science*, **288**, 859-863.

McClung, C.R. (ed.). (1992) *The higher plant Arabidopsis thaliana as a model system for the molecular analysis of circadian rhythms*. Marcel Dekker, NY.

McClung, C.R., Fox, B.A. and Dunlap, J.C. (1989) The *Neurospora* clock gene *frequency* shares a sequence element with the *Drosophila* clock gene *period*. *Nature*, **339**, 558-562.

McFadden, E.R., Jr. (1988) Circadian rhythms. *Am J Med*, **85**, 2-5.

Menaker, M. (2003) Circadian rhythms. Circadian photoreception. *Science*, **299**, 213-214.

Merrow, M., Brunner, M. and Roenneberg, T. (1999) Assignment of circadian function for the *Neurospora* clock gene *frequency*. *Nature*, **399**, 584-586.

Merrow, M., Dragovic, Z., Tan, Y., Meyer, G., Sveric, K., Mason, M., Ricken, J. and Roenneberg, T. (2003) Combining theoretical and experimental approaches to understand the circadian clock. *Chronobiol Int*, **20**, 559-575.

Merrow, M., Franchi, L., Dragovic, Z., Görl, M., Johnson, J., Brunner, M., Macino, G. and Roenneberg, T. (2001) Circadian regulation of the light input pathway in *Neurospora crassa*. *EMBO J.*, **20**, 307-315.

Merrow, M.W. and Dunlap, J.C. (1994) Intergeneric complementation of a circadian rhythmicity defect: phylogenetic conservation of structure and function of the clock gene *frequency*. *EMBO J.*, **13**, 2257-2266.

Moore, R.Y. (1997) Circadian rhythms: basic neurobiology and clinical applications. *Ann. Rev. Med.*, **48**, 253-266.

Moore-Ede, M.C., Sulzman, F.M. and Fuller, C.A. (1982) *The Clocks that time us*. Harvard University Press, Cambridge.

Montgomery, B. and Lagarias C. (2002) Phytochrome ancestry:sensors of bilins and light *Trends in Plant Science*, 1360-1385/02

Nakashima, H. and Fujimura, Y. (1982) Light-induced phase shifting of the circadian clock in *Neurospora crassa* ammonium salts in high pH. *Planta*, **155**, 431-436.

Ninnemann, H. (1979) Photoreceptor for circadian rhythms. In Smith, K.C. (ed.), *Photochemical and Photobiological Reviews*, NY and London, Vol. 4, pp. 207-266.

Ninnemann, H. (1991) Participation of the molybdenum cofactor of nitrate reductase from *Neurospora crassa* in light promoted conidiation. *J. Plant. Physiol.*, **137**, 677-682.

Obrietan, K., Impey, S. and Storm, D.R. (1998) Light and circadian rhythmicity regulate MAP kinase activation in the suprachiasmatic nuclei. *Nat Neurosci*, **1**, 693-700.

Ostareck-Lederer, A., Ostareck, D.H., Standart, N. and Thiele, B.J. (1994) Translation of 15-lipoxygenase mRNA is inhibited by a protein that binds to a repeated sequence in the 3' untranslated region. *Embo J*, **13**, 1476-1481.

Oyama, T., Shimura, Y. and Okada, K. (1997) The Arabidopsis HY5 gene encodes a bZIP protein that regulates stimulus-induced development of root and hypocotyl. *Genes Dev*, **11**, 2983-2995.

Paietta, J. and Sargent, M.L. (1981) Photoreception in *Neurospora crassa*: Correlation of reduced light sensitivity with flavin deficiency. *Proc. Natl. Acad. Sci. USA*, **78**, 5573-5577.

Panda, S., T.K.Sato, Castrucc, A.M., Rollag, M.D., DeGrip, W.J., Hogenesch, J.B., Provencio, I. and Kay, S.A. (2002) Melanopsin (Opn4) requirement for normal light-induced circadian phase shifting. *Science*, **298**, 2213-2216.

Perkins, D.D., Margolin, B.S., Selker, E.U. and Haedo, S.D. (1997) Occurrence of repeat induced point mutation in long segmental duplications of Neurospora. *Genetics*, **147**, 125-136.

Perkins, D.D., Radford, A., Newmeyer, D. and Bjorkman, M. (1982a) Chromosomal loci of Neurospora crassa. *Microbiol Rev*, **46**, 426-570.

Perkins, D.D., Radford, A., Newmeyer, D. and Björkman, M. (1982b) Chromosomal loci of *Neurospora crassa*. *Microbiol. Rev.*, **46**, 426-570.

Pittendrigh, C.S., Bruce, V.G., Rosensweig, N.S. and Rubin, M.L. (1959) Growth patterns in *Neurospora crassa*. *Nature*, **184**, 169-170.

Pittendrigh, C.S. and Minis, D.H. (1964) The entrainment of circadian oscillations by light and their role as photoperiod clocks. *Am. Natural.*, **98**, 261-294.
Preiss, T. and Hentze, M.W. (1999) From factors to mechanisms: translation and translational control in eukaryotes. *Curr Opin Genet Dev*, **9**, 515-521.
Quail, P.H. (2002) Photosensory perception and signalling in plant cells: new paradigms? *Curr Opin Cell Biol*, **14**, 180-188.
Reisz-Porszasz, S., Probst, M.R., Fukunaga, B.N. and Hankinson, O. (1994) Identification of functional domains of the aryl hydrocarbon receptor nuclear translocator protein (ARNT). *Mol Cell Biol*, **14**, 6075-6086.
Rocco, M.B., Nabel, E.G. and Selwyn, A.P. (1987) Circadian rhythms and coronary artery disease. *Am J Cardiol*, **59**, 13C-17C.
Roenneberg, T. and Foster, R.G. (1997) Twilight Times - Light and the circadian system. *Photochem. Photobiol.*, **66**, 549-561.
Roenneberg, T. and Hastings, J.W. (1988) Two photoreceptors influence the circadian clock of a unicellular alga. *Naturwissenschaften*, **75**, 206-207.
Roenneberg, T. and Merrow, M. (1998) Molecular circadian oscillators - an alternative hypothesis. *J. Biol. Rhythms*, **13**, 167-179.
Roenneberg, T. and Merrow, M. (2000) Circadian light input: omnes viae Romam ducunt. *Curr. Biol.*, **10**, R742-R745.
Roenneberg, T. and Merrow, M. (2001a) The role of feedbacks in circadian systems. In Honma, K. and Honma, S. (eds.), *Zeitgebers, Entrainment and Masking of the Circadian System*. Hokkaido Univ. Press, Sapporo, pp. 113-129.
Roenneberg, T. and Merrow, M. (2001b) Seasonality and photoperiodism in fungi. *J. Biol. Rhythms*, **16**, 403-414.
Roenneberg, T. and Morse, D. (1993) Two circadian oscillators in one cell. *Nature*, **362**, 362-364.
Roenneberg, T. and Taylor, W. (1994) Light induced phase responses in *Gonyaulax* are drastically altered by creatine. *J. Biol. Rhythms*, **9**, 1-12.
Roenneberg, T. and Taylor, W. (2000) Automated recordings of bioluminescence with special reference to the analysis of circadian rhythms. *Meth. Enzymol.*, **305**, 104-119.
Ruby, N.F., Brennan, T.J., Xie, X., Cao, V., Franken, P., Heller, H.C. and O 'Hara, B.F. (2002a) Role of melanopsin in circadian responses to light. *Science*, **298**, 2211-2213.
Ruby, N.F., Brennan, T.J., Xie, X., Cao, V., Franken, P., Heller, H.C. and O'Hara, B.F. (2002b) Role of melanopsin in circadian responses to light. *Science*, **298**, 2211-2213.
Russo, V.E. (1988) Blue light induces circadian rhythms in the *bd* mutant of *Neurospora*: double mutants *bd*,*wc-1* and *bd*,*wc-2* are blind. *Photochem. Photobiol.*, **2**, 59-65.
Sambrook, J., Fritch, E.F. and Maniatis T. (1989) *Molecular cloning: A laboratory manual*.
Sargent, M. and Briggs, W.R. (1967) The effect of light on a circadian rhythm of conidiation in *Neurospora*. *Plant Physiol*, **42**, 1504-1510.
Sargent, M.L. and Kaltenborn, S.H. (1972) Effects of medium composition and corbon dioxide on circadian conidiation in *Neurospora*. *Plant Physiol.*, **50**, 171-175.

Sargent, M.L. and Woodward, D.O. (1969) Genetic determinants of circadian rhythmicity in *Neurosproa*. *J. Bacteriol.*, **97**, 861-866.
Schwerdtfeger, C. and Linden, H. (2001) Blue light adaptation and desensitization of light signal transduction in *Neurospora crassa*. *Mol. Microbiol.*, **39**, 1080-1087.
Scott, A. (2000 Dec) Shift work and health. *Prim Care.*, **27(4)**, 1057-1079.
Shearman, L.P., Zylka, M.J., Weaver, D.R., Kolakowski, L.F. and Reppert, S.M. (1997) Two *period* homologs: circadian expression and photic regulation in the suprachiasmatic nuclei. *Neuron*, **19**, 1261-1269.
Shrode, L.B., Lewis, Z.A., White, L.D., Bell-Pedersen, D. and Ebbole, D.J. (2001) vvd is required for light adaptation of conidiation-specific genes of Neurospora crassa, but not circadian conidiation. *Fungal Genet Biol*, **32**, 169-181.
Sokolove, P.G. and Bushell, W.N. (1978) The chi square periodogram: Its utility for analysis of circadian rhythms. *J. Theoret. Biol.*, **72**, 131-160.
Sokolovsky, V.Y., Lauter, F.-R., Müller-Röber, B., Ricci, M., Schmidhauser, T.J. and Russo, V.E.A. (1992) Nitrogen regulation of blue-light-inducible genes in *Neurospora crassa*. *J. Gen. Microbiol.*, **138**.
Somers, D.E., Devlin, P.F. and Kay, S.A. (1998a) Phytochromes and cryptochromes in the entrainment of the *Arabidopsis* circadian clock. *Science*, **282**, 1488-1490.
Somers, D.E., Devlin, P.F. and Kay, S.A. (1998b) Phytochromes and cryptochromes in the entrainment of the Arabidopsis circadian clock. *Science*, **282**, 1488-1490.
Sommer, T., Chambers, J.A., Eberle, J., Lauter, F.R. and Russo, V.E. (1989) Fast light-regulated genes of *Neurospora crassa*. *Nucl. Ac. Res.*, **17**, 5713-5723.
Stanewsky, R., Lynch, K.S., Brandes, C. and Hall, J.C. (2002) Mapping of elements involved in regulating normal temporal period and timeless RNA expression patterns in Drosophila melanogaster. *J Biol Rhythms*, **17**, 293-306.
Stripecke, R., Oliveira, C.C., McCarthy, J.E. and Hentze, M.W. (1994) Proteins binding to 5' untranslated region sites: a general mechanism for translational regulation of mRNAs in human and yeast cells. *Mol Cell Biol*, **14**, 5898-5909.
Sweeney, B.M. and Hastings, J.W. (1960) Effects of temperature upon diurnal rhythms. *Cold Spring Harbor Symp. Quant. Biol.*, **25**, 87-104.
Talora, C., Franchi, L., Linden, H., Ballario, P. and Macino, G. (1999) Role of a white collar-1-white collar-2 complex in blue-light signal transduction. *EMBO J.*, **18**, 4961-4068.
Tamada, T., Kitadokoro, K., Higuchi, Y., Inaka, K., Yasui, A., de Ruiter, P.E., Eker, A.P. and Miki, K. (1997) Crystal structure of DNA photolyase from Anacystis nidulans. *Nat Struct Biol*, **4**, 887-891.
Walden, W.E., Daniels-McQueen, S., Brown, P.H., Gaffield, L., Russell, D.A., Bielser, D., Bailey, L.C. and Thach, R.E. (1988) Translational repression in eukaryotes: partial purification and characterization of a repressor of ferritin mRNA translation. *Proc Natl Acad Sci U S A*, **85**, 9503-9507.
Wang, Z.Y. and Tobin, E.M. (1998) Constitutive expression of the *CIRCADIAN CLOCK ASSOCIATED 1* (*CCA1*) gene disrupts circadian rhythms and suppresses its own expression. *Cell*, **93**, 1207-1217.
Waterhouse, J., Minors, D. and Redfern, P. (1997) Some comments on the measurement of circadian rhythms after time-zone transitions and during night work. *Chronobiol Int*, **14**, 125-132.

White, B.T. and Yanofsky, C. (1993) Structural characterization and expression analysis of the *Neurospora* conidiation gene *con-6*. *Developmental Biology*, **160**, 254-264.

Whitelam, G.C., Patel, S. and Devlin, P.F. (1998) Phytochromes and photomorphogenesis in Arabidopsis. *Philos Trans R Soc Lond B Biol Sci*, **353**, 1445-1453.

Wilsbacher, L.D. and Takahashi, J.S. (1998) Circadian rhythms: molecular basis of the clock. *Curr Opin Genet Dev*, **8**, 595-602.

Yager, L.N., Lee, H., Nagle, D.L. and Zimmerman, J.E. (1998) Analysis of *fluG* Mutations That Affect Light-Dependent Conidiaiton in *Aspergillus nidulans*. *Genetics*, **149**, 1777-1786.

Yan, O.Y., Andersson, C.R., Kondo, T., Golden, S.S., Johnson, C.H. and Ishiura, M. (1998) Resonating circadian clocks enhance fitness in cyanobacteria. *PNAS*, **95**, 8660-8664.

Yang, Y., Cheng, P. and Liu, Y. (2002) Regulation of the *Neurospora* circadian clock by casein kinase II. *Genes Dev*., **16**, 994-1006.

Zigmond, M. (1999) Fundamental Neuroscience. *Academic Press*, **ISBN0127808701**.

Zylka, M.J., Shearman, L.P., Weaver, D.R. and Reppert, S.M. (1998) Three *period* homologs in mammals: differential light responses in the suprachiasmatic circadian clock and oscillating transcripts outside of brain. *Neuron*, **20**, 1103-1110.

8 VERÖFENTLICHUNGEN / PUBLICATIONS

Teile dieser Arbeit wurden bereits veröfentlicht:

Combining Theoretical and Experimental Approaches to Understand the Circadian Clock
Merrow M, Dragovic Z, Tan Y, Meyer M, Sveric K, Mason M, Ricken J, Roenneberg T
Chronobiology International, 2003, Vol. 20/4, 1-17

Light reception and circadian behavior in 'blind' and 'clock-less' mutants of Neurospora crassa.
Dragovic Z, Tan Y, Gorl M, Roenneberg T, Merrow M
EMBO J, 2002 Jul 15 21:14 3643-51

Circadian regulation of the light input pathway in Neurospora crassa.
Merrow M, Franchi L, Dragovic Z, Gorl M, Johnson J, Brunner M, Macino G, Roenneberg T
EMBO J, 2001 Feb 1 20:3 307-15

9 ERKLÄRUNG

Hiermit erkläre ich, daß die vorliegende Dissertation selbständig verfaßt und nur unter Verwendung der ahgegebenen Quellen und Hilfsmittel angefertigt wurde.

Die Dissertation wurde in dieser oder änlicher Form noch keiner anderen Fakultät oder sonstiger Prüfungsbehörde vorgelegt.

10 DANKSAGUNG /ACKNOWLEDGEMENTS / ZAHVALNICA

Ich danke meiner Doktormutter Priv. Doz. Dr. Martha Merrow und meinem Doktorvater Prof. Dr. Till Roenneberg für die erstklassige Anleitung und Unterstützung meiner Arbeit.

Einen besonderes Dank möchte ich Prof. Dr. Ernst Pöppel aussprechen. Sein ständiges Interesse und seine Diskussionbereitschaft haben wesentlich zum Erfolg meiner Arbeit beigetragen.

Einen herzlichen Dank gilt für Vera Schiewe, die mich mit ihrer Arbeit und ihrer Freundschaft unterstüzt hat.

I would like to thank Ying Tan, Margit Görl, Brunner Michael and Lisa Franchi for the scientific collaboration.

Bei Prof. Dr. Judy Johnson und Ina Contag möchte ich mich für die Herstellung der monoklonalen Antikörper bedanken.

Ganz herzlich möchte ich mich bei Hans Distel, Ruth Hoffman, Helmut Klausner, Susanne Piccone, Astrid Bauer und Johanna Raithel für die gute Arbeitsatmosphäre bedanken.

Zahvaljujem se mojim roditeljima Nikoli i Danici za sve ono lepo za sta se roditeljima treba biti zahvalan.

Zahvaljujem Bozi i Mirjani Mokranjac za sveukupnu pomoc i podrsku tokom visegodisnjeg skolovanja.

Zahvaljujem se Srdjanu Dragovicu za tehnicku pomoc prilikom izrade vise experimenta prikazanih u ovom doktoratu.

Ponajvise se ipak zahvaljujem Dejani Mokranjac sto me trpi sve ove godine.

CURRICULUM VITAE

Zdravko Dragovic

21.06.1972.	Born in Belgrade, Yugoslavia
1979-1987	„Svetozar Miletic“ primary school, Belgrade, Yugoslavia
1987-1991	„Zemun Gymnasium“, Belgrade, Yugoslavia
1991-1992	Army service in Bela Crkva, Yugoslavia
1992-1999	Study of Molecular Biology and Physiology at Faculty of Biology, University of Belgrade, Belgrade, Yugoslavia
1999-2004	PhD research in the laboratory of Prof. Dr. Till Roenneberg at Institut für Medicinische Psychologie, Ludwig-Maximilians-Universität München